Karlsruher Institut für Technologie

Phytochrome-dependent light signaling in *Aspergillus nidulans*

Zur Erlangung des akademischen Grades eines

DOKTORS DER NATURWISSENSCHAFTEN

(Dr. rer. nat.)

von der KIT-Fakultät für Chemie und Biowissenschaften

des Karlsruher Instituts für Technologie (KIT)

genehmigte

DISSERTATION

von

M.Sc. Zhenzhong Yu

aus

Shandong, China

Dekan: Prof. Dr. Willem Klopper

Referent: Prof. Dr. Reinhard Fischer

Korreferent: Prof. Dr. Jörg Kämper

Tag der mündlichen Prüfung: 21.10.2016

Erklärung

Ich erkläre, dass ich die Doktorarbeit selbständig angefertigt und keine anderen als die angegebenen Quellen und Hilfsmittel benutzt sowie die wörtlich oder inhaltlich übernommenen Stellen als solche kenntlich gemacht und die Satzung des Karlsruher Institut für Technologie (KIT) zur Sicherung guter wissenschaftlicher Praxis in der jeweils gültigen Fassung beachtet habe.

Karlsruhe, den

_____

Zhenzhong Yu

Publikationsliste

Aus dieser Arbeit sind folgende Publikationen entstanden:

Röhrig, J.*, Yu, Z.*, Han, K.-H. & Fischer, R. (2016). The *Aspergillus nidulans* Velvet-interacting protein, VipA, regulates light-dependent heme biosynthesis. *Mol Microbiol*, in revision.

Yu, Z., Armant, O., & Fischer, R. (2016). Fungi use the SakA (HogA) pathway for phytochrome-dependent light signalling. *Nature Microbiol*, 16019.

Hedtke, M., Rauscher, S., Röhrig, J., Rodríguez‐Romero, J., Yu, Z., & Fischer, R. (2015). Light-dependent gene activation in *Aspergillus nidulans* is strictly dependent on phytochrome and involves the interplay of phytochrome and white collar-regulated histone H3 acetylation. *Mol Microbiol*, 97(4), 733-745.

Weitere Publikationen, die nicht direkt mit dem Thema dieser Arbeit verknüpft sind:

Cai M.*, Zhang Y.*, Hu W., Shen W., Yu Z., Zhou W., Jiang T., Zhou X. & Zhang Y. (2014). Genetically shaping morphology of the filamentous fungus *Aspergillus glaucus* for production of antitumor polyketide aspergiolide A. *Microb Cell Fact* **13**, 73-83.

Yu Z., Cai M., Hu W., Zhang Y., Zhou J., Zhou X. & Zhang Y. (2014). A cyclin-like protein, ClgA, regulates development in *Aspergillus nidulans*. *Res Microbiol* **165**, 462-467.

* Autoren haben in gleichem Maße zu der Arbeit beigetragen.

Abbreviations

BiFC	Bimolecular Flourescence Complementation
bZIP	Basic region-leucine zipper
ChIP	Chromatin immunoprecipitation
CPD	Cyclobutane pyrimidine dimer
dsDNA	Double-stranded DNA
FAD	Flavin-adenine dinucleotide
HKD	Histindine kinase domain
HHK	Hybrid histidine kinase
HK	Histidine kinase
HPt	Histidine phosphotransferase
LOV	Light-Oxygen-Voltage
NES	Nuclear export signal
NGS	Next Generation Sequencing
NLS	Nuclear localization site
OD	Output domain
PAS	Per-ARNT-Sim
PABA	p-aminobenzoic acid
PEST	Proline (P), glutamic acid (E), serine (S) and threonine (T) rich domain
PHR	Photolyase-related domain
RD	Receiver domain
RR	Response regulator
ROS	Reactive oxygen species
SD	Sensor domain
SNP	Single nucleotide polymorphism
ssDNA	Single-stranded DNA
ST	Sterigmatocystin
TCS	Two-component system
TLC	Thin layer chromatography
TF	Transcription factor
WC-1	White collar 1
WC-2	White collar 2
WCC	White-Collar-Complex
WT	Wild type
ZF	GATA type zinc-finger DNA binding domain

Contents

Summary

In order to cope with the ever-changing environment, organisms have evolved to sense and adapt to various environmental cues. Light is one of the most important environmental signals and regulates physiological and morphological processes of many organisms. The filamentous fungus *Aspergillus nidulans* senses red and blue light using the red light receptor, FphA, and the blue light receptors, LreA and CryA.

In a previous analysis light-regulated genes were identified, and the mechanism of light induction was studied for two of them, *ccgA* and *conJ.* The induction is dependent on phytochrome (FphA), but FphA does not bind to the promoter of *ccgA* directly. The effect of other components involved in light perception on light induction of *ccgA* and *conJ* is minor. In order to find new components involved in phytochrome-dependent light sensing, we established an efficient genetic screening approach. The promoter of the light-inducible gene, *conJ*, was fused to the nutritional marker gene *pyr4*, and the plasmid was introduced into an uracil auxotrophic strain. This strain grew like wild type in light, but grew only very poorly in the dark. This strain was used as the parent strain for UV-mutagenesis. Seven *blind* mutants that could not respond to light anymore, and hence formed only small colonies in light, were isolated. Moreover, a dominant mutant, which grew already in the dark in the absence of uracil and uridine, was obtained. In this dominant mutant, *ccgA* and *conJ* were de-repressed in the dark. The responsible mutations in the *blind* mutant M6-9 and the dominant mutant MD3-8, were identified by next generation sequencing (NGS).

The new component identified with the *blind* mutant M6-9 was the stress activated MAP kinase SakA, the homologue of *S. cerevisiae* Hog1. The analysis of the dominant mutant MD3-8 revealed two single-base substitutions (from an ATG codon to a TAG stop codon) in the gene AN1777 that encodes a protein with an N-terminal PHD finger, a TFS2M, which is found in the central region of transcription elongation factor S-II, and a C-terminal SPOC domain (spen paralog and ortholog C-terminal domain). PHD finger-containing proteins are invovled in chromatin remodeling and the SPOC domain points to the involvement in a transcriptional repression complex. The analysis has not been finished but the preliminary results point to chromatin-remodeling processes during light regulation. The role of SakA in light signaling was studied in detail.

In *S. cerevisiae*, the sole two-component system (TCS) phosphorelay and the MAP kinase Hog1 pathway are responsible for osmosensing. In *A. nidulans* SakA is involved in osmo- and other stress-sensing as well as in the regulation of development. The TCS phosphorelay system consists of a hybrid histidine kinase

(HHK), a histidine-containing phosphotransferase (HPt), YpdA, and a response regulator (RR), SskA, and the MAP kinase SakA pathway including the MAPKKK, SskB, the MAPKK PbsB, the MAPK SakA and the transcription factor AtfA, to respond to environmental signals. By real-time RCR, we confirmed that SskA, SskB, PbsB, SakA and AtfA were essential for light induction of *ccgA* and *conJ*. FphA is one of the 15 HHKs in *A. nidulans*. By bimolecular fluorescence complementation (BiFC) and co-immunoprecipitation (CoIP), it was shown that FphA directly interacts with the HPt YpdA. Hence, light plugs into the SakA pathway from upstream YpdA through FphA.

We further analyzed SakA translocation and phosphorylation under different light conditions or salt stress. In white and red light, SakA shuttled from the cytoplasm into the nucleus but in blue light it did not. In an *fphA*-deletion strain, no shuttling was observed, implying FphA is essential for the shuttling. Intriguingly, in an *fphA*-deletion strain SakA shuttling was still induced by salt stress. This demonstrates that osmosensing is independent of FphA. White and red light stimulated SakA phosphorylation, which was confirmed by western blotting and immunostaining using antibodies derived against the phosphorylated form of p38 (the human orthologue of SakA). Phosphorylation of SakA under blue light was only detected by immunostaining. LreA and LreB were not necessary for the blue light induced phosphorylation. In the *fphA*-deletion stain, no phosphorylation was detected. Hence, light activation of the SakA pathway solely depends on FphA.

In another research group, interested in the sulfur metabolism in *A. nidulans*, a transcriptomic analysis revealed that phytochrome expression was strictly controlled by the positive regulator of the sulfur metabolism, MetR. This observation was studied further. Indeed, a *metR1* mutant had a similar phenotype as an *fphA*-deletion stain and light-induction of *ccgA* and *conJ* was impaired. Similarly, expression of the global regulator *veA* was no longer light repressed in both mutants. These results show that FphA represents a link between the sulfur metabolism and VeA-mediated morphogenetic and physiological processes.

In addition to the induction of *ccgA* and *conJ* by light, we found that the two genes could be induced by high temperatures. FphA and SakA were both essential for temperature sensing, suggesting a novel role for FphA as a potential thermosensor and the SakA pathway as a signalling module to adapt to temperature changes.

Zusammenfassung

Organismen haben sich entwickelt, um den wechselnden Umweltbedingungen standzuhalten, damit sie Umweltsignale wahrnehmen und sich als Folge anpassen können. Licht ist einer eines der wichtigsten Umweltsignale und reguliert viele physiologische sowie morphologische Prozesse in vielen Organismen. Der filamentöse Pilz *Aspergillus nidulans* nimmt Rot- und Blaulicht wahr, indem der Rotlichtrezeptor FphA und die Blaulichtrezeptoren LreA und CryA verwendet werden.

In einer früheren Studie wurden lichtregulierte Gene identifiziert und der Mechanismus der Lichtregulation für zwei der Gene, c*cgA* und *conJ,* analysiert. Die Induktion ist abhängig von Phytochrom (FphA), aber FphA bindet nicht direkt an den Promotor von *ccgA* oder *conJ*. Der Effekt von weiteren Komponenten der Lichtperzeption auf die lichtabhängige Induktion ist eher gering. Für die Suche nach neuen Komponenten, die in der phytochrom-vermittelten Lichtwahrnehmung beteiligt sind, wurde eine neue, effiziente genetische Analyse entwickelt. Der Promotor des lichtinduzierbaren Gens *conJ*, wurde mit einem Nährstoffmarker, *pyr4*, fusioniert, und das Plasmid wurde in einen Uracil-auxotrophen Stamm gebracht. Dieser Stamm wuchs wie der Wildtyp in Licht, aber in der Dunkelheit wuchs er nur sehr schlecht. In einer UV-Mutagenese wurde dieser Stamm als Ausgangsstamm verwendet. Dabei wurden sieben *blinde* Mutanten isoliert, die nicht mehr auf Licht reagieren und daher nur kleine Kolonien bildeten. Desweiteren wurde eine dominante Mutante erhalten, die in Dunkelheit in Abwesenheit von Uracil und Uridin wuchs. In dieser dominanten Mutante, waren *ccgA* und *conJ* im Dunkeln dereprimiert. Die verantwortlichen Mutationen der *blinden* Mutanten M6-9 und der dominanten Mutante MD3-8, wurden mittels *next generation sequencing* (NGS) identifiziert.

Die neu identifizierte Komponente der blinden Mutante M6-9 war die stressaktivierte MAP Kinase SakA, das Homolog zu *S. cerevisiae* Hog1. Die Analyse der dominanten Mutante MD3-8 wies zwei Punktmutationen (ATG Codon zu TAG Codon) im Gen An1777 auf. Das von An1777 exprimierte Protein besitzt einen N-terminalen PHD Finger, eine TFS2M Domäne, die in der zentralen Region von Transkriptions-Elongationsfaktor S-II zu finden ist, und eine C-terminale SPOC Domäne (Spen paralog and ortholog C-terminal domain). Das resultierende Protein der Mutante MD3-8 ist ein Peptid dem die SPOC Domäne fehlt. Generell vermitteln PHD Finger Proteine Histon-Methylierungen und Spen Proteine sind Komponenten transkriptioneller Repressionskomplexes. Die Analyse ist noch nicht beendet, aber die vorläufigen Ergebnisse weisen auf eine Rolle von Chromatinmodifikationen in der

Regulation der lichtinduzierbaren Gene hin. Die Funktion von SakA in der Licht-Signaltransduktion wurde im Detail untersucht.

In *S. cerevisiae* ist das einzige Zwei Komponenten-System Phosphorelay und der MAP Kinase Hog1 Signalweg für die Wahrnehmung hoher Salzkonzentrationen zuständig. In *A. nidulans* ist SakA an der Wahrnehmung von osmotischen und anderen Stressformen sowie der Regulation der Entwicklung beteiligt. Das Zwei-Komponenten-Phosphorelay System besteht aus einer Hybrid-Histidinkinase, einer Histidin-beinhaltenden Phosphotransferase, YpdA, einem Responseregulator, SskA, und dem MAP Kinase SakA Singalweg samt der MAPKKK, SskB, der MAPKK PbsB, der MAPK SakA und dem Transkriptionsfaktor AtfA. Mittels real-time RT-PCR wurde nachgewiesen, dass SskA, SskB, PbsB, SakA und AtfA für die lichtabhängige Induktion von *ccgA* und *conJ* essentiell sind. FphA ist eine von 15 HKs in *A. nidulans.* Mittels Bimolekularer Fluoreszenz Komplementation (BiFC) und Co-Immunopräzipitation wurde gezeigt, dass FphA direkt mit dem HPt YpdA interagiert. Daher wird Licht stromaufwärts von YpdA im Signalweg, durch FphA wahrgenommen.

Des Weiteren wurden die SakA Translokalisation und die SakA Phosphorylierung unter verschiedenen Lichtkonditionen oder Salzstress analysiert. In Weiß- und Rotlicht translozierte SakA vom Cytoplasma in den Zellkern, aber in Blaulicht war dies nicht der Fall. In einem *fphA* Deletionsstamm wurde keine Translokation beobachtet, sodaß FphA für die Translokation von SakA essentiell ist. Erstaunlicherweise konnte die SakA Translokation im *fphA* Deletionsstamm durch Salzstress noch induziert werden. Hierdurch wird deutlich, dass die Wahrnehmung von osmotischem Stress unabhängig von FphA ist. Weiß- und Rotlicht stimulierten die SakA Phosphorylierung. Dies wurde mittels Western Blot und Immunodetektion durch Antikörper gegen die phosphorylierte Form von p38 (dem menschlichen Ortholog zu SakA) bestätigt. Phosphorylierung von SakA unter Blaulicht wurde nur durch Immunodetektion bestätigt. LreA und LreB waren nicht für eine blaulichtinduzierte Phosphorylierung notwendig. Daher ist die lichtvermittelte Induktion des SakA Signalweg nur von FphA abhängig.

In einer anderen Arbeitsgruppe, die sich für den Schwefelmetabolismus von *A. nidulans* interessiert, wurde mittels Transkriptomanalyse herausgefunden, dass die Phytochromexpression strikt durch den positiven Regulator des Schwefelmetabolismus, MetR, kontrolliert wird. Dieser Beobachtung wurde hier weiter nachgegangen und die Lichtreaktion der *mtR1* Mutanten analysiert. Die *metR1* Mutante hatte einen ähnlichen Phänotyp wie der *fphA* Deletionsstamm. Die sexuelle Entwicklung wurde dereprimiert im Licht. Tatsächlich konnte *fphA* in der metR1 Mutante nicht mehr exprimiert werden. Wie im *fphA* Deletionsstamm, war die lichtabhängige Induktion von *ccgA* und *conJ* in der *metR1* Mutante beeinträchtigt. Die

veA Expression war reprimiert, wenn der Wildtyp Licht ausgesetzt wurde, jedoch wurde die *veA* Expression im *fphA* Deltionsstamm und in der *metR1* Mutante nicht durch Licht beeinflusst. FphA verbindet also den Schwefelmetabolismus und den SakA Signalweg und VeA-abhängige morphologische und physiologische Prozesse.

Zusätzlich zur Lichtinduktion von *ccgA* und *conJ,* wurde herausgefunden, daß beide Gene durch hohe Temperaturen induziert werden können. FphA und SakA sind beide für die Temperaturwahrnehmung essentiell, wodurch eine neue Rolle von FphA als potentieller Temperatursensor suggeriert wird

Introduction

Fungi are a large community in the environment comprising more than 5 million species and only around 100,000 of them have been described so far (Blackwell, 2011; O'Brien *et al.*, 2005). Most of them are saprophytic organisms. They are an industrially valuable resource for the preparation of antibiotics, amino acids and food additives and are crucial for environmental carbon cycling (Chakraborty *et al.*, 2016; Dufosse *et al.*, 2014; Herr and Fischer, 2014; Mosier *et al.*, 2016). In addition, some of them threat human health as pathogens (Brown *et al.*, 2012; Fisher *et al.*, 2012; Hedayati *et al.*, 2007; Kim, 2016; Nielsen and Heitman, 2007). Fungi are widespread underground in soil or in organic matters, and this environment is relatively stable with respect to darkness, nutrition, temperature, humidity and oxygen. However, huge amounts of organic matter are found on the ground surface, where fungi may be exposed to different and very unstable environmental conditions. Dry conditions on the soil surface make the mycelium desiccate quickly and UV light may cause damage of the DNA and an increase of harmful reactive oxygen species (ROS) (Bahn *et al.*, 2007; Gessler *et al.*, 2007; Rodriguez-Romero *et al.*, 2010). The alternations between day and night and seasonal changes make the environment ever-changing. In order to adapt to the changing environments, fungi have evolved to sense various internal and external cues, one of which is light. Light as one of the most important natural resources is closely linked with the lives on the earth. Photosynthesis fundamentally provides the energy for human, animals, plant and even microbes. Besides the critical role in photosynthesis, light as an informational cue regulates physiological and developmental processes of many organisms during their life cycle (Blumenstein *et al.*, 2005; Dasgupta *et al.*, 2016; Fischer, 2008; Idnurm and Heitman, 2005; Kami *et al.*, 2010; Rodriguez-Romero *et al.*, 2010; Rohrig *et al.*, 2013).

Although fungi are heterotrophic orgamisms, many species use light as informational cue. In the zygomycetous fungus *Phycomyces blakesleeanus*, an impressive light response is the phototropism of the macrophore that grows towards light. Light inhibits microphore development but promotes the synthesis of carotenoid in the mycelium (Idnurm *et al.*, 2006). In the ascomycete *Neurospora crassa*, light induces carotenoid synthesis, which colors the colony orange (Zalokar, 1954). Light also induces branching making the colony appear more compact in light than in the dark (Lauter *et al.*, 1998). Maximum asexual sporulation also requires light exposure. The formation of protoperithecia (female sexual structures) in *N. crassa* is induced by blue light, and the phototropism of perithecial (fertilized perithecia) beaks is controlled by blue light (Harding

and Melles, 1983; Innocenti *et al.*, 1983). In *Trichoderma atroviride*, blue light activates conidiation (Casas-Flores *et al.*, 2004). In the entomopathogenic fungus *Metarhizium robertsii* and the plant pathogenic fungus *Colletotrichum acutatum* visible light increases the production of conidia and the conidia produced in light are more tolerant to UV-B radiation (de Menezes *et al.*, 2015; Rangel *et al.*, 2011). Light inhibits mating and haploid fruiting of the human fungal pathogen *Cryptococcus neoformans* (Idnurm and Heitman, 2005). In the marine fungus *Halorosellinia* sp. (No. 1403), light enhances the growth and the polyketide production in bioreactor cultures (Zhang *et al.*, 2016). In *Monascus ruber*, growth and pigment production are influenced by light intensity (Buhler *et al.*, 2015).

In *Aspergillus nidulans*, light triggers the balance betwwen asexual and sexual development **(Fig. 1A&B)**. In light, more green conidiopores are produced, but in dark sexual fruit bodies are preferentially formed. The biosynthesis of sterigmatocystin (ST) which is a precursor of aflatoxin, is repressed upon light in *A. nidulans* **(Fig. 1C)** (Blumenstein *et al.*, 2005; Purschwitz *et al.*, 2008).

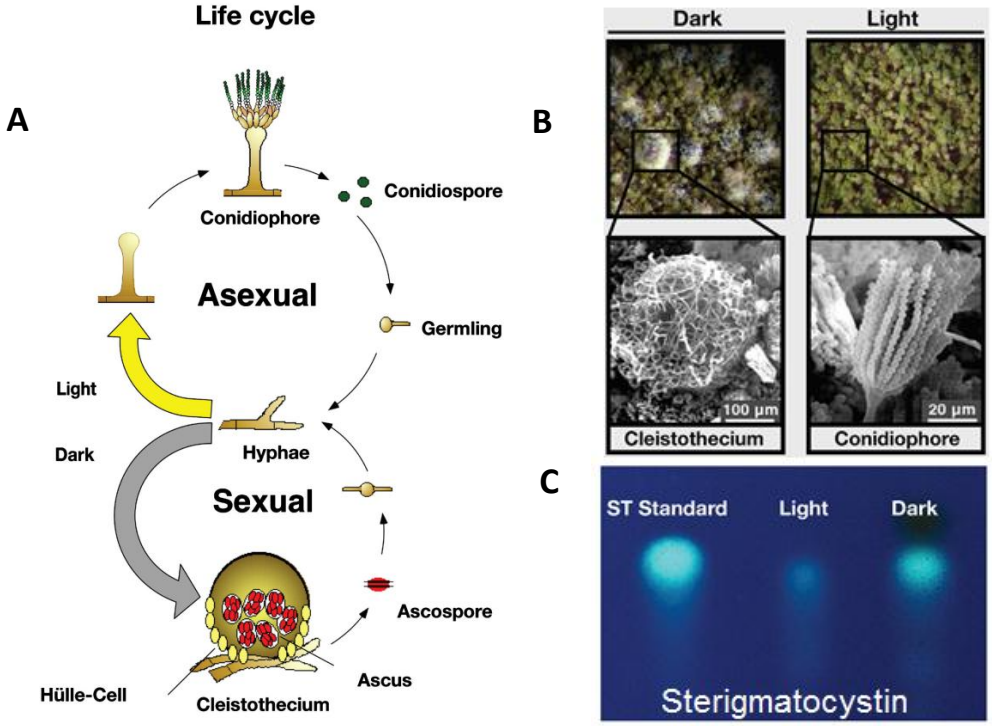

Fig. 1. Light responses in *A. nidulans*. (A) Light promotes asexual development and inhibits sexual development. **(B)** In dark, more cleistothecia are formed, while conidiospores dominate in light. **(C)** Sterigmatocystin (ST) synthesis is repressed in light. ST were detected with thin layer chromatography (TLC) (Bayram *et al.*, 2010).

1 The light perception apparatus

1.1 Red light receptor phytochromes in plants, fungi and bacteria

Fungi perceive external light signals by employing different photoreceptors. *A. nidulans* senses red light, which was first reported in 1990 (Mooney and Yager, 1990). Red light induces conidiation in *A. nidulans*, whereas far-red light represses it. The *brlA* gene, encoding a regulator of conidiophore development, was activated in red light. These findings suggest the existence of fungal red light receptor. In comparison to the study of fungal red-light sensing, however, research on red light perception in plants had started already in 1950s (Butler *et al.*, 1959) and the red light receptor was named phytochrome in 1960 (Borthwick and Hendricks, 1960). In 1990s, phytochromes outside the plant kingdom were reported in cyanobacteria *Synecbocystis PCC6803* and *Fremyella adiplosipbon* (Kaneko *et al.*, 1996; Kehoe and Grossman, 1996; Lamparter *et al.*, 1997). Several years later, phytochrome-like proteins were discovered in heterotrophic bacteria *Deinococcus radiodurans* and *Pseudomonas aeruginosa* (Bhoo *et al.*, 2001; Davis *et al.*, 1999). Before long, spectroscopic evidence for phytochrome-like proteins in *Physarum polycephalum* was obtained (Lamparter and Marwan, 2001). In 2005, the complete phytochrome-like sequences in the fungal genomes of *N. crassa*, *Aspergillus fumigatus* and *A. nidulans* were identified (Karniol *et al.*, 2005). In the same year, the function of phytochrome (FphA) in *A. nidualns* was analyzed (Blumenstein *et al.*, 2005). These findings imply that the evolution of phytochromes has undergone millions of years before the emergence of plant phytchromes. However, the cyanobacterial or non-cyanobacterial origin of canonical plant phytochrome is still under debate (Buchberger and Lamparter, 2015; Karniol *et al.*, 2005; Kooss and Lamparter, 2016; Li *et al.*, 2015; Rottwinkel *et al.*, 2010).

Phytochromes are dimeric proteins in which a conserved cysteine residue covalently attaches a linear tetrapyrrole, bilin, serving as a chromophore. The bound bilin undergoes a reversible photo-isomerization in response to red and far-red light resulting in structural changes of phytochrome **(Fig. 2)** (Abe *et al.*, 1985; Bae and Choi, 2008). Assembled with bilin, phytochrome is ready to absorb red light (666 nm). This form is called Pr form and is considered as biologically inactive form. After the absorption of red light, the Pr form is converted to the Pfr form, ready to absorb far red light (730 nm), and considered as biologically active form. All plant phytochromes comprise an N-terminal photosensor domain and a C-terminal domain **(Fig. 3)**. The sensor domain contains four subdomains, two PAS (Per-ARNT-Sim) domains (designated as P1 and P2), one GAF domain and one PHY (Phytochrome) domain **(Fig. 3)**. The P1 domain of plant phytochrome PHYA regulates the stability of the Pr and the Pfr form. However, the P1

domain is unnecessary for plant phytochrome PHYB (Wagner *et al.*, 1996). Truncated *Arabidopsis* PHYB (lacking the first 57 amino acids) has full activity. P2 and GAF domains compose the photosensor domain, which is conserved in most plants and responsible for binding the chromophore to the conserved cysteine residue in GAF domain (Lamparter *et al.*, 2004). P2 and GAF are both necessary for the function of the photosensing and deletion of either of them results in a nonfunctional photosensor domain. The crystal structure shows the P2 and GAF domains in *Deinococcus* bacteriophytochrome are tightly linked by a trefoil knot (Wagner *et al.*, 2005; Wagner *et al.*, 2007). The C-terminal domain comprises three subdomains, the PAS-A, PAS-B and the histidine kinase related (HKRD) domains **(Fig. 3)**, which is inactive (Boylan and Quail, 1996). Plant phytochromes dimerize through a dimerization motif, which overlaps part of PAS-A and PAS-B domains. This region also contains a nuclear localization site (NLS). P1, PAS-A and PAS-B domains are unique in plants and the function of P1 domain differs in different plants (Bae and Choi, 2008; Boylan and Quail, 1996).

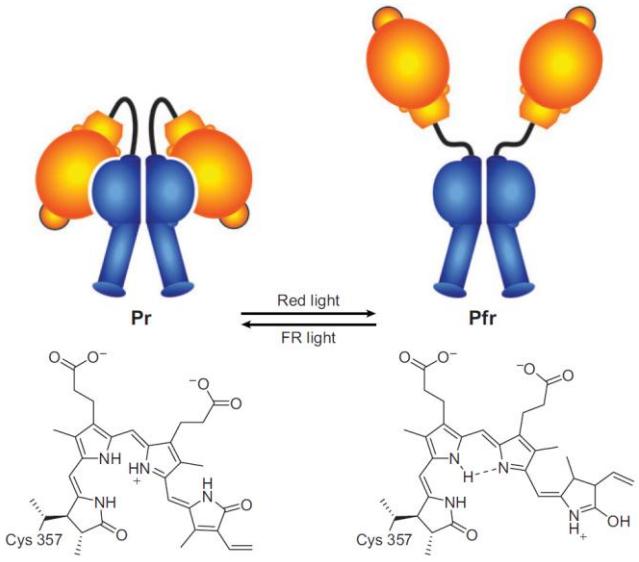

Fig. 2. Conformation change of plant phytochrome caused by photoisomerization of phytochromobilin upon red and far-red light. Dimeric phytochromes covalently bind phytochromobilin, a linear tetrapyrrole bilin compound. The phytochromobilin undergoes photoisomerization at C15-C16 double bond upon red light (666 nm) and far-red light (730 nm), which results in the conformation change of phytochrome between Pr and Pfr forms. In red light, Pr is converted to Pfr that is considered biologically active. In dark or far-red light, Pfr is converted to Pr that is considered biologically inactive (Bae and Choi, 2008).

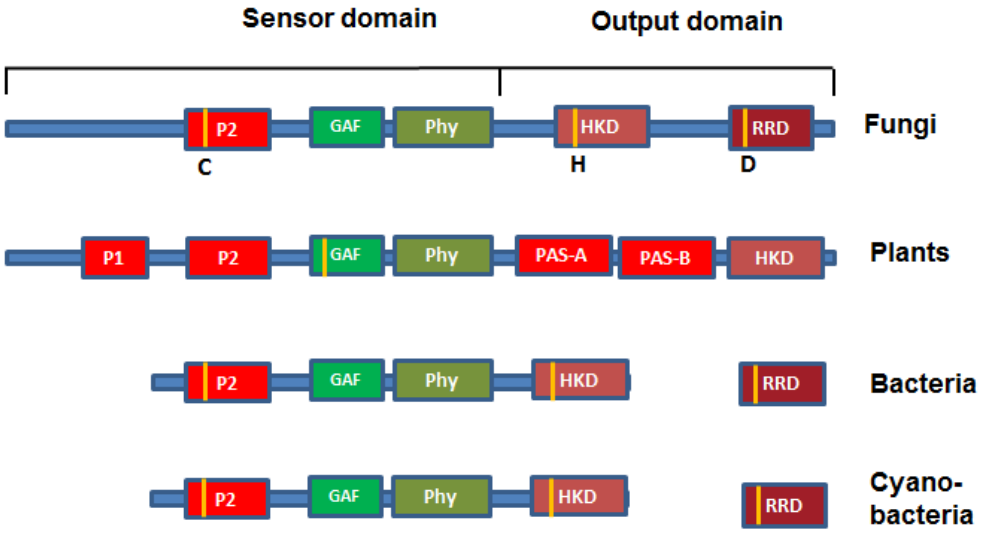

Fig. 3. Domain structure of phytochromes in fungi, plants and bacteria. P1, P2, PAS-A and PAS-B all belong to PAS (Per-ARNT-Sim) domains; GAF, GAF domain (vertebrate cGMP-specific phosphodiesterases, cyanobacterial adenylate cyclases, and formate hydrogen lyase transcription activator FhlA); Phy, phytochrome domain; HKRD, histidine kinase domain; RRD, response regulator domain.

The photosensor domain of phytochrome in fungi and bacteria comprises P2, GAF and PHY domains, but lacking the P1 domain **(Fig. 3)**. The first reported phytochrome in fungi is *A. nidulans* phytochrome FphA (Blumenstein *et al.*, 2005). Similar phytochrome-like proteins also exist in several other ascomycetous fungi such as *A. fumigatus*, *Gibberella moniliformis*, *N. crassa*, and the basidiomycetes *Ustilago maydis*, and *Cryptococcus neoformans* but not in *Saccharomyces cerevisiae*, *Schizosaccharomyces pombe*, *Candida albicans* or *Ashbya gossypii*. In *A. nidulans*, the Pr form is initially synthesized in the dark, absorbs maximally at 705 nm and turns into the Pfr form (758 nm absorption maximum) (Blumenstein *et al.*, 2005; Brandt *et al.*, 2008). The N-terminus varies from plant phytochromes, because it consists of a variable extension and is responsible for the stabilization of the Pfr form (Brandt *et al.*, 2008). Instead of being bound to the conserved cysteine residue in the GAF domain as in plants, the chromophore is bound to the conserved cysteine residue in P2. The fungal output domain contains a HKRD and a response regulator domain (RRD) **(Fig. 3)**. Bacterial phytochromes have no RRD, but they have corresponding response regulators (RRs) **(Fig. 3)**. To date only for the *A. nidulans* FphA a light-driven histidine kinase activity has been shown. The autophosphorylation activity strongly depends on red light (Brandt *et al.*, 2008). Although the Pfr form appears to be an active histidine kinase, the Pr form has also weak autophosphorylation activity. Phosphoryl group transfer from the histidine residue (H770) in the HKRD to the aspartate residue (D1181) in the RRD has been

demonstrated (Brandt *et al.*, 2008). Deletion of phytochrome in *A. nidualns* leads to a slight reduction of conidiation, but facilitates sexual development in light and ST production (Purschwitz *et al.*, 2008). This implies phytochrome balances asexual and sexual development and inhibits ST production.

In N. crassa, two orthologues of phytochrome, PHY-1 and PHY-2, have been identified (Borkovich *et al.*, 2004). PHY-2 has chromphore binding abilibty *in vitro* and PYH-1 exclusively localizes in the cytoplasm (Froehlich *et al.*, 2005). *phy-1* and *phy-2* mutants do not demonstrably show global changes of light-inducible gene expression (Chen *et al.*, 2009). However, *con-10* mRNA accumulates in the PHY-2 mutant, implying a small subset of genes probably regulated by PHY2 (Olmedo *et al.*, 2010). The expression of *phy-1* and *phy-2* is independent of light, but the expression of them is higher in late sexual development than in early sexual development (Wang *et al.*, 2016). And light mediates the initiation of sexual development through phytochromes. Protoperithecial development commences earlier in *phy-2*-deletion strain, when cultured under red light, implying the negative regulatory role for sexual development (Wang *et al.*, 2016). Phytochromes are likely to balance asexual and sexual development in *N. crassa* as in *A. nidulans* (Purschwitz *et al.*, 2008; Wang *et al.*, 2016).

1.2 White collar complex (WCC)

N. crassa perceives blue light with the blue light senor white collar-1 (WC-1) that forms heterodimer with white collar 2 (WC-2) in the White-Collar-Complex (WCC) (Ballario and Macino, 1997; Ballario *et al.*, 1996; Linden and Macino, 1997). WC-1 utilizes FAD (flavin-adenine dinucleotide) as chromophore (Froehlich *et al.*, 2002; He *et al.*, 2002). Upon illumination, its LOV (Light-Oxygen-Voltage) domain covalently binds FAD at the conserved cysteine residue (Cheng *et al.*, 2003). Additionally, WC-1 harbors a GATA type zinc-finger DNA binding domain (ZF) and two PAS domains **(Fig. 4)**, which modulate protein-protein interactions (Ballario *et al.*, 1998; Ballario *et al.*, 1996; Lee *et al.*, 2003). WC-1 forms a heterodimer with WC-2 via the PAS domain (Ballario *et al.*, 1998). WC-2 also contains a ZF domain in the C-terminus (Cheng *et al.*, 2002; Collett *et al.*, 2002; Linden and Macino, 1997).

The orthologues of WC-1 and WC-2 in *A. nidulans* are LreA and LreB, respectively (Purschwitz *et al.*, 2008). They have the same domain organization as WC-1 and WC-2. The 836 amino acid long LreA has a LOV domain, two PAS domains, a NLS, and a ZF domain at the C-terminus **(Fig. 4)**. The 417 amino acid long LreB has a PAS domain, a NLS and a ZF at the C-terminus. Different to the important role of the WCC in the *N. crassa* light response, deletion of *lreA* or *lreB* does not abolish the light-inducible conidiation. Deletion of *lreA* or *lreB* leads to enhanced conidia production both in dark and in light. *lreA*- and *lreB*-deletion strains also show a defect in the formation of

cleistothecia and the synthesis of ST (Purschwitz *et al.*, 2008). Therefore, the WCC of *A. nidulans* slightly represses asexual development and promote sexual development and ST production.

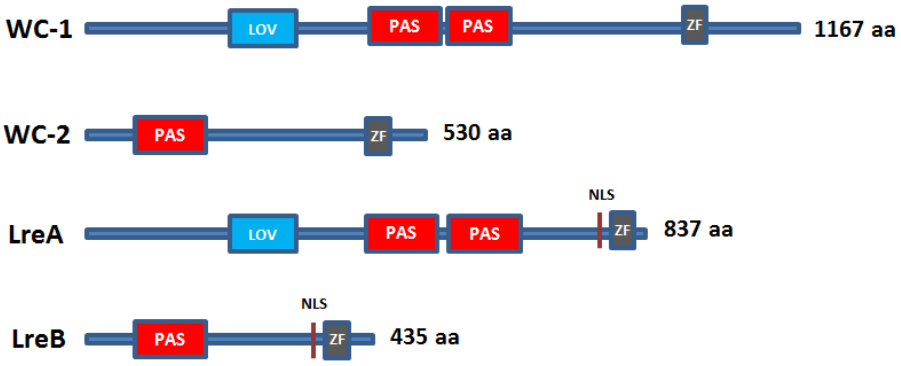

Fig. 4. Domain organization of *N. crassa* WC-1 and WC-2, and *A. nidulans* LreA and LreB. The bule-light receptors WC-1 and LreA both harbor a LOV (Light-Oxygen-Voltage) for FAD (flavin-adenine dinucleotide) binding, two PAS (Per-ARNT-Sim) domains for protein interactions, and a GATA type zinc-finger DNA binding (ZF) domain. WC-2 and LreB both contain a PAS and a ZF domain.

In *Trichoderma atroviride*, the homologs of WC-1 and WC-2, Blr1 and Blr2 are essential for light-induced conidiation (Casas-Flores *et al.*, 2004). Proteomic analysis in the *blr1*-deletion strain revealed many of down-regulation proteins in the dark, while in the *blr2*-deletion strain up-regulation of proteins in dark is predominant, suggesting Blr1 functions independent of Blr2 (Sanchez-Arreguin *et al.*, 2012).

1.3 Cryptochromes in fungi

Cryptochromes are the blue-light receptors regulating circadian clock, growth and development in higher eukaryotes and presumably evolved from DNA photolyase protein family (Bayram *et al.*, 2008a; Liu *et al.*, 2016; Ono *et al.*, 2013; Pedmale *et al.*, 2016). Photolyases and cryptochromes are widely distributed in eubacteria, archaea and eukaryotes (Bayram *et al.*, 2008a; Cashmore *et al.*, 1999; Sancar, 1994; Todo *et al.*, 1996). DNA photolyases (DNA repair enzymes) use blue light to repair DNA damages (cyclobutane pyrimidine dimers (CPDs) and 6-4 pyrimidine pyrimidone photoproducts). Photolyases together with cryptochromes form the cryptochrome/photolyase superfamily that is composed of six subgroups: class I CPD photolyases; class II CPD photolyases; animal cryptochromes ((6-4) photolyases); plant cryptochromes; and CRY-DASH proteins (Bayram *et al.*, 2008a; Daiyasu *et al.*, 2004; van der Schalie and Green, 2005). CPD photolyase absorbs a photon (blue light) which causes the excitation of an electron from the cofactor FAD. The excited electron is transferred to the CPD bound by the

enzyme and the damaged DNA is repaired by CPD cleavage (Sancar, 1994; Sancar, 1990). Cryptochromes are mainly characterized by an N-terminal photolyase-related (PHR) domain and C-terminal region of varying length. PHR is conserved in cryptochromes and harbors the cofactor FAD responsible for the electron transfer. In *A. nidulans*, only one photolyase/croptochrome-encoding gene *cryA* was identified. CryA belongs to the class I CPD photolyases and exhibits DNA repair acivity. However, beyond being a DNA repair enzyme, CryA inhibits sexual development by repressing the expression of regulator encoding genes related to fruiting body formation (Bayram *et al.*, 2008a). *N. crassa* CRY-1 is a DASH-type cryptochrome that can bind single- and double-stranded DNA (ssDNA and dsDNA, respectively), ssRNA and dsRNA *in vitro* (Froehlich *et al.*, 2010; Selby and Sancar, 2006). Deletion of *cry-1* does not change global gene expression (Chen *et al.*, 2009), but perhaps changes the expression of a small subset of genes (Olmedo *et al.*, 2010). In *T. atroviride*, cryptochrome/photolyase genes regulate the expression of *blr1*-independent genes and the deletion of *cry1* leads to a drastic reduction of photoreactivation capacity, as well as a change of gene expression upon blue and red light illumination (Garcia-Esquivel *et al.*, 2016).

1.4 Opsins

Opsins are a group of membrance-embeded proteins with seven transmembrane helices and bound retinal as chromophore (Brown, 2004). *N. crassa* opsin NOP-1 binds retinal and undergoes a slow photocycle and with long-lived intermediates (Bieszke *et al.*, 1999a; Bieszke *et al.*, 1999b). *nop-1* is a light-inducible gene and the mRNA accumulates during asexual and sexual development, but not during vegetative growth (Bieszke *et al.*, 1999a; Wu *et al.*, 2014). It has been suggested that NOP-1 regulates mRNA accumulation of a subset of genes regulated by light and conidiation (Bieszke *et al.*, 2007; Olmedo *et al.*, 2010). *A. nidulans nopA* is predicted to encode an opsin-like protein but *nopA*-deletion strains have no detectible phenotype, and hence the function of *nopA* is still unknown (Ruger-Herreros *et al.*, 2011).

1.5 The LOV-domain protein, VIVID (VVD)

VVD, a blue light receptor, functions in photoadaption of *N. crassa* and the encoding gene *vvd* is an early light-inducible gene (Chen *et al.*, 2010; Heintzen *et al.*, 2001; Hunt *et al.*, 2010; Malzahn *et al.*, 2010; Schwerdtfeger and Linden, 2003). The LOV domain of VVD binds FAD and causes a conformational change upon light exposure(Lamb *et al.*, 2009; Vaidya *et al.*, 2011; Zoltowski and Crane, 2008; Zoltowski *et al.*, 2007; Zoltowski *et al.*, 2009). VVD localizes in the nucleus and physically interacts with WCC to inhibit its transcriptional activity (Hunt *et al.*, 2010; Malzahn *et al.*, 2010). At a certain light intensity, the WCC-mediated light response is attenuated by VVD, which prepares the light

signaling system to respond to stronger light (Heintzen *et al.*, 2001; Schwerdtfeger and Linden, 2001; Schwerdtfeger and Linden, 2003). Colony of *vvd* mutants are bright orange in constant light, suggesting increased carotenoid production and higher activity of the WCC (Heintzen *et al.*, 2001; Schwerdtfeger and Linden, 2003). In *A. nidulans* photoadaption occurs probabaly as well. The *brlA* mRNA accumulation is transient and decreases, when the mycelia are illuminated more than 1 hour (Ruger-Herreros *et al.*, 2011). Photoadaption is also observed in *P. blakesleeanus* (Rodriguez-Romero and Corrochano, 2006; Sanz *et al.*, 2009). However, in *Aspergillus or Phycomyces*, the homolog of VVD has not been found yet (Idnurm *et al.*, 2010; Ruger-Herreros *et al.*, 2011).

1.6 Global regulator of secondary metabolism VelvetA (VeA)

VeA is an interaction partner of FphA (Purschwitz *et al.*, 2009; Rodriguez-Romero *et al.*, 2010) and is well known for its important role in morphogenetic and metabolic pathways by interacting with diverse proteins (Bayram *et al.*, 2008b; Kato *et al.*, 2003; Kim *et al.*, 2002; Sprote and Brakhage, 2007). VeA belongs to the velvet family proteins **(Fig. 5)**, which coordinate development and secondary metabolism (Bayram and Braus, 2012; Bayram *et al.*, 2008b; Park *et al.*, 2014). Besides VeA, the velvet family proteins in *A. nidulans* include VelB, VelC and VosA, regulate sexual development, spore viability and also spore maturation (Ahmed *et al.*, 2013; Bayram and Braus, 2012; Ni and Yu, 2007; Sarikaya Bayram *et al.*, 2010).

The studies on VeA started in the 1960s after a UV-mutagenesis screening (Kafer, 1965). Mutation of *veA* results in a shift from sexual to asexual development even in the dark. Because asexual sporulation is light-independent and the strain grows very well in the drak, the *veA1* mutation was kept in most *A. nidulans* laboratory strains (Adams *et al.*, 1998). The *veA1* gene produces a truncated VeA protein **(Fig. 5)** due to the point mutation in the initiation code ATG (Kim *et al.*, 2002). VeA1 remains mainly cytoplasmic independently of light, whereas wild type VeA accumulates in the nucleus in the dark and localizes mainly in the cytoplasm upon light exposure (Stinnett *et al.*, 2007).

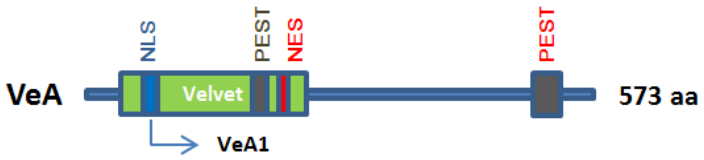

Fig. 5. Structure of VeA in *A. nidulans*. VeA contains a velvet domain (green box), typical for velvet family proteins, a bipartite NLS (blue box), a nuclear export signal (NES) (red box), two PEST (rich in: proline (P), glutamic acid (E), serine (S) and threonine (T)) motifs (black box), which

are typical for proteins with a high turnover and often become phosphorylated. Blue arrow indicates the truncated protein, VeA1 (Rauscher *et al.*, 2016).

VeA interacts with the red light receptor FphA in the nucleus. Although FphA is a hybrid histidine kinase (HHK), deletion of *fphA* does not abolish phosphorylation (Purschwitz *et al.*, 2009). In the dark, VeA, forming a heterodimer with the velvet protein VelB in the nucleus, interacts with the potential methyltransferase LaeA (Bayram *et al.*, 2008b). LaeA is a global regulator of the secondary metabolism in *A. nidulans* (Bok and Keller, 2004). The VelB/VeA/LaeA heterotrimer connects development and secondary metabolism (Bayram *et al.*, 2008b; Sarikaya-Bayram *et al.*, 2015). The other interaction partners identified so far are the methyltransferases VipC, VapB (Sarikaya-Bayram *et al.*, 2014), LlmF (Palmer *et al.*, 2013) and Velvet-interacting protein A, VipA. VipC-VapB methyltransferase heterodimer is tethered to the plasma membrane by the FYVE-like zinc finger protein VapA (Sarikaya-Bayram *et al.*, 2014). Upon certain environmental signals, the VipC-VapB methyltransferase heterodimer is released and enters the nucleus to interact with VeA. VapB methyltransferase diminishes histone 3 lysine 9 trimethylation (H3K9me3) in the nucleus to modulate differentiation. The methyltransferase LlmF is a negative regulator of sterigmatocystin production and asexual development by influencing VeA subcellular localization. Deletion of *limF* leads to accumulation of VeA in nucleus (Palmer *et al.*, 2013). A recent study revealed *A. nidulans* VeA undergoes multi-phosphorylation to trigger developmental processes and ST synthesis. Double mutations of T167 to valine and T170 to glutamic acid in VeA exert most obvious effects on development and *veA* gene expression (Rauscher *et al.*, 2016). These results suggest regulation of the multiple VeA activities by protein interactions, subcellular localizations and phosphorylations.

2 Signal transduction during light signaling in *A. nidulans* and *N. crassa*

2.1 Light signaling in *N. crassa*

In *N. crassa*, more than 31% of expressed genes are affected after exposure to light (Wu *et al*., 2014). The transcription of light-inducible genes is hierarchical (Chen *et al*., 2009). Recently, approximately 400 direct targets of the WCC have been identified by ChIP-seq and 28 of them are transcriptional factors (TFs) (Smith *et al*., 2010). Activated WCC induces early light-inducible genes by directly binding to the promoter of these genes including the TFs encoding genes. TFs further activate downstream genes. For instance, submerged protoperithecia-1 (SUB-1), one of the early light-inducible TFs, is essential for

a large set of the late light-inducible genes (Chen *et al*., 2009). SUB-1 interacts with another transcription factor FF-7 to modulate chromatin modification in combination with WCC (Sancar *et al.*, 2015).

Chromatin remodeling mediates the induction of the light-inducible genes such as *albino-3 (al-3)* and *vivid (vvd)*. A strain with mutated histone H3 (hHK14Q) phenocopies the *wc-1* mutant strain and the light-induction of *al-3* and *vvd* is strongly reduced. The *ngf-1* gene encodes a histone acetyltransferase (HAT), a homologue of the yeast GCN5. *ngf-1* mutants are defective in photoinduction (Grimaldi *et al*., 2006). NGF-1 interacts with WC-1, which is independent of light. Both of them are present at the light-inducible gene promoters in the dark, but the histone tail is inaccessible. Upon illumination, the WCC conformation is changed and NGF-1 acetylates histone H3 giving rise to the induction of light-inducible genes (Brenna *et al*., 2012). On the contrary, methylation of histone H3 represses light-inducible genes. Lack of the methyltransferase DIM-5 causes an increase of the transcription of two light inducible genes, *frq* and *vvd*. In the absence of H3K9me3 under light conditions, WC-2 binding to the pLRE in the *frq* promoter is enhanced (Ruesch *et al*., 2014). FRQ, encoded by *frq* and WCC are the base for the circadian feedback loops. The Clock ATPase CATP associates with the *frq* locus and other target genes of the WCC and facilitates histone removal at these loci to activate clock-dependent gene expression (Cha *et al.*, 2013). SWI/SNF, a nucleosome remodeling complex, interacts with WCC and is required for both circadian remodeling of nucleosome at the *frq* locus and rhythmic *frq* expression. However, the SWI/DNF complex is not required for light induction of the *frq* gene. More likely, the WCC recruits the SWI/DNF complex to activate *frq* expression and thus initiate the circadian clock (Wang *et al.*, 2014).

The WCC binds to the promoter to activate *frq* expression and FRQ along with other proteins can inhibit WCC activity by physically interacting with it (Dasgupta *et al.*, 2016; Froehlich *et al.*, 2002; He *et al.*, 2006; Schafmeier *et al.*, 2008; Tataroglu *et al.*, 2012). During the course of circadian day, FRQ is stabilized and then inactivated through phosphorylation (Baker *et al.*, 2009), resulting in releasing and reactivation of the WCC (Larrondo *et al.*, 2015). Some kinases and phosphatases have been described that modify WCC activities. CK-1a and CK-II phosphorylate and inactivate the WCC in a FRQ-dependent manner and another kinase GSK3 can promote WCC degradation (He *et al.*, 2006; Tataroglu *et al.*, 2012). Phosphatases PP2A and PP4 dephosphorylate and activate WCC (Cha *et al.*, 2007; Schafmeier *et al.*, 2005). Protein kinase A (PKA) and protein kinase C (PKC) repress light-inducible gene expression and the latter interacts with the WCC directly (Cha *et al.*, 2008; Franchi *et al.*, 2005; Huang *et al.*, 2007). The light signaling pathway in *N. crassa* is summarized in Fig. 6 (Dasgupta *et al.*, 2016).

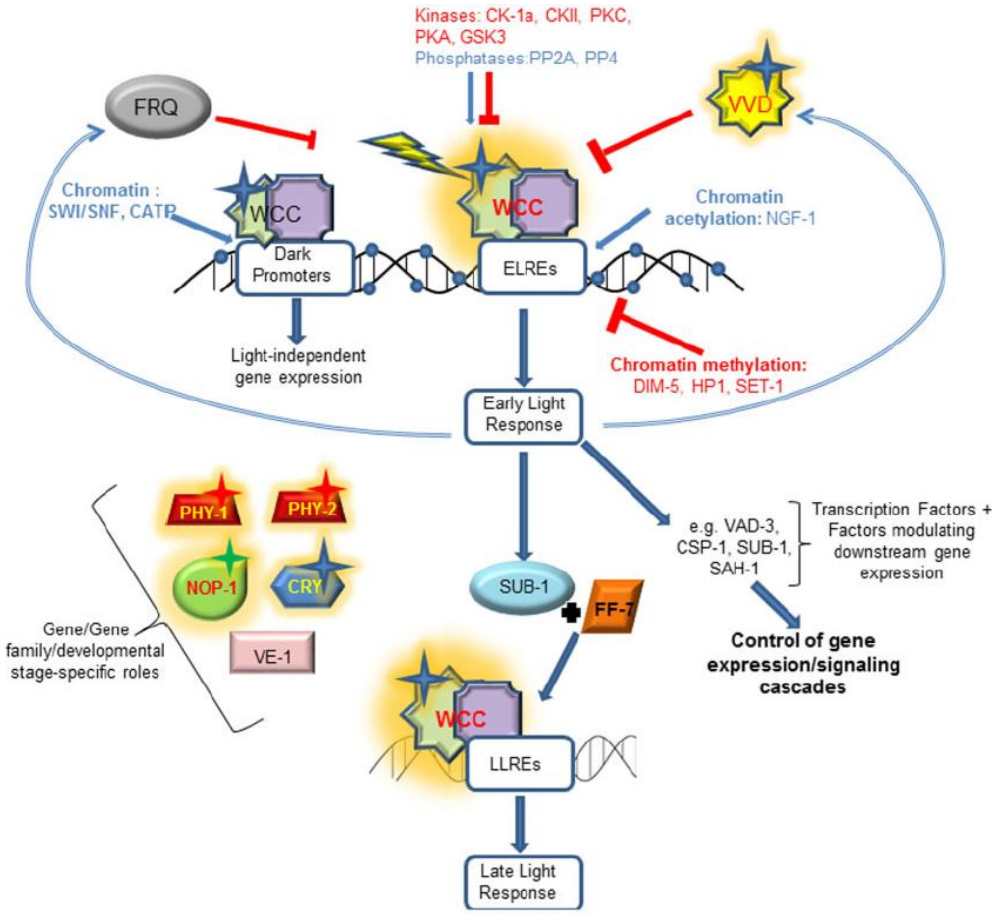

Fig. 6. Model of light signaling in *N. crassa*. WCC transiently binds to early light-responsive emlements (ELREs) in light to induce the expression of early light-responsive genes, such as *sub-1*, *frq*, *vvd* and other transcription factor genes. The transcription factors control the expression of downstream genes. SUB-1 interacts with FF-7 in combination with WCC control late light responses by modulating chromatin remodeling. FRQ inhibits WCC activity rhythmically and VVD forms a dynamic pool with WCC to commence photoadaptation. NGF-1 mediated chromatin acetylation promotes gene expression, whereas chromatin methylation represses light responses. The SWI/SNF complex and CATP modulate light-independent gene expression. Other light receptors (PHY-1, PHY-2, NOP-1 and CRY), and VE-1 likely modulate light responses by controling a small subset of genes (Dasgupta *et al.*, 2016).

2.2 Light signaling in *A. nidulans*

When *A. nidulans* mycelia was exposed to light for 30 min, 425 genes were up-regulated and 108 genes are down-regulated (Ruger-Herreros *et al.*, 2011). Some of the light-inducible genes are predicted to be involved in processes, such as circadian clock, conidiation, carbon metabolism, transport, redox reactions, or stress responses. Some other genes are putative transcription factors that probably play a role in the light signaling pathway. Upon illumination, the master regulator gene of conidiation, *blrA*, is

induced and *blrA* upstream genes, *fluG* and *flbA-C* are up-regulated meanwhile, which explains why light favors conidiation of *A. nidulans*. Two other light-inducible genes are *conJ* and *conF*, homologs of *N. crassa con-10* and *con-6*. These two genes are conserved in filamentous fungi (Suzuki *et al*., 2013). *conJ* and *conF* are induced by short light exposure, but under long-term illumination, the expression level of them is coordinated with asexual development. ConJ and ConF localize in the cytoplasm and partially in the nucleus and contribute to conidia germination and desiccation resistance. *conJ* and *conF* double-deletion strains produce higher cellular amounts of glycerol and erythritol. *ccgB*, a homolog of *N. crassa* clock-control and glucose-repressed gene *ccg-1*, displays the highest induction level among all the light-inducible genes under light conditions (Ruger-Herreros *et al.*, 2011). Intriguingly, *ccgB* appears to be duplicated in the genome of *A. nidulans* but not in other fungi, such as *A. fumigatus* and *A. niger* (Ruger-Herreros *et al*., 2011). The *ccgA* gene together with *conJ* have been used for mechanistic studies of light induction. The induction of *ccgA* is strictly regulated by phytochrome (Hedtke *et al.,* 2015). The light-induction of *ccgA* is completely abolished in *fphA*-deletion strains, whereas the impact of *lreA*- and *lreB*-deletion on *ccgA* induction is minor. In the dark, *ccgA* is partially de-repressed in *veA*-deletion strains. However, FphA doses not bind to *ccgA* promoter directly. Instead, LreA binds to the *ccgA* promoter in the dark and is released from the promoter in light. LreA binding to the *ccgA* promoter is VeA-dependent. VeA binds to the promoter both in the dark and in light, which is in agreement with the repressing role of VeA on *ccgA* expression. VeA binding to the *ccgA* promoter is FphA-dependent. *ccgA* expression is also modulated by histone H3 acetylation. In light, more acetylated hH3K9 is present in the promoter of the *ccgA*, promoting light-induction, whereas in *fphA*- or *lreA*-deletion strains, less acetylated hH3K9 is detected in the promoter. LreA interacts with the acetyltransferase GcnE and with the histone deacetylase HdaA in the nucleus. Based on the study of light-induction of *ccgA*, a light signaling model was proposed **(Fig. 7)** (Hedtke *et al.*, 2015). In the dark, LreA and VeA recruit both GcnE and HdaA to the *ccgA* promoter locus. LreA inhibits GcnE acetylation activity and thus *ccgA* is repressed by de-acetylation. In light, LreA is released from the promoter and VeA and FphA activate GcnE to promote histone acetylation. *ccgA* is induced by light eventually.

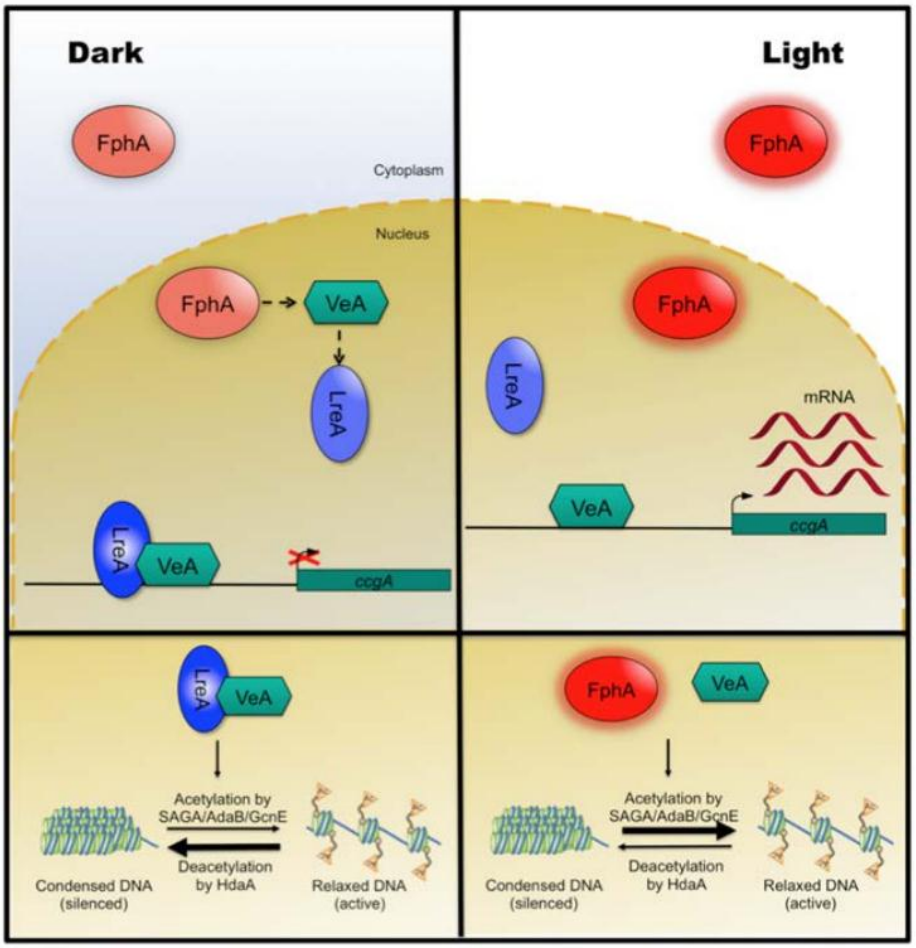

Fig. 7. Proposed model of light signaling in *A. nidulans* based on the studies of the light-inducible genes *ccgA* and *conJ* (Hedtke *et al*., 2015). In the dark, LreA and VeA bind to the *ccgA* promoter and recruit both acetyltransferase GcnE and deacetylase HdaA. The activity of GcnE is inhibited by LreA and thus *ccgA* is silenced. In light, LreA is released from the *ccgA* promoter locus. VeA and FphA promote GcnE activity and *ccgA* is induced eventually.

3 Aim of this project

In previous studies it was shown that many light-inducible genes strictly depend on phytochrome. However, phychrome does not bind directly to the promoters of the light-inducible genes *ccgA,* and although the LreA/LreB dimer and VeA bind to these promoters, the influence on the transcription of *ccgA* is minor. Therefore, the mechanism of light sensing and signaling remained elusive. In this study, we aimed at establishing a screening method to discover novel components involved in light signaling.

Results

1 Screening for *blind* or constitutive-active mutants

1.1 Screening for *blind* mutants

1.1.1 Construction of the parent strain used for UV-mutagenesis

To identify new components involved in light signaling, we tried to establish a smart screening system, which could identify *blind* mutants. To this end, first a parent strain was constructed, in which the selectable marker, *N. crassa pyr4,* was placed under the control of a light-inducible promoter. We anticipated that that should lead to light-dependent growth of the strain on minimal medium lacking uracil and uridine. In *A. nidulans*, over 400 genes were induced when the mycelia was exposed to light for 30 minutes. *conJ* is one of the light-inducible genes and was up-regulated 60 folds **(Fig. 8A)**. The corresponding putative promoter region (2 kb) was used for the construction of the plasmid pZY19, in which *pyr4* was placed under the control of this promoter **(Fig. 8B)**. The plasmid was transformed into wild type (SKV104). The only source for orotidine-5-phosphate decarboxylase was thus the light-controlled *pyr4* gene **(Fig. 8C)**.

As we expected, this strain could grow healthily in light on minimal medium agar without uracil and uridine (U/U) and grew very slowly in the dark **(Fig. 8D)**. When uracil and uridine were added, the parent strain grew like wild type in the dark. When conidia were spread with glass beads on a minimal medium plate without uracil and uridine only small white colonies were formed after three days **(Fig. 8E)**.

To make sure the parent strain still responds well to light and the light-dependent growth was not due to other plasmid-dependent factors, the relative expression of *ccgA*, *conJ* and *pry4* was measured by quantitative real-time PCR. All three genes were up-regulated after exposure to light **(Fig. 8F)**. The transcription patterns of *ccgA* and *conJ* were similar to wild type. These results suggested that growth of the parent strain in light was indeed due to the induction of the *pyr4* gene. The parent strain was used to isolate slow-growing mutants, which were putatively *blind*.

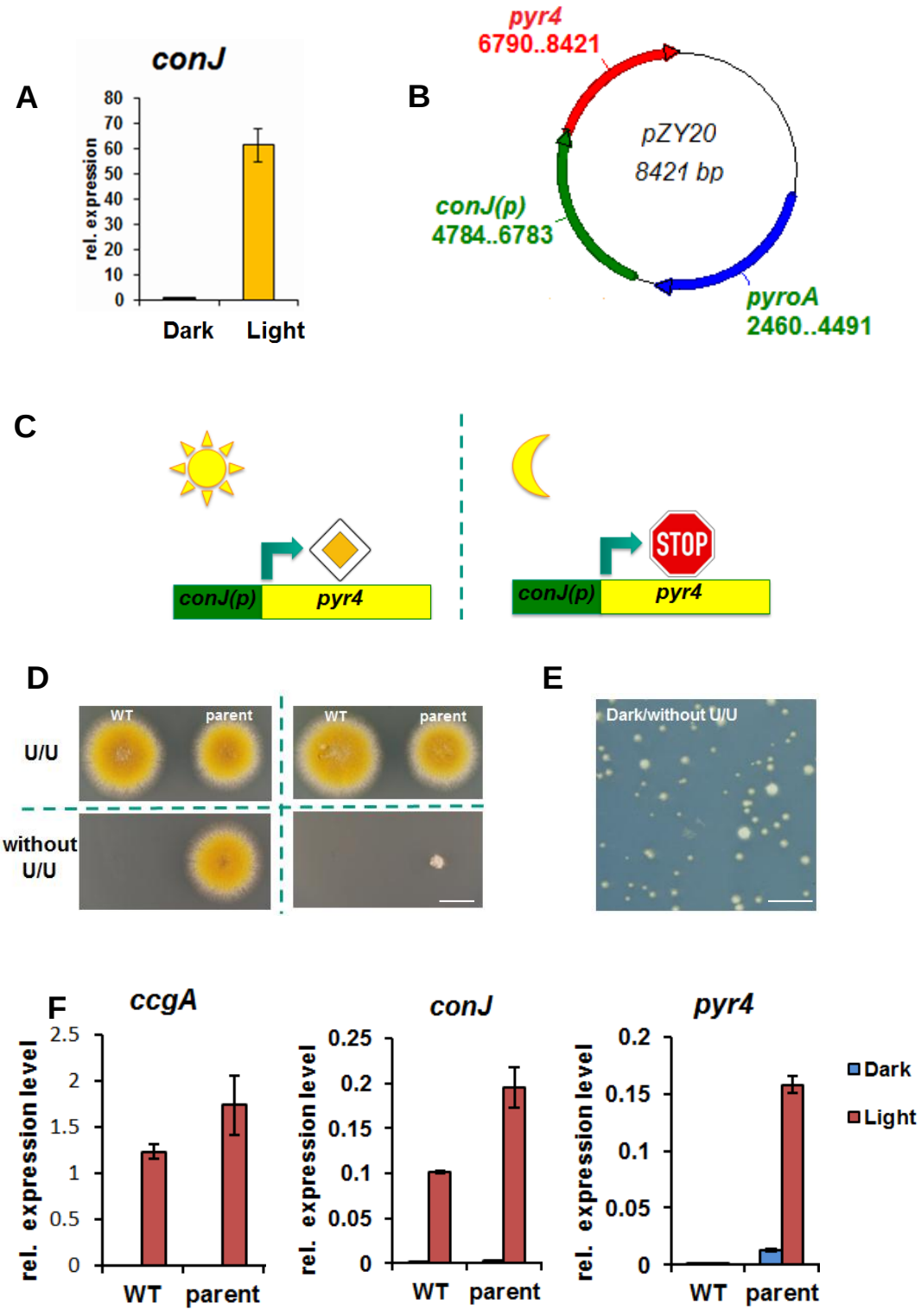

Fig. 8. Construction of the parent strain used for UV-mutagenesis. (A) Expression of the light-inducible gene *conJ* in light. Conidia were incubated on the surface of liquid minimal medium in six plates and cultivated overnight at 37°C in the dark. Three plates were exposed to white light. To purify the RNA, the mycelia was harvested under green light and frozen immediately in liquid nitrogen. The H2B gene was used as reference gene and the expression levels were further normalized to the *conJ* gene in the dark. The error bars represent standard deviations calculated

from three independent biological replicates. **(B)** Map of plasmid pZY20. The plasmid contains the *conJ(p)::pyr4* cassette and the *A. fumigatus pyroA* gene used as selection marker for transformations and crossings. **(C)** Model of *N. crassa pyr4* gene expression under the control of light. Under the control of the *conJ* promoter, the *pyr4* gene is induced in light. **(D)** Phenotype of the parent strain under the control of light. Same amount of conidia were inoculated on supplemented minimal medium with or without uracil and uridine (U/U). The plates were incubated in the dark or in light for three days at 37°C. Scale bar, 1 cm. **(E)** Phenotype of the parent strain grown up from single spores. Conidia were distributed on the minimal medium plate supplemented with PABA and incubated in the dark at 37°C for three days. Only slow-growing colonies were formed. Scale bar, 1 cm. **(F)** Expression of *ccgA*, *conJ* and *pyr4* in the parent strain upon illumination. The illumination experiment and RNA purification were performed as described above. The expression level was normalized to H2B. The error bars represent standard deviations calculated with three independent biological replicates.

1.1.2 Identification of *blind* mutants after UV-light mutagenesis

Our hypothesis was, that mutagenesis of an essential component of light signaling would lead to a failure of the induction of light-inducible genes and thus of the *pyr4* nutritional marker gene. The *blind* mutant was supposed to have a slow-growing phenotype after UV treatment **(Fig. 9A)**. In order to do a UV mutagenesis, the proper UV dose was analyzed first. A fresh conidia suspension was adjusted to 1.2×10^4 conidia/ml. 400 µl conidia suspension were added to Ø 14 cm Petri dish with 100 ml solid minimal medium supplemented with uracil, uridine and PABA. Conidia were distributed evenly using Ø 3 mm glass beads. The plates were irradiated with different doses (0 mJ, 10 mJ, 15 mJ, 20 mJ and 25 mJ) of UV light and incubated for three days in light at 37 °C to calculate the survival rate **(Fig. 9B)**. For the following screening, we chose 15 mJ UV-light to treat the conidia on the plates to get a survival rate of 25%. After UV treatment, the plates were placed in white light and incubated for 3 days at 37 °C. Most of the alive conidia grew to normal sized colonies and few slow-growing colonies were formed **(Fig. 9C)**. To eliminate fitness mutants from the slowing-growing mutants, the putative *blind* mutants were transferred to fresh minimal medium plates with or without uracil and uridine. The ones whose phenotype was rescued by uracil and uridine were the putative *blind* mutants **(Fig. 9D)**.

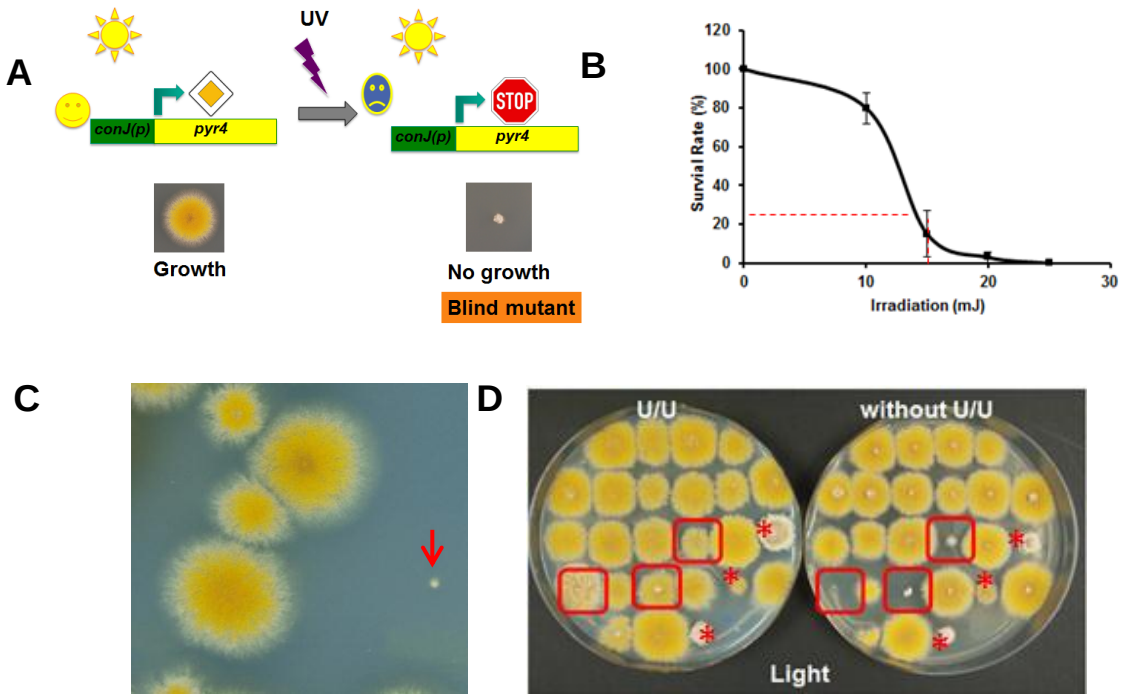

Fig. 9. Screening for putative *blind* mutants after UV-mutagenesis. (A) Strategy of UV-mutagenesis. UV treatment possibly mutates an essential component for light signaling. Some mutants are supposed to grow slowly even in light due to the failure of *conJ(p)::pyr4* induction. **(B)** Survival rate of the conidia after different doses of UV treatment. Survival rates of the conidia after exposure to 0 mJ, 10 mJ, 15 mJ, 20 mJ and 25 mJ UV light were calculated with three biological replicates. **(C)** Phenotype of the putative *blind* mutant on the screening plate after UV-treatment. The slow-growing mutant is indicated with a red arrow. **(D)** Slow-growing colonies were transferred to new plates with or without uracil and uridine to eliminate fitness mutant. The mutants marked with a red box are the putative *blind* mutants. Strains with other fitness defects are labeled with an asterisk (*).

1.1.3 Light response of putative *blind* mutants

During the screening, we obtained approximately 32,000 survivors and among them, 476 mutants, which formed small colonies on minimal medium in light. Of these, only five grew to normal sized colonies on medium supplemented with uracil and uridine **(Fig. 10A)**. In addition, three strains grew better than in the dark, but slower than the other five strains and sporulation of them was impaired **(Fig. 10A)**. The other slow-growing colonies probably had mutations in other pathways, which impaired hyphal growth.

In order to distinguish a mutation in the *conJ* promoter or the inserted *pyr4* gene from a mutation in a gene encoding an upstream regulator of *conJ*, the expression of the endogenous *conJ* gene and a second light-inducible gene, *ccgA*, was quantified by real time PCR. The values were normalized to the constitutive H2B (histone) gene. In seven

strains both genes were not light inducible, whereas in mutant M17-3 light induction was not affected **(Fig. 10B)**. Thus seven blind mutant strains were isolated. Mutant M17-3 may harbor mutations in the *conJ(p)::pyr4* cassette.

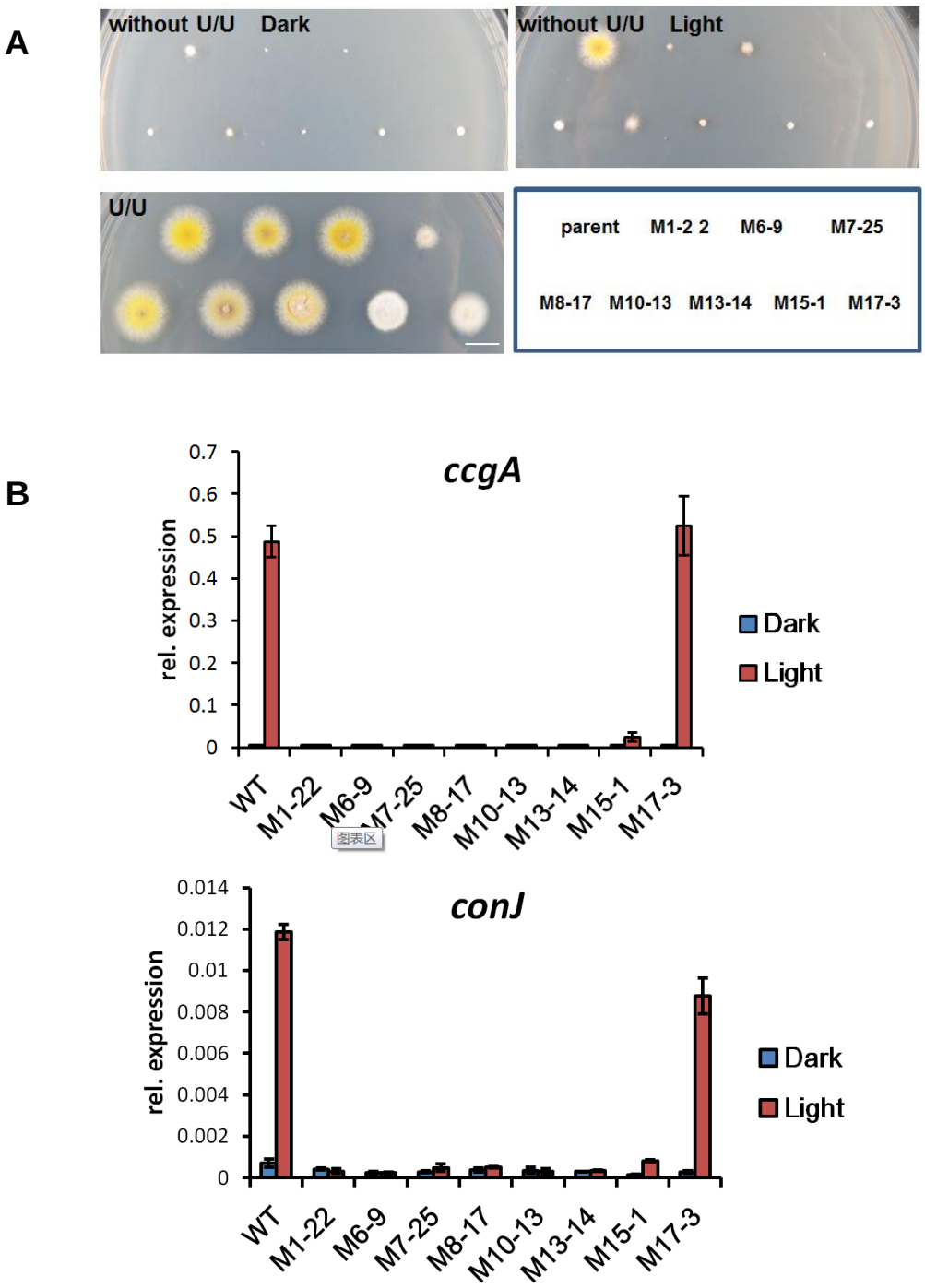

Fig. 10. Light response of putative *blind* mutants. (A) Phenotype of the parent strain and the *blind* mutants in response to light. Same amounts of conidia were inoculated on supplemented minimal medium with or without uracil and uridine (U/U). The plates were incubated in the dark or in light for three days at 37°C. Lower right box indicates the name of the strains. Scale bar, 1 cm. **(B)** Expression of *ccgA* and *conJ* in wild type and the mutants. Fresh conidia were inoculated on

the surface of supplemented liquid minimal medium and cultured 18 h in the dark at 37°C. The mycelia were harvested under green light conditions directly or after 30 min illumination with white light and frozen in liquid nitrogen for RNA isolation. The expression levels were normalized to H2B gene. The mean values were calculated from three biological replicates and the error bars represent the standard deviation.

1.1.4 Phytochrome complemented mutant M10-13

Considering the possibility that the phenotype of the *blind* mutants was caused by a mutation in FphA, all mutants were tested for complementation with the *fphA* gene. Mutants were co-transformed with the plasmid pJR17 (pCR2.1-TOPO containing the entire *fphA* gene) and pCK17 (pCR2.1-TOPO containing the *pabaA* gene). Indeed, mutant M10-13 was complemented by the *fphA* gene, and the strain grew well in light in the absence of uracil and urindine **(Fig. 11A)**. In order to determine the mutation in *fphA* causing the loss of function, the *fphA* gene was amplified from mutant M10-13 genomic DNA and sequenced. A deletion of C on position 2308 in the open reading frame of the *fphA* gene was detected, which leads to premature translation termination of *fphA* **(Fig. 11B&C)**. The putative polypetide lacks the essential histidine kinase (HKD) and response regulator domain (RRD). None of the other six mutants could be complemented by *fphA*, suggesting mutations in other genes.

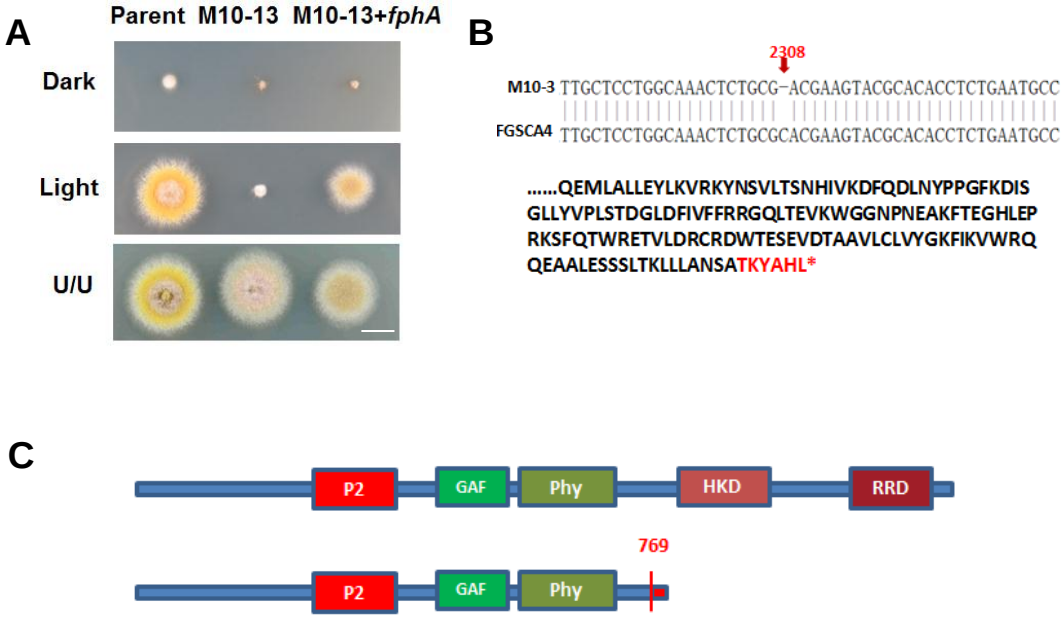

Fig. 11. Phytochrome is mutated in mutant M10-13. (A) The slow-growing phenotype of M10-13 in light is rescued by re-complementation of the strain with the *fphA* gene. M10-3 was co-transformed with the plasmid pJR17 (pCR2.1-TOPO containing the entire *fphA* gene) and

pCK17 (pCR2.1-TOPO containing the *pabaA* gene). Colonies were cultured on supplemented minimal medium for 2.5 days under the indicated conditions. Scale bar, 1 cm. **(B)** Illustration of the mutation in the *fphA* gene. A one-nucleotide deletion was detected. **(C)** Illustration of the frame-shift mutation leading to premature translation termination of *fphA*. The truncated protein lacks HKD and RRD domains.

1.1.5 Identification of the mutation in mutant M6-9 by whole genome sequencing

Mutants obtained after UV mutagenesis are likely to contain several thousands of mutations (Tan *et al.*, 2014). To eliminate background mutations in the *blind* mutants, we crossed them to wild type. Perhaps due to the numerous mutations on the genome after UV-treatment, crossings appeared to be difficult for these mutants. By crossing them to different wild type strains, M6-9 was successfully crossed to wild type SJR3 **(Fig. 12A)**. Therefore, we analyzed mutant M6-9 first, although the crossing of the other mutants also worked after changing the wild type strains. Five progenies of mutant M6-9 were chosen to check the light response by measuring the *ccgA* and *conJ* expression levels **(Fig. 12B)**. In these five progenies, P2-7 and P1-7 were blind to light. P2-7 was crossed to SJR3 again **(Fig. 12A)**. Afterwards, the progeny strains, which grew slowly in the dark on the minimal medium without uracil and uridine were collected.

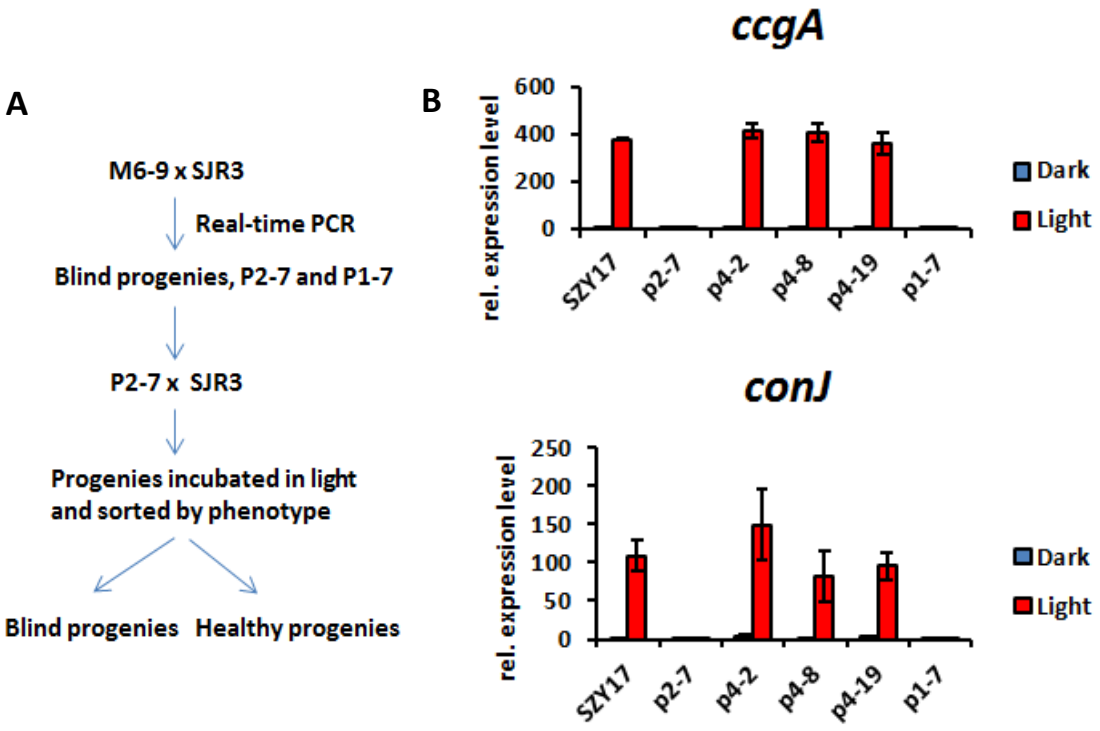

Fig. 12. Elimination of background mutations in mutant M6-9 by crossing it to witd-type. (A) Crossing history of the *blind* mutant M6-9. After the first round of crossing, *conJ* and *ccgA*

expression was checked. The *blind* progeny p2-7 was crossed to wild type once more. The progenies harboring the *conJ::pyr4* cassette were screened on supplemented minimal medium without pyridoxine. The *blind* and healthy progenies were simply distinguished by culturing them on minimal medium plates without uracil and uridine in light. *Blind* progenies showed a slow-growing phenotype under this culture condition. **(B)** Light response of the progenies after the first cross. Five progenies were chosen to check the light response. Illumination experiment and RNA isolation were performed as described above. The expression levels were normalized to H2B. The mean values were calculated from three biological replicates and the error bars represent the standard deviation.

According to the growth phenotype, the collected progeny strains were divided into two groups, 28 *blind* progenies and 28 healthy progenies. All the strains were inoculated on the surface of supplemented liquid medium separately and cultured overnight. Mycelia of seven progenies respectively were mixed and ground in a mortar with liquid nitrogen for genomic DNA purification. Genomic DNA of 28 wild type and 28 mutant progenies was combined respectively and subjected to NGS **(Fig. 13A)**. After alignment of the reads against the reference genome, we checked the depth of coverage along the different chromosomes and could not detect any large insertions or deletions. We thus focused on single nucleotide polymorphisms (SNP). Background mutations present in both the mutant and the wild type strain were first removed. We found two potential frame shift mutations in the genes CADANIAG00003997 and CADANIAG00001630 (located at the genomic coordinate II:379061 and VIII:1735159 respectively) as well as one potential missense variant leading to a P/R substitution at the position II:303934 in the first exon of the CADANIAT00003967 gene. After visual inspection of these 3 potential causative mutations, we could validate that the mutation in the gene CADANIAG00001630 encoding SakA/HogA leads to a frame shift at the amino acid position G111 as a consequence of one nucleotide deletion **(Fig. 13B&C)**.

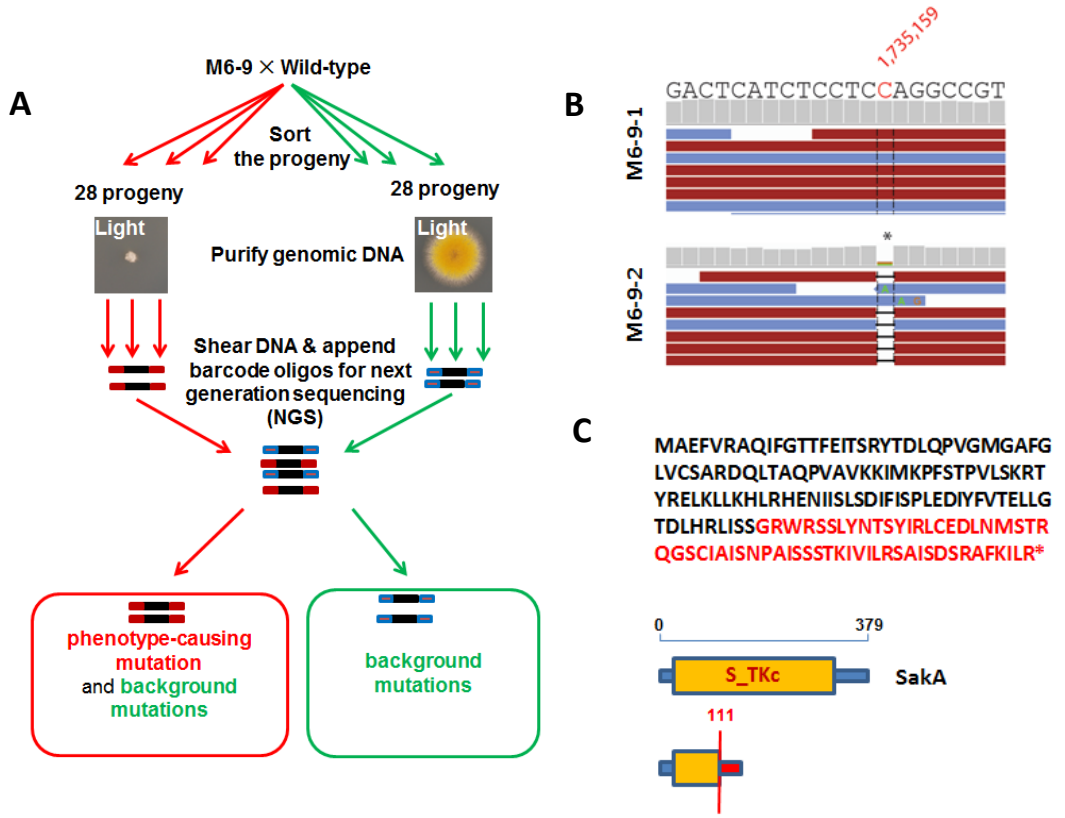

Fig. 13. Identification of the mutation in the mutant M6-9 by whole genome sequencing (NGS). (A) Scheme of identifying the responsible mutation in mutant M6-9 by next generation sequencing (NGS)**.** Fresh conidia were inoculated on the surface of supplemented liquid minimal medium in the plates and cultured overnight at 37 °C. Mycelia from every seven plates were mixed and collected for genomic DNA extraction. The genomic DNA from *blind* and healthy strains were pooled separately. The mixed genomic DNA was subjected to NGS. The responsible mutation was identified by comparing the genome of the two pools. **(B)** A 1 nt deletion was detected in the *sakA* gene. **(C)** The translated protein of the mutated *sakA* gene lacks the kinase domain.

1.2 Screening for constitutive-active mutants (dominant mutants)

1.2.1 Isolation of dominant mutants

Besides the novel components which could activate the light-inducible genes, we presumed that unknown negative regulators exist which repress the activation of light-inducible genes in the dark. The UV-mutagenesis system probably could help to produce some dominant mutants in which the light-inducible genes were constitutively active **(Fig. 14A)**. Therefore, a dominant mutant should grow well in the dark, when uracil and uridine was absent. The negative regulator could be identified in the same way as described above.

To isolate dominant mutants, the same UV-treatment method was performed as described above. After UV-treatment, the plates were incubated in the dark instead of in light for 3 days. Mutants growing faster than the others were picked for further analysis **(Fig. 14B)**. In total, we obtained approximately 6,400 survivors. Surprisingly, more than 100 mutants showed improved growth. Considering that the dominant phenotype was possibly caused by the reverse mutation of the intrinsic *pyrG89* gene, the expression of light inducible-genes was checked. As a first start, only several of them were checked in the by real-time PCR.

Four mutants (MD3-8, MD5-1, MD5-15 and MD6-6) which grew faster than the parent strain in the absence of uracil and uridine in the dark were selected **(Fig. 14C)**. Mutant MD5-15 and MD6-6 grew slower than the parent strain even in the presence of uracil and uridine, suggesting mutations in genes related to vegetative growth. The expression of *ccgA* and *conJ* in all four mutants was checked with real-time PCR **(Fig. 14D)**. In the dark, *ccgA* and *conJ* were induced in mutant MD3-8 and even in light the expression level is up-regulated ~4 folds in comparison to the parent strain, whereas in the other three mutants, the expression patterns were the same as wild type. Therefore, we focused on mutant MD3-8 first and the other mutants were stored for future studies.

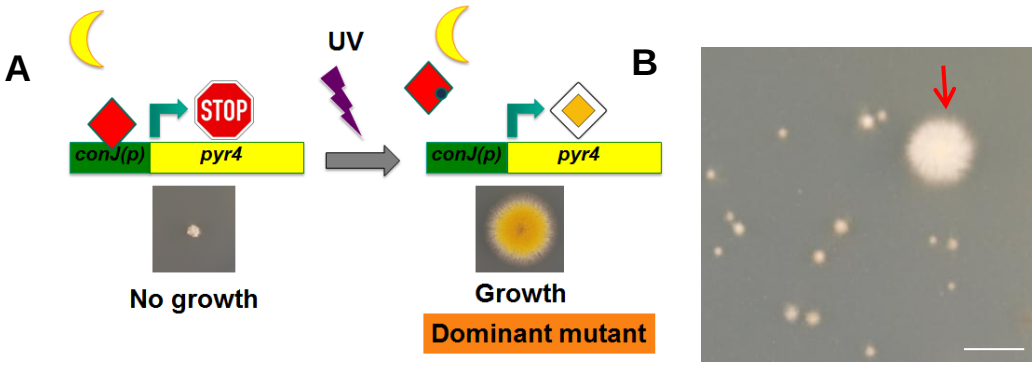

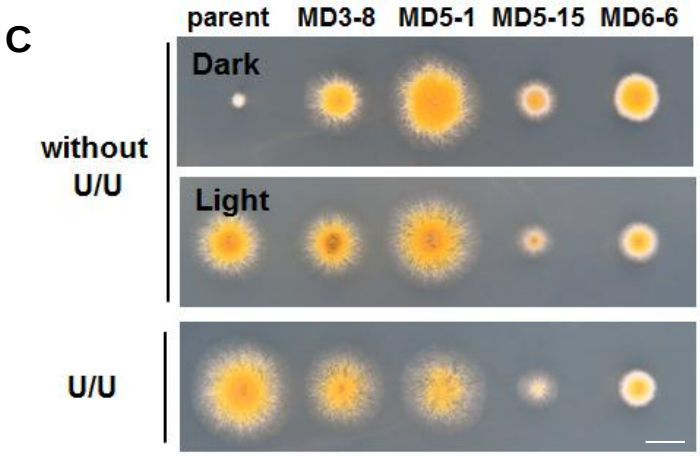

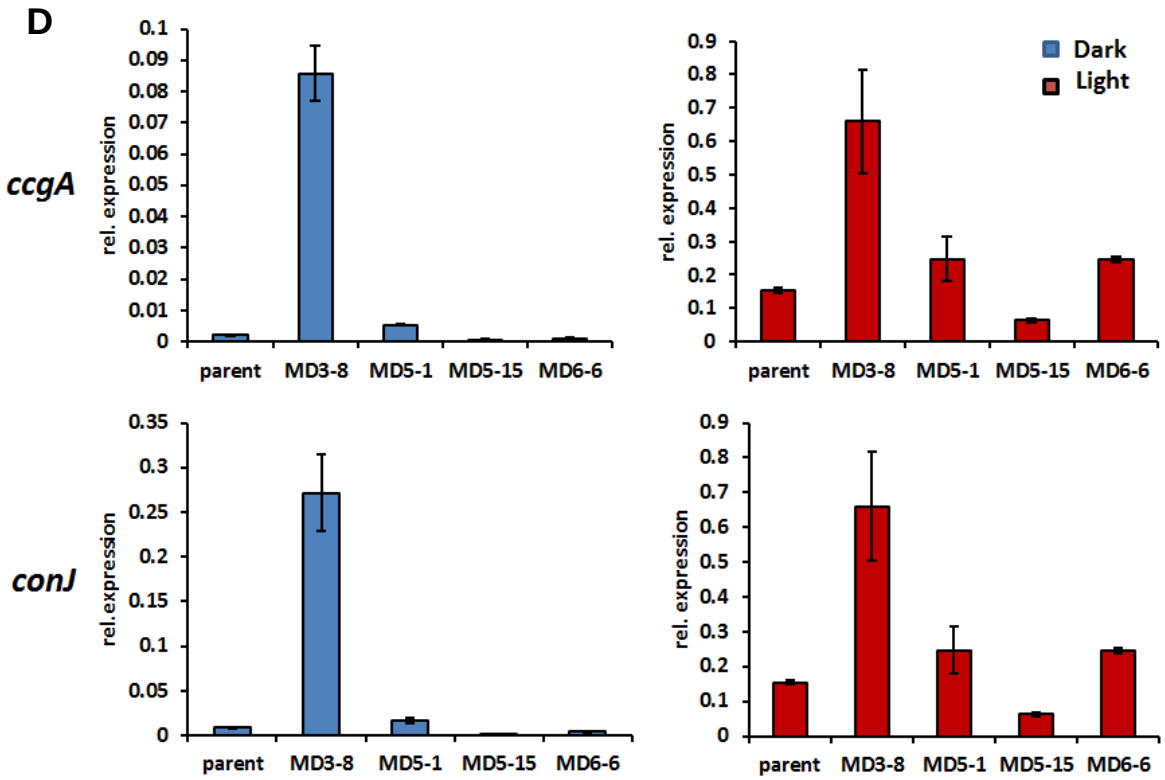

Fig. 14. Screening for dominant mutants. (A) Strategy of screening for dominant mutants by UV-mutagenesis. After UV-treatment, a repressor of a light-inducible promoter is mutated and thus the dominant mutant can grow in the dark independently of uracil and uridine. **(B)** Picture of the colonies obtained after mutagenesis. After the UV treatment, the plates were incubated in the dark for 3 days. Red arrow indicates the putative dominat mutant. Scale bar, 1 cm. **(C)** Phenotype of the dominant mutants (MD3-8, MD5-1, MD5-15 and MD6-6). Conidia of each strain were inoculated on minimal medium with or without uracil and uridine and cultured for 2.5 days in the dark or in light. Scale bar, 1 cm. **(D)** Expression of *ccgA* and *conJ* in wild type and dominant mutants. Fresh conidia were inoculated on the surface of supplemented liquid minimal medium and cultured 18 hours in the dark at 37°C. The mycelia were harvested under green light conditions directly or after 30 min illumination with white light and frozen in liquid nitrogen for RNA isolation. The expression levels were normalized to H2B. The mean values were calculated from three biological replicates and the error bars represent the standard deviation.

1.2.2 Identification of responsible variations in the dominant mutant MD3-8

To eliminate the numerous background mutations, the mutant needed to be crossed several times. However, based on previous experience, the crossing for mutants is different, which might be caused by the multiple mutations. To facilitate crossings, we created some new strains by crossing the parent strain to wild type (SJR3). One strain (SZY64) habored the *conJ::pyr4* cassette and needed arginine to grow. It displayed a

light-dependent growth phenotype on argine supplemented minimal medium agar plate in the absence of uracil and uridine and could be crossed to the mutants that needed PABA easily. After each crossing, all the progeny strains habored the the *conJ::pyr4* cassette and hence it was easier to collect more progenies with different phenotype for genome sequence.

The mutant M3-8 was crossed to SZY64 and the dominant progeny PD-6 was further crossed to the parent strain **(Fig. 15A)**. After two rounds of crossings, we got many progenies, some of which showed the dominant phenotype and some of which did not **(Fig. 15B)**. The progenies were sorted by the phenotype. To test if light-inducible genes were indeed derepressed in dominant progenies we choose two dominant and one normal progeny to check the light response. Indeed, *ccgA* and *conJ* were highly transcribed in two progenies compared to wild type and in the normal progeny *ccgA* and *conJ* still were repressed **(Fig. 15C)**.

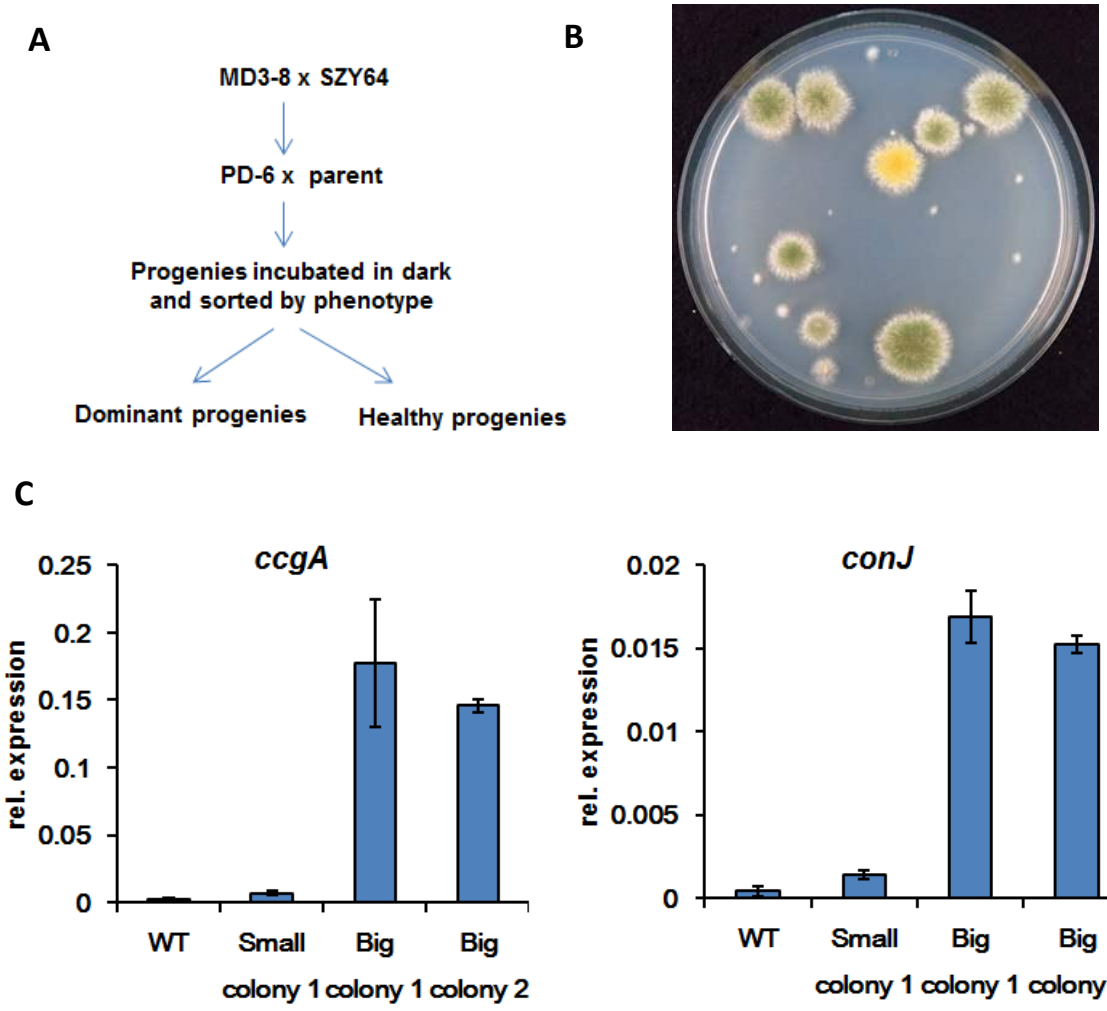

Fig. 15. Elimination of background mutations of mutant MD3-8 by crossing. (A) Crossing history of mutant MD3-8. **(B)** Phenotype of the progenies. After the second round of crossing, the

ascospore suspension was spread on a minimal medium plate without uracil and uridine and cultured 3 days in the dark. **(C)** *ccgA* and *conJ* expression of progenies was checked. After two rounds of crossings, one progeny from wild typle like (small colony 1) and two strains from dominant progenies were cultured for 18 hours in the dark at 37°C and RNA was extracted as described above. The mycelia were harvested under green light conditions and directly frozen in liquid nitrogen for RNA isolation. The expression levels were normalized to H2B. The mean values were calculated from three biological replicates and the error bars represent the standard deviation.

In total, 54 dominant progenies and 35 normal strains were collected. To reduce the work for purifying genomic DNA, the mycelia of the progenies were premixed before grinding as we did above. The genomic DNA was subjected to NGS. By comparing the genome sequences, two single nucleotide substitutions were detected in the gene AN1777 in the MD3-8-1 genome **(Fig. 16A)**. The mutations were not present in MD3-8-2 and the published reference genome. The mutations in MD3-8-1 change an ATG codon at position 1312 to a TAG stop codon, causing premature termination of the translation **(Fig. 16A)**. The gene AN1777 that encodes a protein with an N-terminal PHD (plant homeodomain) finger, a TSF2M, which is found in the central region of transcription elongation factor S-II and a C-terminal SPOC (spen paralog and ortholog C-terminal domain) domain **(Fig. 16B)**. PHD finger-containing proteins are invovled in chromatin remodeling (Aasland *et al.*, 1995; Shi *et al.*, 2007) and the SPOC domain points to the involvement in a transcriptional repression complex (Ariyoshi and Schwabe, 2003). The premature peptide lacks SPOC domain.

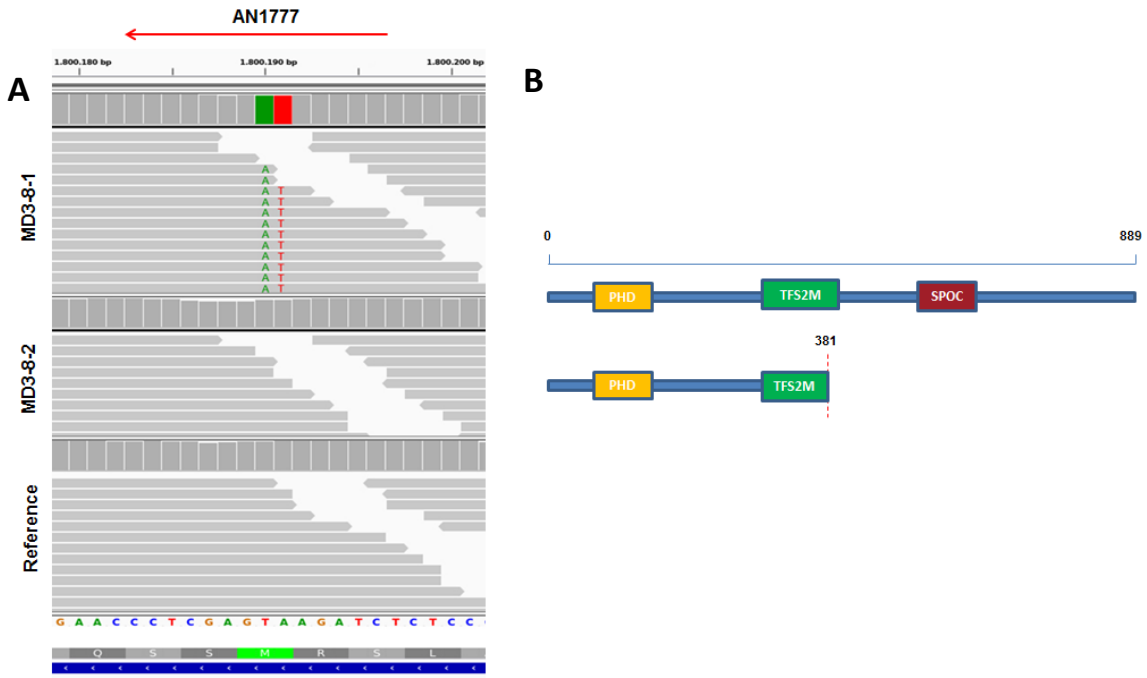

Fig. 16. Identification of the responsible mutation in dominant mutant MD3-8. (A) Illustration of two single nucleotide substitutions in MD3-8-1. **(B)** Structure of the protein AN177 and the premature peptide.

2 SakA pathway involved in light signaling

2.1 The *sakA* gene rescued the light response of mutant M6-1

By whole genome sequencing, we successfully identified the mutation in the *sakA* gene in the mutant M6-9. To confirm it, the mutation should be complemented by a wild-type copy of *sakA.* To this end, the *sakA* gene was amplified from wild-type genomic DNA and ligated to the pJet1.2 vector, yielding pZY21. This plasmid together with pCK17 were co-transformed to M6-9 and the positive transformants were screened by PCR. The transformant harboring the wild-type *sakA* gene grew well on minimal medium without uracil and uridine under light. Indeed, the wild-type *sakA* gene restored the phenotype of mutant M6-9 **(Fig. 17 A)**. Therefore, the mutation in the *sakA* gene in mutant M6-9 is the responsible mutation for the slow-growing phenotype. The MAPK SakA pathway **(Fig. 17B)** is responsible for osmotic and oxidative stress sensing in *A. nidulans*. Therefore, it appears that light signaling and stress sensing at least partially share the same pathway.

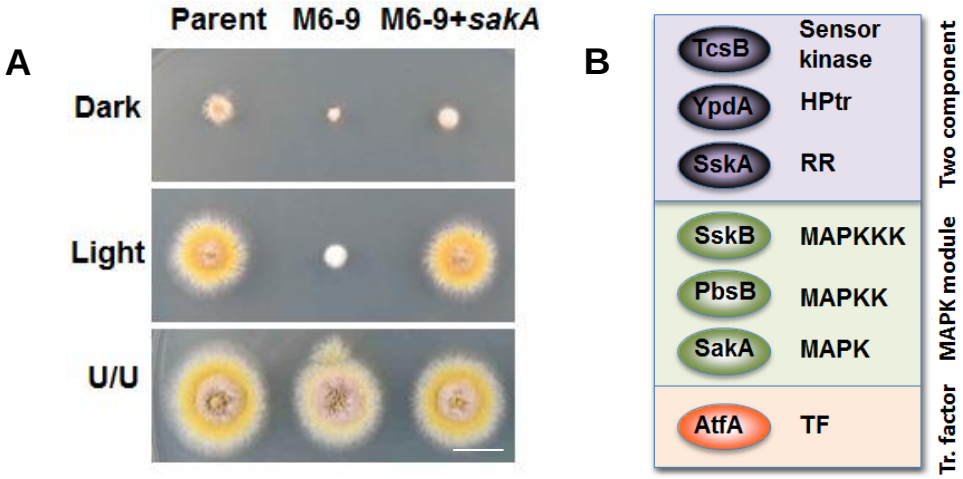

Fig. 17. Impact of the *SakA* signaling pathway on light sensing. (A) Colonies of wild type (SJR2) and the *sakA* mutant strain (SZY31) grown on agar plates for 2 days under illumination conditions. Scale bar, 1 cm. **(B)** Simplified scheme of the two-component system and MAPK module involved in osmo- and stress sensing in *A. nidulans*.

2.2 The SakA pathway is essential for light signaling

To verify whether the light-signaling pathway utilizes other components of the osmosensing pathway, we checked the expression level of *ccgA* and *conJ* upon light induction in *ΔsskA*, *ΔsskB, ΔpbsB, ΔsakA* and *ΔatfA* strains. In these mutants, *ccgA* and

conJ could not be induced anymore **(Fig. 18)**. Since *ypdA* is essential, *ΔypdA* is unavailable (Vargas-Perez *et al.*, 2007).

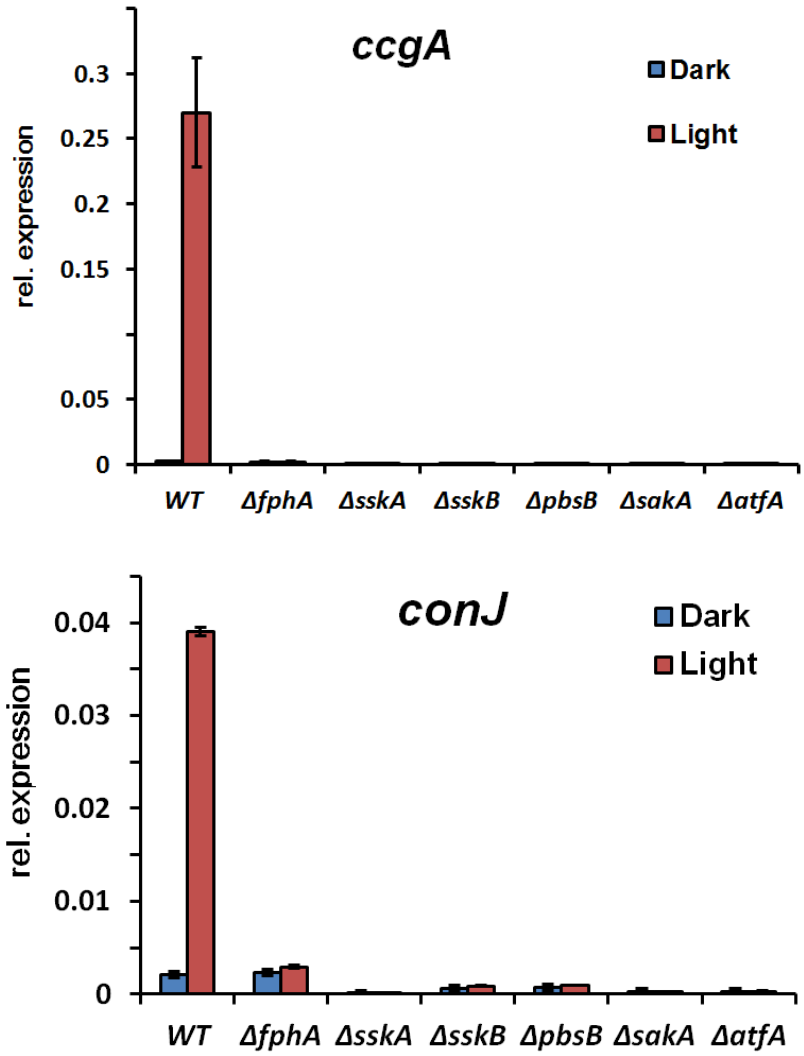

Fig. 18. *ccgA* and *conJ* induction analyzed in different deletion strains. Fresh conidia harvested from wild type (SJR2), *ΔfphA* (SJP1), *ΔsskA* (SZY41), *ΔsakA* (SZY31) and *ΔatfA* (SZY42) were inoculated on the surface of supplemented liquid minimal medium and cultured for 18 h in the dark at 37°C. The grown mycelium was exposed to light or kept in the dark for 30 min and frozen in liquid nitrogen for RNA isolation. The expression levels of *ccgA* and *conJ* were measured by real-time PCR. The mean values were calculated from three biological replicates and the error bars represent the standard deviation.

2.3 Light-inducible genes *ccgA* and *conJ* could be induced by osmotic stress

After the discovery of the link between light and stress signaling, we asked whether the light-inducible genes could be induced under osmotic stress. The wild-type strain was

cultured in the dark for 18 hours and afterwards salt stress was imposed for 30 minutes. The expression levels of *ccgA* and *conJ* were measured by real-time PCR and normalized to the H2B gene. Indeed, *ccgA* and *conJ* were both induced after the osmotic stress was imposed **(Fig. 19A)**. This suggests that growth of the parent strain used for UV mutagenesis should also be able to grow in the absence of light but in the the presence of salt. Furthermore, all *blind* mutants should not be able to grow on such medium if other components of the SakA pathway would be affected. In order to test the other *blind* mutants for defects in salt-stress signaling, we cultured all *blind* mutants in minimal medium supplemented with PABA and 0.5 M NaCl for 3 days at 37 °C in the dark. Only the wild type and M10-13 could grow **(Fig. 19B)**, which suggested that in the other mutants the MAPK SakA pathway was defective.

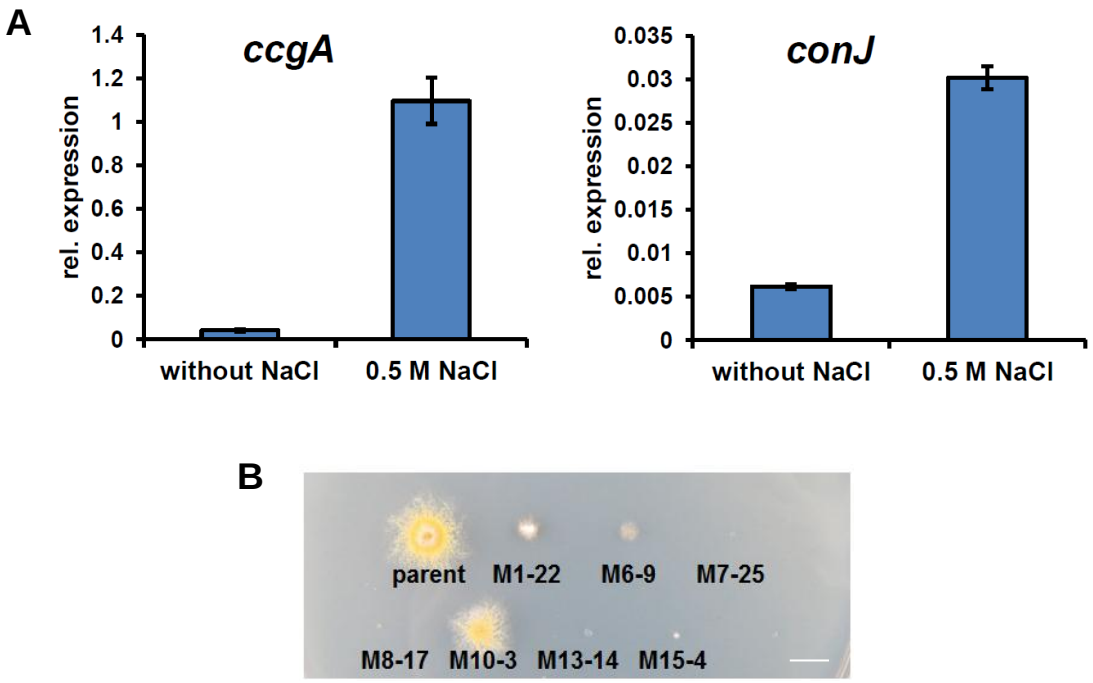

Fig. 19. Expression of *ccgA* and *conJ* and phenotype of the *blind* mutants under salt stress. **(A)** *ccgA* and *conJ* expression was up-regulated under salt stress. Conidiospores (1×10^6 spores/ml) were cultured in 300 ml flasks with 60 ml of liquid supplemented minimal medium at 37 °C shaken at 180 rpm. After 18 hours, 8.6 ml pre-warmed minimal medium with 4 M NaCl, or without NaCl for the control, were added to each flask. After 30 min stimuli, mycelia were collected by filtering through miracloth and frozen immediately in liquid nitrogen for RNA isolation. The mean values were calculated from three biological replicates and the error bars represent the standard deviation. **(B)** Phenotype of the mutants under salt stress. Parent strain and mutant M6-9 grew normally in the dark at 37 °C on supplemented minimal medium containing 0.5 M NaCl without uracil and uridine. The colonies were incubated 2.5 days. Scale bar, 1 cm.

2.4 Mutations found in *pbsB* and *sskB* in M1-22 and M15-1 respectively

After knowing that other components of the SakA pathway could be affected in the other *blind* mutants, we aimed at determining the mutations. To this end we simply amplified the full length of the genes, *sskA*, *sskB*, *pbsB*, *sakA* and *atfA*, and subjected them to sequencing. Some single-base mutations in the *pbsB* gene of mutant M1-22 were detected and these mutations resulted in 9 single amino acid mutations that probably lead to a nonfunctional polypeptide **(Fig. 20A)**. An insertion in *sskB* in mutant M15-1 was detected, which causes a frame-shift mutation. The product of the mutated *sskB* gene produces a premature peptide lacking the intact catalytic domain **(Fig.20B)**.

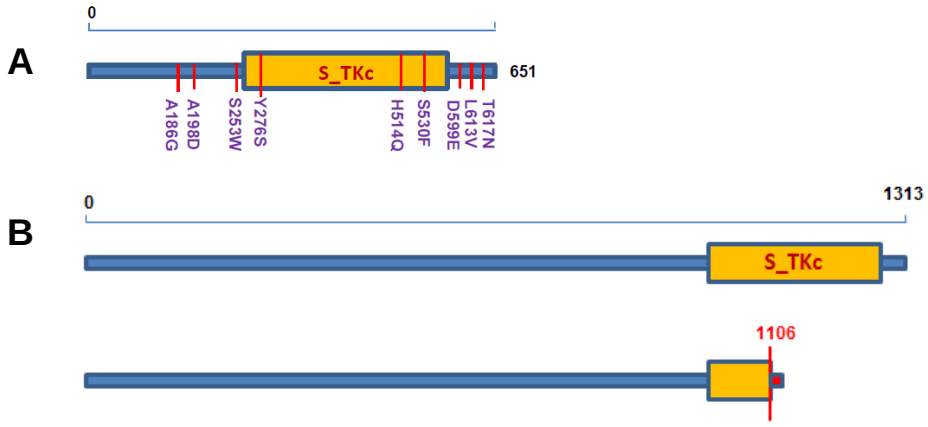

Fig. 20. Variations found in *pbsB* and *sskB* in M1-22 and M15-1 respectively. (A) Several single-base substitutions were detected in the *pbsB* gene in M1-22. **(B)** A one-nucleotide insertion was found in the *sskB* gene in M15-1.

3 Light activation of the SakA pathway depends on phytochrome

3.1 The balance between asexual and sexual development is shifted towards sexual development in the *sakA*-deletion strain

In order to obtain a *sakA*-deletion strain in a *veA* wild-type background, the strain TFLΔsakA-03 was crossed to wild type (SJR3), yielding SZY31. After 2.5 days of culture, the *sakA*-deletion strain had the same colony size with wild type, but produced less green conidia **(Fig. 21A&B)**. Both wild-type and *sakA*-deletion strains produced more conidia in light than in the dark. But the *sakA*-deletion strain only produced 15% of conidia compared to wild type in the dark and 20% in light. With respect to sexual development, sexual development of wild type was repressed in light and production of cleistothecia reduced to 20% compared to dark conditions, while the *sakA*-deletion strain produced the same amount of cleistothecia in light and dark and the same amount as wild type in the dark. Taken together, the results show that the light response in the *sakA* mutant is largely impaired.

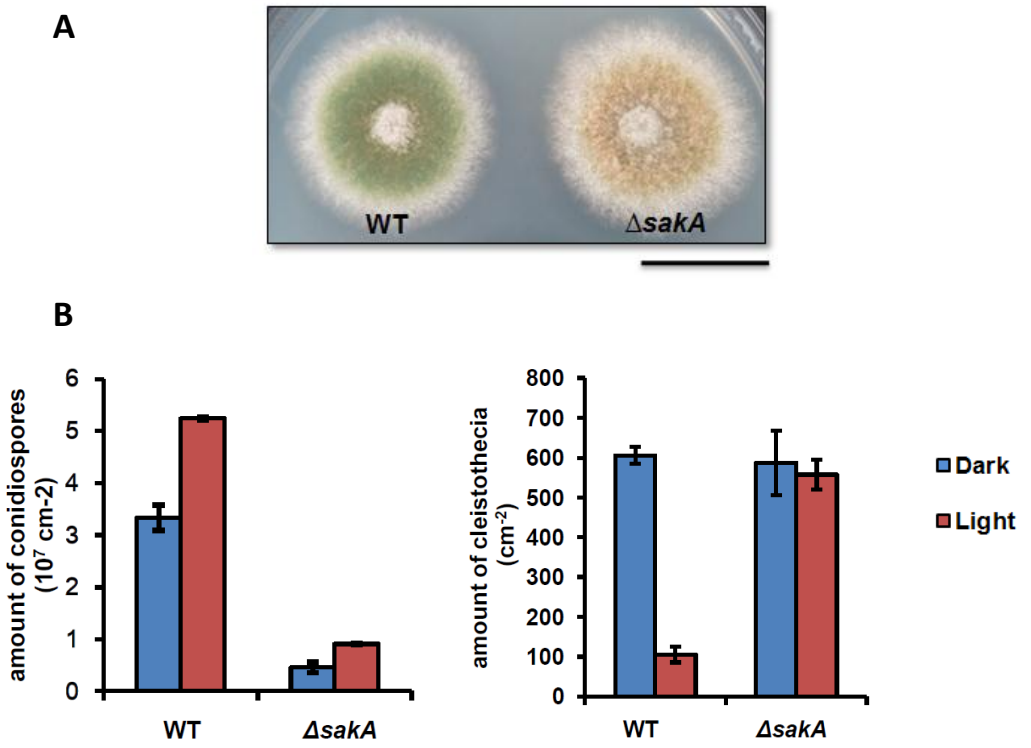

Fig. 21. Vegetative growth and asexual and sexual development of a *sakA*-deletion strain compared to wild type. (A) The *sakA*-deletion strain produced less green conidia as compared to wild type. The colonies grew 2.5 days on supplemented minimal medium. Scale bar, 1 cm. **(B)**

Quantification of the conidiospore production of wild type and the *sakA*-deletion strain in the dark and in light. Fresh conidia were added to supplemented minimal medium containing 7.5% agar to a final concentration of 1×10^6 spores/ml and 2 ml of the medium were poured onto minimal medium agar plates. All plates were incubated at 37 °C in the dark for 12 hours and then half of them were exposed to light. After 5 days of cultivation, 3 pieces of agar were cut out with a hole puncher of Ø 8 mm from each plate. To wash off the conidia, each agar disk was put into a 2 ml Eppendorf tube with 1ml water containing 1% Tween and shaken at 200 rpm for 1 hour at 37 °C. Conidia were then counted in a Neubauer chamber. Cleistothecia were counted under the stereo microscope. The mean values were calculated from three biological replicates and the error bars represent the standard deviations.

3.2 Cross talk between light signaling and osmosensing

To analyze the cross talk between light signaling and osmosensing, different SakA pathway mutants were imposed to light or salt stress on agar plates. The diameters of the colonies were measured after 4 days of culturing **(Fig. 22)**. In the dark, the growth between different strains displayed no difference, but in light, the growth of six deletion strains was slightly inhibited, compared to wild type. When salt stress was imposed, the growth of all the strains was promoted. But under salt stress, *ΔsskA*, *ΔsskB, ΔpbsB, ΔsakA* and *ΔatfA* grew slower than wild type, especially*ΔsskA*. When light and salt stress were applied together, the growth of wild type and *ΔfphA* was similarly inhibited in comparison to the growth solely under salt stress. However, *ΔsskA*, *ΔsskB, ΔpbsB, ΔsakA* and *ΔatfA* did not respond to light under salt stress. Therefore, salt stress overrides the light stimulus in this case.

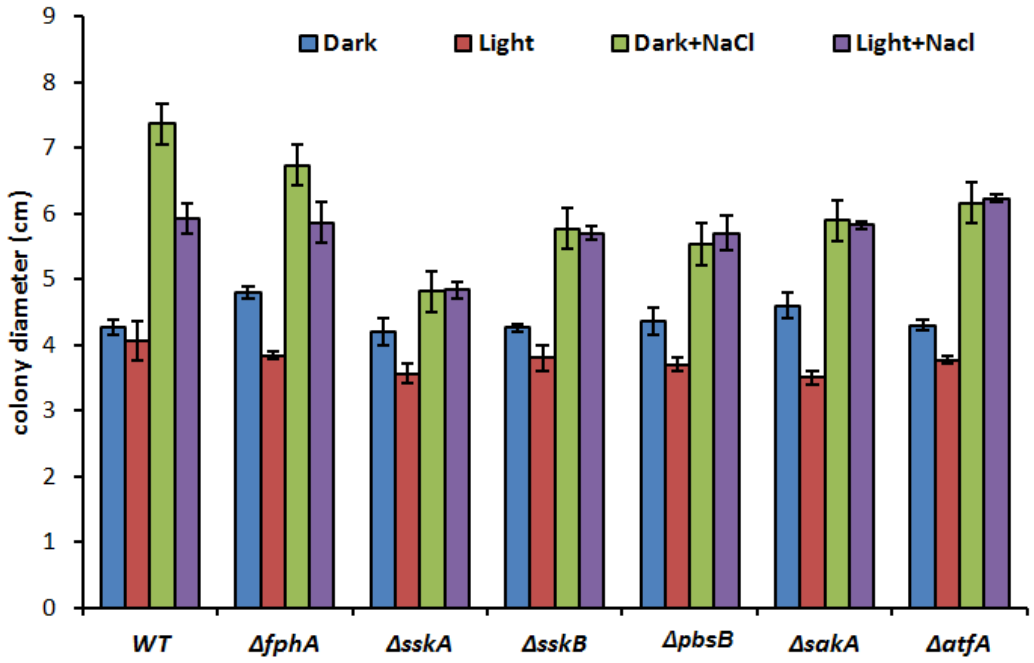

Fig. 22. Radial growth of different deletion strains under light or salt stimuli. Strains used here are SJR2 (WT), SJR10 (*ΔfphA*), SZY41 (*ΔsskA*), A1166 (*ΔsskB*), A1293 (*ΔpbsB*), SZY31 (*ΔsakA*) and SZY42 (*ΔatfA*). Same amount of conidia of different strains were inoculated on supplemented YPD medium plates with or without 0.6 mM NaCl. The plates were incubated in the dark or light for 4 days at 37 °C. The diameter of each colony was measured and the mean values were calculated with three independent biological replicates. The error bars represent the standard deviations.

3.3 Phytochrome interacts with the histidine-containing phophotransfer protein, YpdA

To figure out from where light signaling integrated into the SakA pathway, the interactions of FphA with TscB, YpdA and SskA were analyzed by bimolecular fluorescence complementation (BiFC). Only in the case with YpdA, nice yellow fluorescence was detected in the cytoplasm but not in the nucleus **(Fig. 23A)**. Considering the possibility of false positive signals in the BiFC system, co-immunoprecipitation (CoIP) was performed **(Fig. 23B)**. FphA was tagged with HA and YpdA was tagged with GFP. Under the *alcA* promoter, FphA-HA and YpdA-GFP were well expressed in minimal medium with 2% threonine. HA agrose precipitated FphA-HA very well. FphA-HA successfully precipitated YpdA-GFP, further confirming the interaction. Intriguingly, YpdA localized in both cytoplasm and nucleus **(Fig. 23C)**, when it was expressed under the *alcA* promoter.

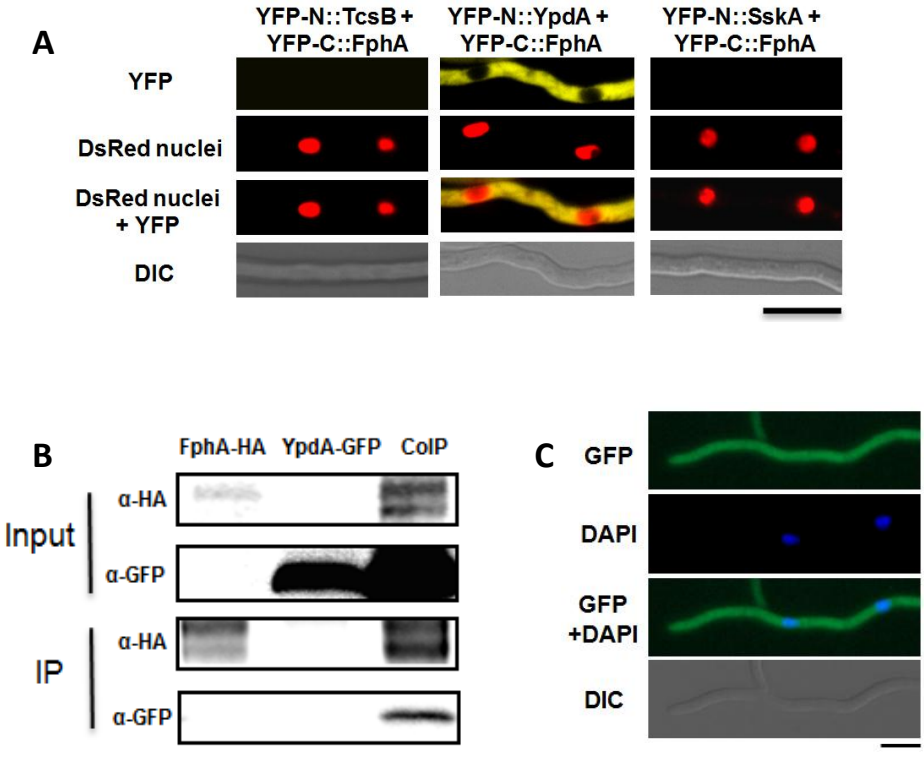

Fig. 23. Phytochrome interacts with YpdA in the cytoplasm and YpdA localizes in both cytoplasm and nucleus. (A) YpdA and SskA were fused to the N-terminal half of YFP respectively and both plasmids were transformed separately with plasmid pJP5 (*alcA::YFP-CT::fphA; pyr4*) into strain SKV103. Strains were cultured in supplemented liquid minimal medium containing 2% threonine and 0.2% glucose. This results in low-level expression of the construct. Scale bar, 10 µm. **(B)** Co-immunoprecipitation of FphA and YpdA. YpdA was fused to GFP and FphA was HA-tagged. The strains were culture in liquid minimal medium at 37 °C containing 2% threonine and 0.2% glucose for 24 hours at 180 rpm. Protein was purified and precipitated with anti-HA agarose. **(C)** YpdA localization. The *ypdA* open reading frame was fused to GFP and expressed under the control of the *alcA* promoter (pZY35). The plasmid was transformed into wild type (SJR2). The strain used for microscopy was cultured on glass slides with 2% glycerol supplemented minimal medium supplemented with 0.2% glucose. Scale bar, 10 µm.

3.4 Overexpression of the RR domain of FphA activates *ccgA* and *conJ* expression

After showing that FphA interacts with YpdA, the next question was how the SakA pathway is activated after this interaction. There is evidence that the phosphorylgroup from YpdA can be transferred to FphA (Azuma *et al.*, 2007). The phosphotransfer occurred to the aspartate residue 1181 in the RR of FphA. Therefore we hypothesized that light activation of FphA could lead to conformational changes of the protein and exposure of the RR. In order to test this hypothesis, we overexpressed GFP-tagged FphA, HKRR, and RR domains using the *alcA* promoter in the dark. Surprisingly, overexpression of RR domain induced *ccgA* and *conJ* expression and thus mimicked the light response **(Fig. 24)**.

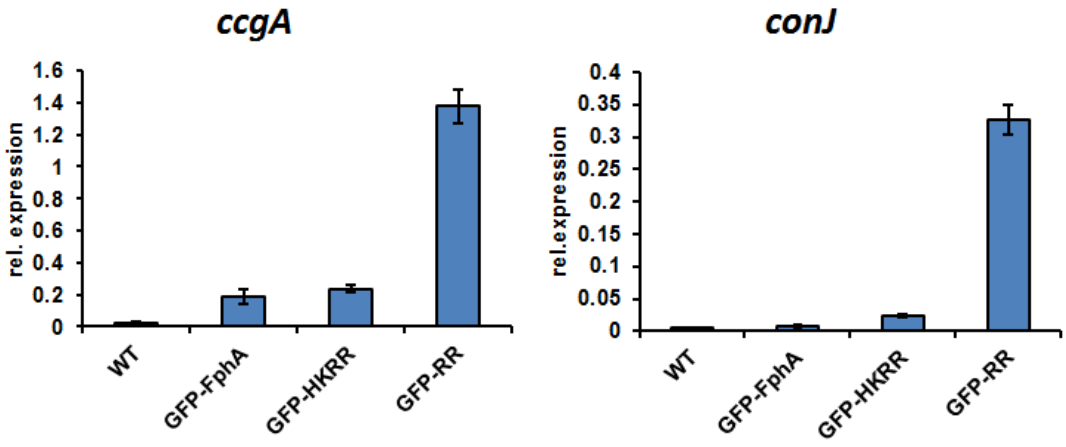

Fig. 24. Overexpression of the RR domain of FphA in the dark induces the expression of *ccgA* and *conJ*. Strains used here are GR5 (wild type), SSM9 (GFP-FphA), SJP109 (GFP-HKRR) and SJP66 (GFP-RR). All strains were in inoculated on the surface of liquid minimal medium supplemented with 2% threonine and 0.2% glucose for 18 hours. RNA was purified as described

above. The expression level was normalized to H2B. The mean values were calculated from three independent replicates and the error bars represent standard deviation.

3.5 SakA localization upon light stimuli

The SakA pathway is responsible for stress sensing. It was shown that imposed stress causes SakA phosphorylation and shuttling into the nuclei (Balazs *et al.*, 2010). To analyze the SakA localization upon illumination, we amplified *sakA(p)::sakA::gfp* cassette from the satrain TFL6. The cassette was transformed to different strains. In the dark, the GFP signal was distributed in nuclei and cytoplasm evenly in wild type **(Fig. 25A)**. In white and red light, brighter nuclei were observed in wild type. However, blue light did not cause the accumulation of the GFP signal in nuclei. In a *ΔfphA* strain, illumination could not cause SakA shuttling anymore neither in white, red or blue light. In *ΔlreA* and *ΔlreB* strains, the shuttling occurred normally upon white and red light **(Fig. 25B)**. Imposed salt stress led to SakA shuttling into nuclei in all the strains mentioned above. SakA shuttling is thus independent of phytochrome in case of salt stress signaling.

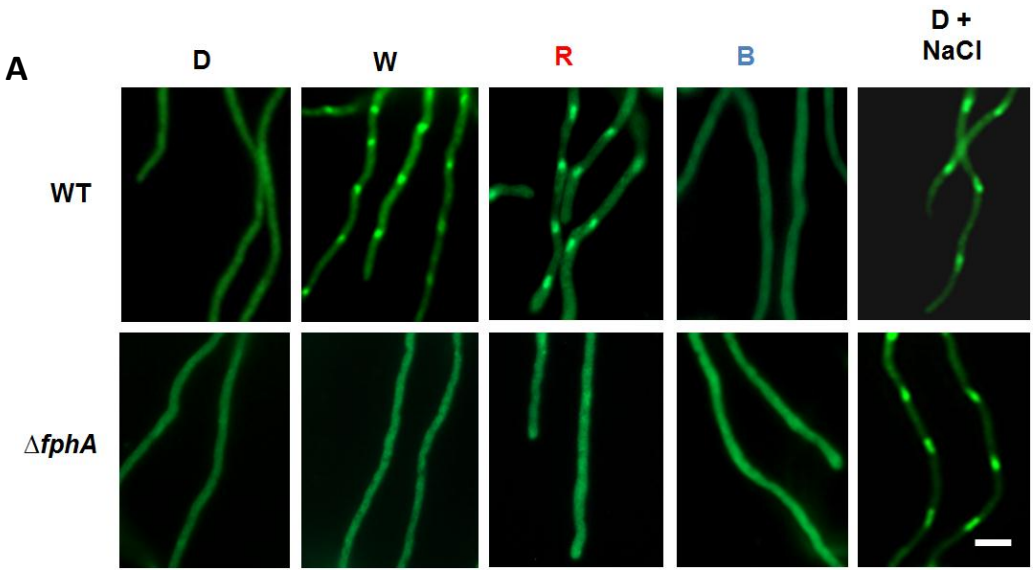

B

	WT	Δ*fphA*	Δ*lreA*	Δ*lreB*
Dark				
White	●		●	●
Red	●		●	●
Blue				
NaCl	●	●	●	●

Fig. 25. SakA shuttling and phosphorylation after light exposure. (A) SakA localization in wild type (SZY34) and an *fphA*-deletion strain (SZY37). GFP tagged SakA was expressed under the

control of the *sakA* native promoter. The strains were cultured on supplemented minimal medium in the dark (D) and grown for 16 hours. The mycelia were fixed in the dark (dim-green light) directly or after 5 min of illumination in white light (W). To impose salt stress, minimal medium was replaced by minimal medium with 0.5 M NaCl and incubated 10 min before fixation. **(B)** Summary of SakA shuttling in wild type (SZY34), Δ*fphA* (SZY37), Δ*lreA* (SYZ35) *and* Δ*lreB* (SYZ35) upon light stimuli or salt stress. A black dot indicates shuttling of SakA.

3.6 SakA phosphorylation in different mutants under different light conditions

To analyze the phosphorylation status of SakA upon light western blots were performed with different stains. In order to make sure the mycelia were fully illuminated, we also used the surface culture by inoculating the conidia on the surface of the liquid medium and culturing 18 hours in the dark before illumination. The influence of white light on SakA phosphorylation was checked first with wild type and *ΔfphA.* After the exposure, more phosphorylated SakA was detected in wild type, whereas in the *ΔfphA* strain the phosphorylation of SakA was not changed upon the light stimulus **(Fig. 26A&B)**.

To figure out whether blue and red light both induced SakA phosphorylation, the effect of red and blue light on SakA phosphorylation in wild type was further analyzed. The mycelia were illuminated with red or blue light respectively for 10 min or 20 min. Red light induced SakA phosphorylation after 10 min and 20 min illumination but blue light did not **(Fig. 26A&B)**.

Next, we analyzed SakA phosphorylation in wild-type, *ΔfphA*, *ΔlreA* and *ΔlreAΔlreB* strains. Smilar to the white light stimulus, red light could not cause SakA phosphorylation in the *ΔfphA* strain. With respect to LreA and LreB, red light induced SakA phosphorylation in *ΔlreA* and *ΔlreAΔlreB* but blue light could not **(Fig. 26C&D)**. These results were consistent with the above studies that blue light could not cause SakA shuttling in the nucleus and the the shuttling depended on FphA.

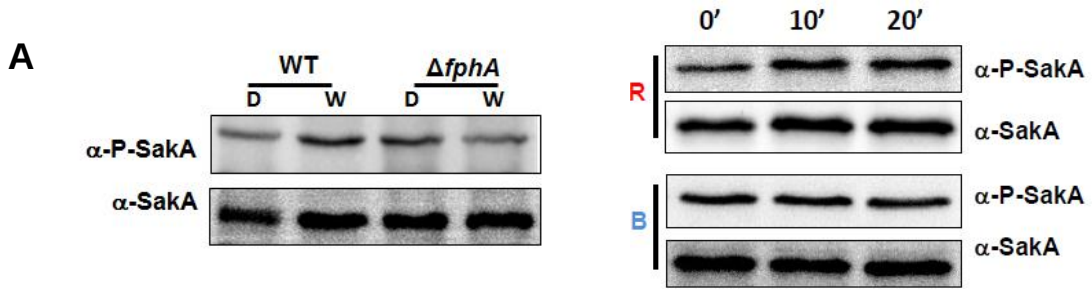

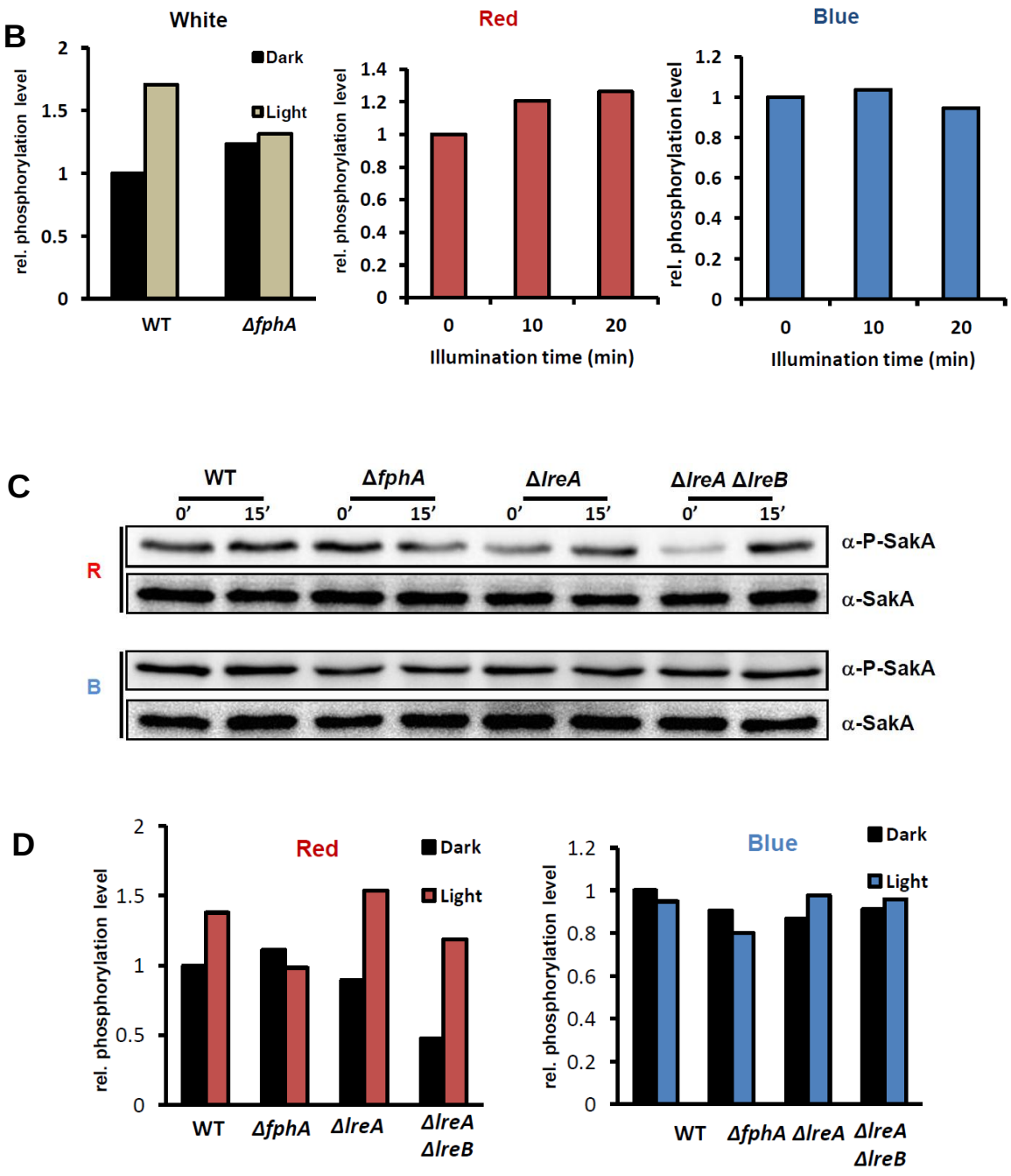

Fig. 26. Phosphorylation of SakA in wild type under different illumination conditions. (A) Phosphorylation of SakA in white (W), red I and blue (B) light. Fresh conidia were inoculated on the surface of liquid minimal medium and incubated for 18 hours in the dark. The mycelium was harvested directly in the dark or after 15 min illumination in white, or 10 or 20 min illumination in red or blue light and frozen in liquid nitrogen immediately for protein extraction. 35 µg crude extract of each sample were loaded onto the SDS PAGE and processed for the western blot. **(B)** Quantification of SakA phosphorylation. The relative phosphorylation levels of SakA were analyzed with ImageJ. **(C)** Analysis of the phosphorylation level in wild type (SJR2), the *fphA*-deletion strain (SJR10), the *lreA*-deletion and the *lreA/lreB*-double-deletion strain (SSR91). Under different illumination conditions. **(D)** Quantification of the bands displayed in **(C).**

Considering the possibility that the surface culture was suffering from diverse stresses, the phosphorylation level of SakA in wild type in submerged culture was also analyzed. Wild type was cultured in flasks and then mycelia were divided into different flasks for illumination. Here, only white and red light induced the SakA phosphorylation, consistent with the results obtained with surface cultures **(Fig. 27)**.

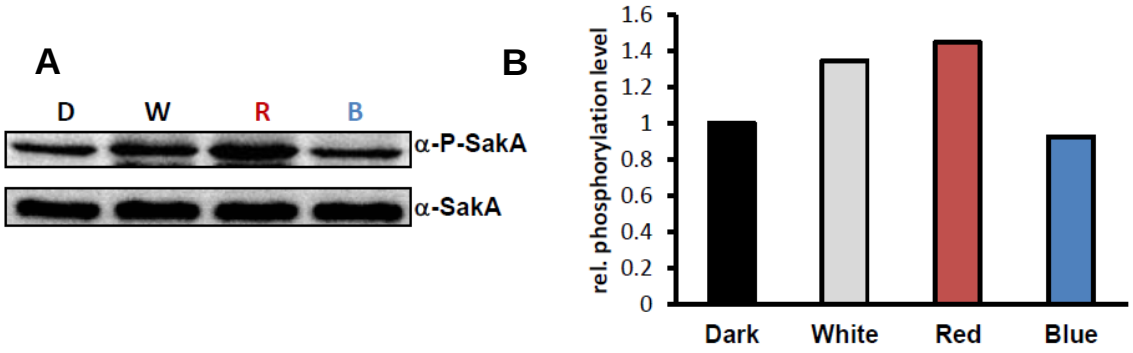

Fig. 27. Phosphorylation of SakA in submerged-cultured wild type under diffent illumination conditions. (A) Conidiospores (1×10^6 spores/ml) were inoculated into a 2 l flask with 400 ml of liquid supplemented minimal medium, incubated at 37 °C and shaken at 180 rpm. Each 50 ml culture was transferred into a 300 ml flask, which had been pre-warmed at 37 °C in light chambers. Three flasks were placed into white, red and blue light chambers separately and one was put into a dark chamber. After 15 min illumination, the mycelium was filtrated and frozen immediately in liquid nitrogen for protein extraction and Western blotting. The graph illustrates the relative phosphorylation levels. **(B)** Quantification of the bands displayed in (A).

Since the increase of SakA phosphorylation was not very significant even in white and red light, we performed immunostaining experiment to check the phosphorylation level of SakA. In white and red light, bright signals were observed in wild type and no signal was detected in an *fphA*-deletion strain **(Fig. 28)**, which is in agreement with the western blot results. However, blue light also caused the SakA phosphorylation though the signal was not as strong as in the case of white and red light. In an *fphA*-deletion strain after blue light exposure, no signal was detected. More intriguingly, the deletion of *lreA* or *lreA*/*lreB* did not affect the sakA phosphorylation in blue light **(Fig. 28)**.

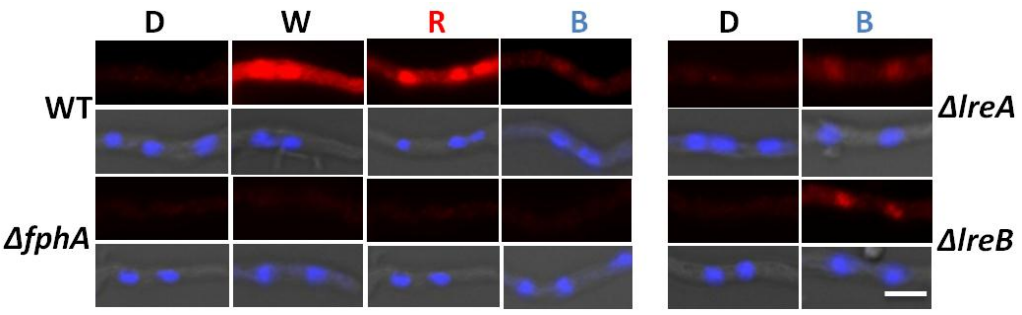

Fig. 28. Immunostaining of wild type (SJR2), the *fphA*-deletion strain (SJR10), and the *lreA*-(SSR66) and *lreB*-deletion strains (SJR70). Conidia were germinated on cover slips at room temperature and then exposed 5 min to white (W), red I and blue (B) light and immediately fixed and processed for immunostaining (upper row of pictures). Nuclei were stained with DAPI (lower row of pictures). Scale bar, 5 µm.

4 MetR strictly regulates phytochrome expression independently of light

4.1 FphA expression in a *metR1* mutant

MetR is a positive regulator of the sulfur metabolism system in *A. nidulans* (Natorff *et al.*, 2003). Recently, the group of Jerzy Brzywczy (Warshaw, Poland) found in a transcriptomic analysis that MetR regulates *fphA* expression (unpublished data). If MetR indeed regulates *fphA* expression, *metR1* mutants should be *blind* and phenocopy an *fphA*-deletion strain. In this chapter, we analyzed the light response of a *metR1* mutant in which MetR is nonfunctional.

First, the expression data obtained in the transcriptomic analysis were validated by quantitative real time RT PCR **(Fig. 29)**. Same expression levels of *fphA* in light and dark were detected in wild tpe. However, in the *metR1* mutant, *fphA* was not expressed anymore neither in dark or light. *fphA* expression is thus independent of light in wild type and MetR indeed is essential for *fphA* expression.

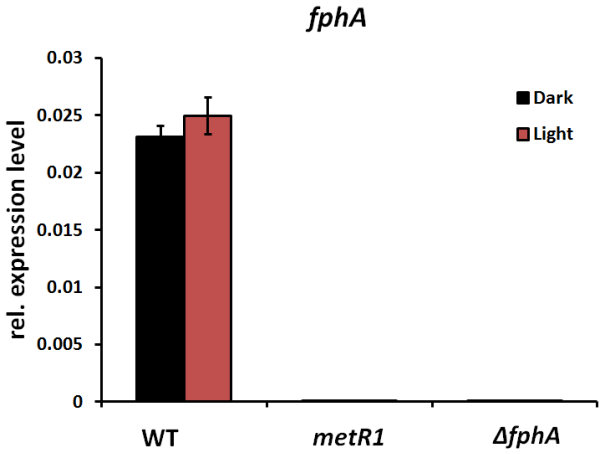

Fig. 29. Expression analysis of *ccgA* and *conJ* in wild type (SJR2), the *metR1* mutant (SZY61) and *fphA*-deletion strain (SJR10). Fresh conidia were inoculated on the surface of supplemented liquid minimal medium and cultured 18 h in the dark at 37 °C. The mycelia were harvested under dim-green light directly or after 30 min illumination with white light and frozen in liquid nitrogen for RNA isolation. The expression levels were normalized to H2B. The mean values were calculated from three biological replicates and the error bars represent the standard deviation.

4.2 *ccgA* and *conJ* expression in a *metR1* mutant

Since the light-inducible genes are strictly regulated by FphA, we hypothesized that the

induction of *ccgA* and *conJ* is controlled by MetR. The light response of a *metR1* mutant was checked by real-time PCR. Indeed in the *metR1* mutant, *ccgA* and *conJ* could not be induced anymore **(Fig. 30)**.

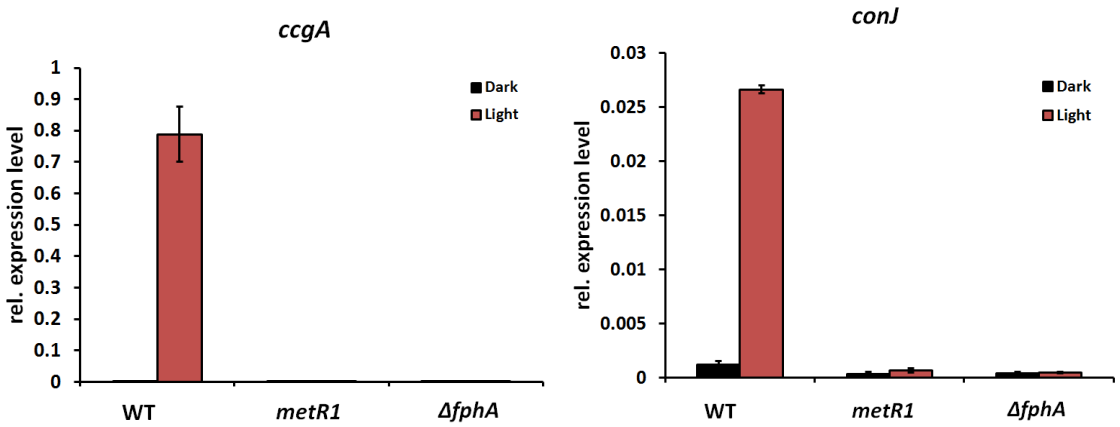

Fig. 30. Expression analysis of *ccgA* and *conJ* in wild type ((SJR2), the *metR1* mutant (SZY61) and *fphA*-deleton strain (SJR10). Fresh conidia were inoculated on the surface of supplemented liquid minimal medium and cultured 18 h in the dark at 37°C. The mycelium was harvested under green light conditions directly or after 30 min illumination with white light and frozen in liquid nitrogen for RNA isolation. The expression levels were normalized to H2B. The mean values were calculated from three biological replicates and the error bars represent the standard deviation.

4.3 Asexual and sexual development in the *metR1* mutant

Light promotes asexual development and inhibits sexual development (Purschwitz *et al.*, 2008). After 5 days of incubation, wild type produced less ceistothecia in light than in dark, whereas light did not inhibit cleistothecia formation in the *metR1* mutant, which produced same amounts of cleistothecia in dark and light **(Fig. 31)**. Asexual development of the *metR1* strain was normal.

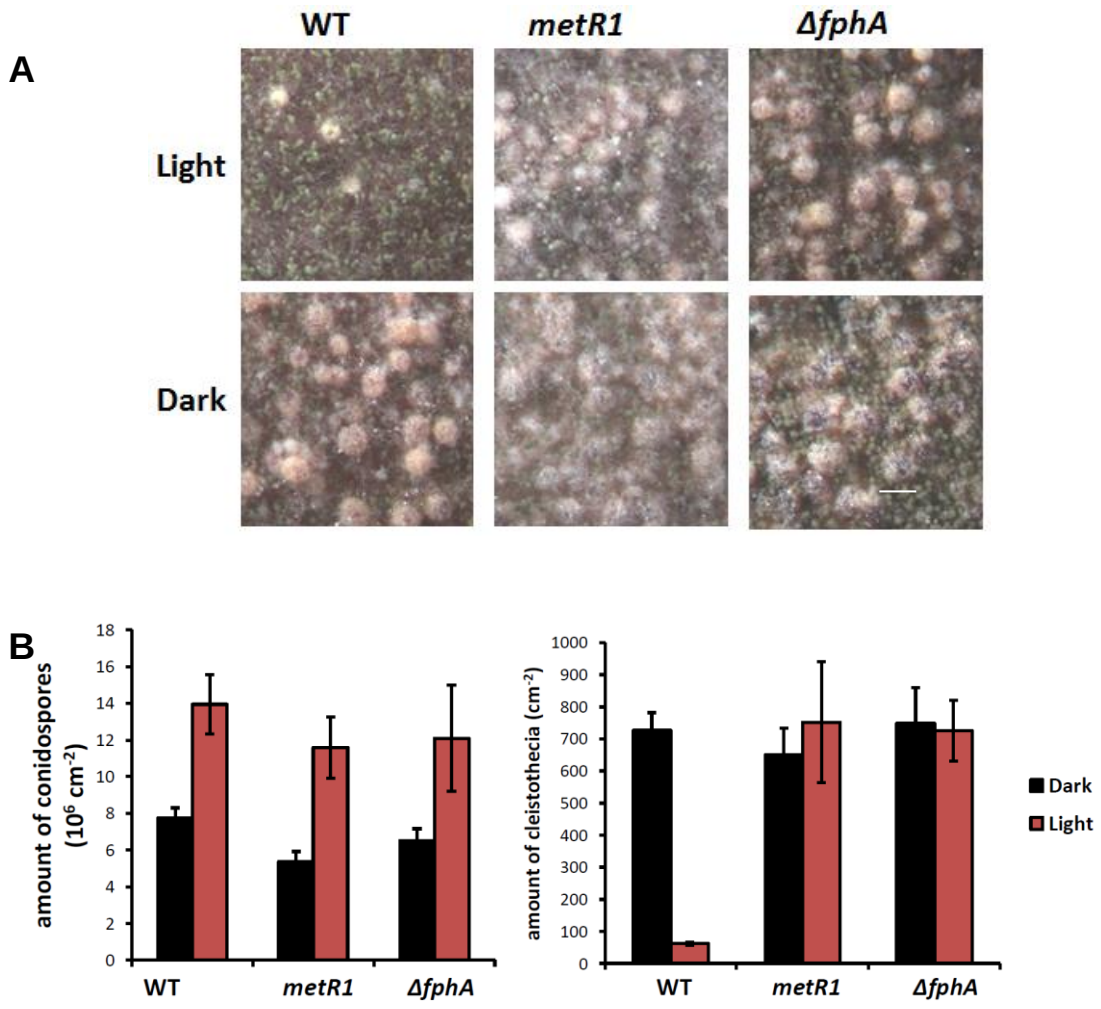

Fig. 31. Phenotype of wild type (SJR2), the *metR1* mutant (SZY61) and the *fphA*-deletion strain (SJR10). (A) Scale bar, 500 µm **(B)** Quantification of conidiospores and cleistothecia. Conidiospores and cleistothecia were quantified as described above.

4.4 *VeA* expression in the *metR1* mutant and the *fphA*-deletion strain

Light represses *veA* expression (Ruger-Herreros *et al.*, 2011). Consistent with this, in wild type, *veA* expression was inhibited in light **(Fig. 32)**. However, in the *fphA*-deletion stain, *veA* expression was not affected by light. *veA* expression was also independent of light in the *metR1* mutant.

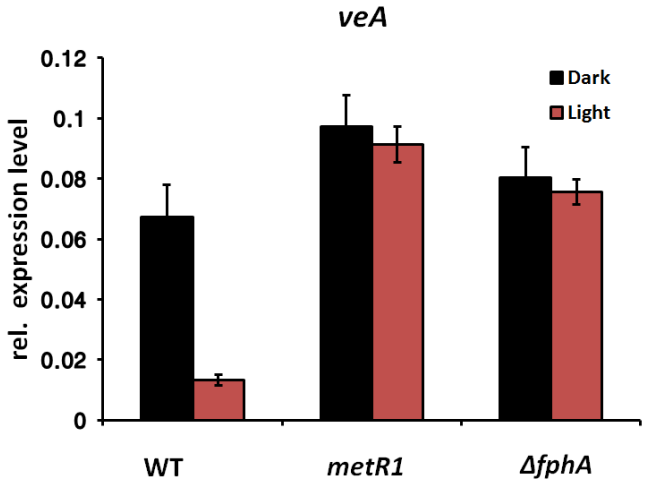

Fig. 32. Expression analysis of *veA* in wild type (SJR2), the *metR1* mutant (SZY61) and the *fphA*-deleton strain (SJR10). Fresh conidia were inoculated on the surface of supplemented liquid minimal medium and cultured 18 h in the dark at 37 °C. The mycelia were harvested under green light conditions directly or after 30 min illumination with white light and frozen in liquid nitrogen for RNA isolation. The expression levels were normalized to H2B. The mean values were calculated from three biological replicates and the error bars represent the standard deviation.

5 Phytochrome and the SakA pathway are involved in temperature sensing

5.1 *ccgA* and *conJ* are induced by high temperatures

Recently, there was some evidence that bacterial phytochrome could act as a protein-based „thermometer“ (Kim *et al.*, 2014; Njimona and Lamparter, 2011; Njimona *et al.*, 2014). It was shown that temperature affects the kinase activity of bacterial phytochrome and the absorption spectra of its sensory core (PAS-GAF-PHY) *in vivo* (Kim *et al.*, 2014; Njimona and Lamparter, 2011; Njimona *et al.*, 2014). Therefore, we asked whether *A. nidulans* FphA could act as thermometer and cause the induction of *ccgA* and *conJ*. Hence, we measured *ccgA* and *conJ* expression after the stains were subjected to a temperature shift.

Mycelia of wild type and an *fphA*-deletion strain were exposed to 50 °C for 30 or 60 minutes after the incubation at 37 °C in the dark. *ccgA* and *conJ* were both induced **(Fig. 33)**. Moreover, the expression of *ccgA* and *conJ* was attenuated in *fphA*-deletion strains in comparison to the wild-type strain. After 60 minutes exposure, the expression levels of *ccgA* and *conJ* were less than 30% of their expression in wild type. Therefore, FphA is likely to be required for the induction of *ccgA* and *conJ* at high temperature.

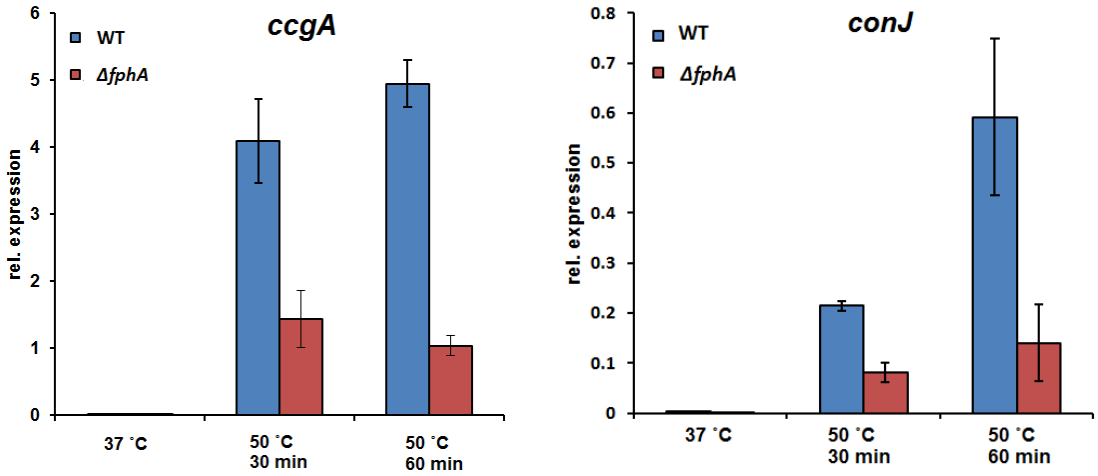

Fig. 33. *ccgA* and *conJ* induction at high temperature stress. Fresh conidia were inoculated on the suface of supplemented minimal medium and cultured for 18 hours in the dark. To impose high temperature stress, some of the plates were moved to another incubator prewarmed to 50 °C and incubated for 30 or 60 minutes. RNA was isolated as described above. Expression levels were normalized to H2B. The mean values were calculated from three biological replicates and the error bars represent the standard deviation.

5.2 FphA and the SakA pathway are required for the high temperature response

To test whether the SakA pathway is involved in temperature sensing, we used the parent strain that we used for mutagenesis, the mutants M6-9 and M10-3 and the complemented strains to check their phenotype at different temperatures **(Fig. 34)**. In the parent strain the *pyr4* gene is under the control of the *conJ* promoter and if *conJ* is temperature induced, the strain should grow better at higher tempertures. Indeed, at 42 °C, the parent strain grew well on minimal meidium without uracil and uridine, while at 28 and 37 °C, it grew very slowly. However, the *sakA*-defective mutant, M6-9 and the *fphA*-defective mutant, M10-13, did not grow at 42 °C, whereas the corresponding complemented strains grew as well as the parent strain. As a control growth was monitored in light.

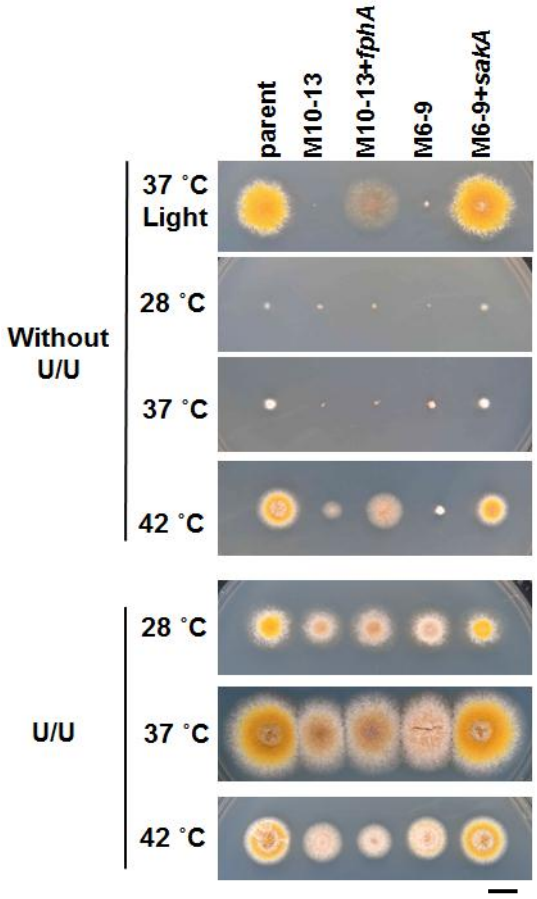

Fig. 34. Phenotype of the parent strain, M6-9, M10-3 and two complemented strains. Same amounts of conidia of each strain were inoculated and incubated for 3 days under the conditions as indicated. Scale bar, 1 cm.

Discussion

1 A powerful screening system for the identification of novel regulators involved in light signaling

Mutagenesis has been applied to sceen mutants with interesting phenotypes, which often helped to discover some novel components and metabolic or morphogenetic pathways.. In the 1960s, Leland H. Hartwell isolated approximately 400 temperature-sensitive mutants of *S. cerevisiae* by mutagenesis and the temperature-sensitive lethal mutants arrested the cell cycle at different, defined stages, which was the key to identify essential genes that control the progression through the cell cycle and replication and mitosis (Hartwell, 1967; Hartwell *et al.*, 1970; Johnson and Downes, 2002). Due to the contribution to the cell cycle research of *S. cerevisiae*, Leland H. Hartwell shared 2001 the Nobel prize in physiology or medicine with Paul Nurse and Tim Hunt. In the developmental research of *Drosophila* and zebrafish, mutatgesis was also widely used to isolate mutants with developmental defects (Karim *et al.*, 1996; Vihtelic and Hyde, 2002). The work of Christiane Nüsslein Volhard on *Drosophila* was honored with the nobel prize in 1995. In *A. nidulans*, mutagenesis was also used to collect temperature-sensitive mutants that were defective in nuclear division, septation or distribution of nuclei and the studies on *nim* (never in mitosis), *bim* (blocked in mitosis), *sep* (fail to form septa) and *nud* (abnormal nuclear distribution) mutants contributed to the understanding of the cell cycle of *A. nidulans* (Morris, 1976; Morris, 1975; OSMANI, 1996). In plants, mutagenesis was applied to screen mutants that exhibited phenotypes of photoreceptor mutants, by which a number of putative steps involved in light signaling signaling were characterized (Chory, 1993). In *N. crassa*, some new white collar mutants that did not respond to blue light were created by UV-mutagenesis (Degli-Innocenti and Russo, 1984). After a set of light-inducible genes, such as *albino-3* responsible for carotenoid synthesis, was described (Arpaia *et al.*, 1995; Baima *et al.*, 1991; Nelson *et al.*, 1989; Schmidhauser *et al.*, 1990), a new screening system for mutants with altered response to blue light was established (Carattoli *et al.*, 1995). In this system, the light-inducible promoter of *albino-3* was fused to the amino acid permease gene *mtr* and the strain carrying this cassette could uptake neutral aliphatic and aromatic amino acids, as well as the toxic analogs in light. Therefore, the strain was sensitive to *p*-florophenylalanine in light but resistant in dark. With this strain, two mutants, that were resistant to *p*-florophenylalanine in blue light and lost the ability to uptake tryptophan were isolated. The light-inducible genes of two mutants could not be induced by light very well. A similar

approach was also used to isolate clock output pathway mutations (Vitalini *et al.*, 2004).

In 2011, a set of light-inducible genes were identified in *A. nidulans* by genome-wide expression analyses (Ruger-Herreros *et al.*, 2011), which provided us enough light-inducible promoters that probably can been used to establish a similar screening system as mentioned above. Indeed, we successfully constructed a parent strain with the promoter of the light-inducible gene *conJ*. Actually, the *ccgA* promoter also was used in the beginning of constructing a parent strain. However, the tranformants constructed with the *ccgA* promoter grew healthily in dark. The *ccgA* exression level is much higher than the one of *conJ* in both dark and light (data not shown). Obviously the expression level of the *ccgA* promoter construct was high enough in the dark to support growth. In contrast, the parent strain with the *conJ* promoter showed a slow-growing phenotype, which is critical for the success of the whole screening strategy for *blind* and dominant mutants. The slow-growing phenotype helped us to easily distinguish the putative *blind* and dominant mutants from tens of thousands of colonies after UV-treatment and tremendously improved the efficiency of the screening. Most of the dominant mutants were not analyzed until now and more novel components related to light signaling will be revealed in the future. If there were genes only induced in blue or in red light, the promoters of the corresponding genes could be used to set up a screening system to identify specific components required for specific wavelengts.

NGS has enabled us to study *A. nidulans* by mutagenesis very efficiently, very rapidly and with relatively low costs. It has become an everyday tool for biological studies and is already widely used in whole genome sequencing, RNA sequencing, genome-wide DNA-protein interaction analyses, genome-wide DNA methylation analyses, microbial diversity analyses in humans and in the environment and several other applications. Recently, this method has revolutionized fungal studies. Some industrial strains such as *Aspergillus niger* and *Trichoderma reesei* earlier screened by mutagenesis and already wildly used in industry now can be analyzed though NGS to identify variations that confer the strains commercial value, which in turn probably helps researcher to genetically modify and create more valuable industrial strains (Lichius *et al.*, 2015; Niu *et al.*, 2016; Yin *et al.*, 2014). *A. fumigatus* is a human pathogen and emerging azole resistance of it caused extensive concern in the past decade. NGS may help to unravel the molecular basis azole resistance (Abdolrasouli *et al.*, 2015; Camps *et al.*, 2012). In *N. crassa,* some classical mutants were sequenced and analyzed to identify significant additional genetic variations (McCluskey *et al.*, 2011). Combined with classical mutagenesis, NGS has helped to screen novel genes involved in pathogenicity, antifungal drug resistance, protein secretion and intracellular transport in fungi (Blum *et al.*, 2016; He *et al.*, 2014; Huang *et al.*, 2015; Tan *et al.*, 2014).

The perfect combination of traditional mutagenesis and NGS is revolutionizing the research of many biological systems.

2 Fungi use the TCS and MAPK SakA pathway to sense and adapt to environmental signals

2.1 *A. nidulans* uses a TCS to transmit the light signal

To survive in the ever-changing environment, organisms need to sense and respond to the various environmental cues. In bacteria, two-component systems (TCSs) are the major signal perceiving devices. The prototypical two-component system comprises a sensor histidine kinase (HK), which is responsible for the sensing of the external signal, and a response regulator (RR) mediating the signaling output **(Fig. 35A)** (Alvarez *et al.*, 2016; Capra and Laub, 2012; Mascher *et al.*, 2006; Nixon *et al.*, 1986; Ronson *et al.*, 1987; Skerker *et al.*, 2005; Stock *et al.*, 2000). HK harbors a sensor domain (SD) and a histindine kinase domain (HKD), which is further dissected into a specific histidine (H) residue and a catalytic domain. Response regulators (RR) are subdivided into a receiver domain (RD), harboring a conserved aspartate (D) residue, and an output domain (OD). The input domain perceives the stimuli leading to auto-phosphorylation of the conserved histidine residue, which donates the phosphoryl group to the conserved aspartate residue in the RD. The signal is eventually transmitted by the OD domain through protein-protein interactions or directly regulating gene transcription. In more elaborate two component system, an additional RR and a histidine phosphotransferase (HPt) are involved and the phosphoryl group is transferred in a phosphorelay (H -> A -> H -> A) **(Fig. 35B)** (Alvarez *et al.*, 2016; Capra and Laub, 2012; Stock *et al.*, 2000). In different phosphorelay systems, RD or both RD and HPt can be fused to the N terminus of a HK to form a hybrid histidine kinase (HHK) **(Fig. 35B)**. Analysis of some bacterial genomes reveals that in most cases the number of HK proteins tends to be the same as the number of RR proteins (Wuichet *et al.*, 2010), although in cyanobacteria a larger number of RRs are found.

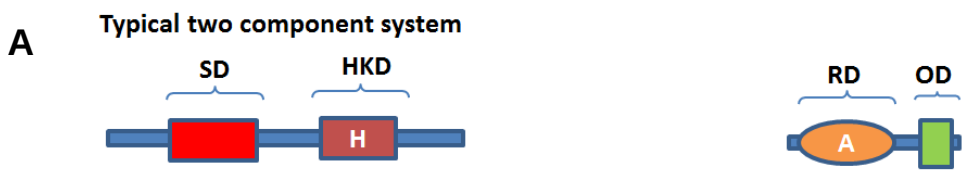

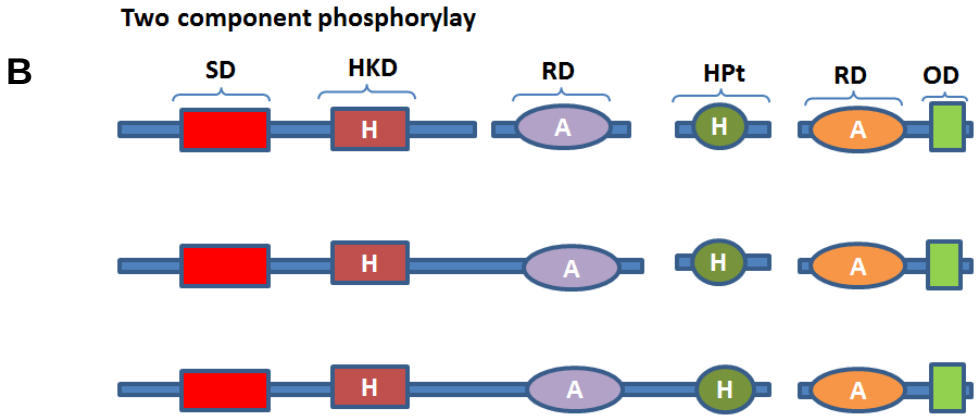

Fig. 35. Organization of two-component systems and two component phosphorelays in bacteria. (A) Prototypical two-component system comprises a histidine kinase (HK) and a response regulator (RR). The sensing domain (SD) perceives the signal, which promotes the autophosphorylation of a conserved histidine (H) in the histidine domain (HKD). The phosphorylated histidine donates the phosphoryl group to the conserved aspartate (D) in the receiver domain (RD) of the response regulator (RR), resulting in outputting the signal from the output domain (OD) by protein-protein or protein-DNA interactions. In the absence of a signal, the RR undergoes dephosphorylation by spontaneous hydrolysis of phosphor-aspartyl bond or by the phosphatase activity of the cognate HK or another protein (phosphatase X). **(B)** In two-component phosphorelay systems, the phosphoryl group is transferred by multiple-step phosphorelays. The phosphoryl group is transferred from HKD to a RD and further to a histidine phosphotransferase (HPt). HPt gives the phosphoryl group to another RD. HKD, RD and HPt can exist in one, in two or in three different proteins (Modified according to Fig. 1, Alvarez *et al.*, 2016).

TCS phosphorelays also exist in slime molds, fungi and plants. In fungal genomes, 1 to 21 HHKs encoding genes are predicted (Alvarez *et al.*, 2016; Bahn, 2008; Catlett *et al.*, 2003; Hagiwara *et al.*, 2016; Posas *et al.*, 1996; Vargas-Perez *et al.*, 2007). More surprisingly, only one HPt and one to four RRs are econded (Alvarez *et al.*, 2016; Azuma *et al.*, 2007; Hagiwara *et al.*, 2016; Posas *et al.*, 1996; Vargas-Perez *et al.*, 2007). A well-studied TCS phosphorelay is the Sln1p-Ypd1p-Ssk1p phosphorelay in *S. cerevisiae*. *S. cerevisiae* has one HHK (Sln1p), one HPt (Ypd1p) and two RRs (Ssk1p and Skn7p) (Posas *et al.*, 1996). Sln1p is an osmotic sensor and the osmotic signal is transmitted by the Sln1p-Ypd1p-Ssk1p phosporelay to the downstream MAPK Hog1p pathway (Santos and Shiozaki, 2001) **(Fig. 36)**. *A. nidulans* possesses 15 HHKs (TcsA, TcsB, NikA, HysA and others), one HPt (YpdA) and four RRs (SskA, SrrA, SrrB and SrrC) (Azuma *et al.*, 2007; Vargas-Perez *et al.*, 2007). The two-component signaling protein TcsA, is involved in conidiation and controls the localization of DevR, encoded by a basic-region helix-loop-helix (bHLH) protein-encoding gene devR. The *devR*-deletion strain has the same phenotype as the *tcsA*-deletion strain (Tuncher *et al.*, 2004). TcsB is the homologue of Sln1p and overexpression of the *tcsB* cDNA suppresses the lethality of a

temperature-sensitive osmosensing-defective *sln1-ts* yeast mutant (Furukawa *et al.*, 2002). However, *tcsB* cDNAs encoding a TcsB variant in which the conserved histidine and aspartate residues are replaced, cannot complement the *sln1-ts* mutant. These results imply TcsB functions as an osmosensing histidine kinase. Unexpectedly, the *tcsB*-deletion strain has no detectable phenotype with respect to development or morphology under salt stress, suggesting that *A. nidulans* has a more complex osmosensing system than *S. cerevisiae* (Furukawa *et al.*, 2005; Furukawa *et al.*, 2002). NikA plays roles in fungicide responses and osmosensing (Hagiwara *et al.*, 2007b; Hagiwara *et al.*, 2009b). HysA is involved in ROS production (Hayashi *et al.*, 2014). FphA is a red light receptor (Blumenstein *et al.*, 2005). The other HHKs in *A. nidulans* have not been studied in detail, though the expression of GFP-tagged HHKs during the life cycle has been analyzed (Suzuki *et al.*, 2008). The sole HPt, YpdA, is essential (Vargas-Perez *et al.*, 2007). SskA and SrrA are both involved in osmosensing and required for sensitivity to fungicide (Hagiwara *et al.*, 2007a; Vargas-Perez *et al.*, 2007). With respect to adaption of oxidative stress, SrrA but not SskA is required (Vargas-Perez *et al.*, 2007). SrrB has no conserved aspartate residue and SrrC is a short protein only harboring a RRD domain wihtout any other features. *srrB*- or *srrC*-deletion strain has no detectable phenotype (Hagiwara *et al.*, 2007a). The direct interaction between FphA and YpdA and the necessity of SskA for the induction of light-inducible genes demonstrate that the light signal is transmitted from FphA to SskA through YpdA. However, whether the light signal goes to other RRs is not investigated yet in this study.

2.2 Retrograde phosphorelay from YpdA to FphA

Under low-osmolarity conditions, Sln1p is autophosphorylated in the specific histidine residue in the HKD and the phosphoryl group is further transferred to the aspartate residue in the RRD. Afterwards, this phosphoryl group is transferred to HPt, Ypd1p and then to the RR, Ssk1p. The phosphorylated Ssk1p cannot interact with Ssk2p/Ssk22p which in turn cannot be autophosphorylated in this case, resulting in the inactivation of the downstream Hog1p MAPK cascade **(Fig. 36)** (Maeda *et al.,* 1994; Posas *et al.,* 1996). High osmolarity stress blocks Sln1p autophosphorylation leading to a low phosphorylation level of Ssk1p and unphosphorylated Ssk1p binds to Ssk2p/Ssk22p promoting the autophosphorylation of Ssk2p. Phosphorylated Ssk2p further activates Pbs2p. Activated Pbs2p in turn activates the Hog1p MAPK **(Fig. 36)** (Maeda *et al.,* 1995; Posas and Saito, 1998). Skn7p serves as a transcription factor when it receives the osmotic signal from Sln1 (Li *et al.*, 1998). Moreover, Skn7p is responsible for oxidative stress signaling, but this role is independent of Sln1p (Lee *et al.*, 1999; Li *et al.*, 1998; Morgan *et al.*, 1997). In oxidative stress sensing, the transcription factor Yap1p

cooperates with Skn7p to activate some oxidative stress-related genes **(Fig. 36)** (Morgan *et al.*, 1997).

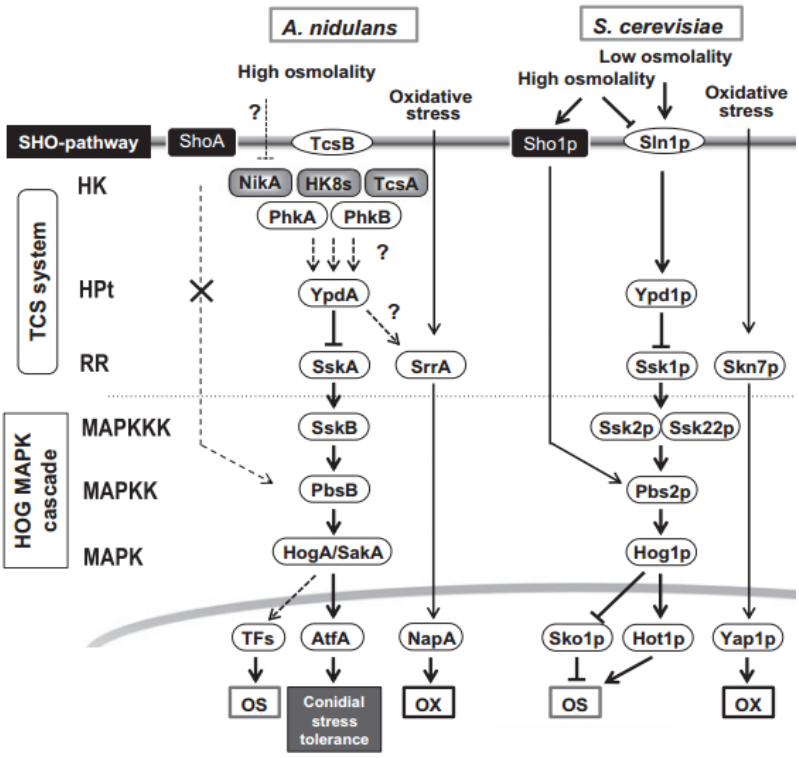

Fig. 36. Comparison of signaling components in the HOG pathway in *A. nidulans* and *S. cerevisiae* (Hagiwara *et al.*, 2016)**.** Only the osmolality and oxidative stresses are shown. In *S. cerevisiae* Sho1p activates Pbs2p under high osmolarity stress, whereas the homologous pathway of *A. nidulans* is nonfunctional. The interplay between HKs and YpdA in *A. nidualns* is not established (dotted arrows). OS, osmotic stress response; OX, oxidative stress response.

From 15 HHKs of *A. nidulans*, only the auto-phosphorylation of FphA and HysA has been proven *in vitro*, because the conditions triggering the auto-phosphorylation of the other HKs are unclear. (Brandt *et al.*, 2008; Hayashi *et al.*, 2014). The auto-phosphorylation of recombinant FphA is dependent on light and the phosphoryl group can be transferred from the conserved histidine residue in the HKD to conserved aspartate residue in the RRD of a second monomer (Brandt *et al.*, 2008). The well-studied intermolecular trans-phosphorylation of HHKs in *A. nidulans* is HysA (Hayashi *et al.*, 2014). HysA undergoes autophosphorylation *in vitro* and the phosphoryl group is transferred from the conserved histidine residue to the conserved aspartate residue in the RRD. And then the phosphoryl group is transferred to YpdA which further donates the phosphoryl group to SrrA (Azuma *et al.*, 2007). Beyond the HHKs in *A. nidulans*, the HHK ArcB of *Escherichia coli* can also phosphorylate SrrA through YpdA. In *A. nidulans*, the interaction between HKs, HPt and RRs has not been shown *in vivo*

before this study. The interaction between YpdA and FphA and the necessity of FphA and SskA for light signaling imply the possibility of FphA-YpdA-SskA phosphorelay. However, if FphA donates the phosphoryl group in light, SskA will be phosphorylated and thus the SakA pathway will be inactivated, which is inconsistent with the fact that light activates the SakA pathway. Instead of functioning as a donor, FphA could accept the phosphoryl group from YpdA. This has been demonstrated *in vitro* and the aspartate residue 1181 (D1181) in the RRD is essential for the phosphoryl group transfer (Azuma *et al.*, 2007). Indeed, *ccgA* and *conJ* genes cannot be induced in an *fphA*^{D1181A} mutant in which the aspartate residue 1181 was mutated to the alanine residue (Hedtke *et al.*, 2015). Overexpression of the RR domain indeed induces *ccgA* and *conJ* expression, implying the retrograde phosphorelay *in vivo*. It is likely that in light the essential aspartate residue in RR domain is exposed to YpdA, which lead to phosphoryl group goes from YpdA to FphA instead of to SskA. Thus, unphosphorylated SskA activates SakA pathway. In the dark, other HKs keep YpdA phosphorylated.

2.3 MAPK SakA pathway is a hub for light and other environmental signals

The high osmolarity glycerol (Hog) MAPK pathway was identified in yeast and is required for the adaption to various environmental stimuli, such as oxidative, high osmolarity, ultraviolet radiation, and heat stress (Hohmann, 2002; Krantz *et al.,* 2009). In *S. cerevisiae*, the Hog1 pathway has two upstream osmosensing branches (Sln1p and Sho1p). Sln1p activates Ssk2p/Ssk22p MAPKKKs by TCS phosphorelay in high osmoslarity and Sho1p, another hybrid histidine kinase as an osmolarity sensor, activates Pbs2p phosphorylation **(Fig. 36)** (Gustin *et al.*, 1998; Hohmann, 2002; Posas and Saito, 1997). Similar to *S. cerevisia*, the Hog1 pathway in *Candida albicans* is required to cope wiht high osmolarity stress. In addition, the Hog1 pathway is also activated by oxidative stress. Activation of this pathway is important for the survival of *C. albicans* within phagocytes that produce oxidative stress (Alonso-Monge *et al.,* 1999). In *N. crassa*, the OS MAPK pathway is homologous to the *S. cerevisia* Hog1 pathway. Besides the function on the response to osmolarity, fungicide, oxidative stress, the MAPK OS pathway works as the output pathway of the circadian clock (Banno *et al.*, 2007; de Paula *et al.*, 2008; Jones *et al.*, 2007; Krantz *et al.*, 2006; Lamb *et al.*, 2012; Lamb *et al.*, 2011; Noguchi *et al.*, 2007; Vitalini *et al.*, 2007). The WCC indirectly regulates the rhythmic expression of the *hpt-1* gene which encodes HPt or directly binds to the promoter of the *os-4* MPKKK gene in response to light and rhythmically in constant light (Lamb *et al.*, 2011). In this way, the circadian clock controls rhythmic phosphorylation of the p38-like MAPK OS (de Paula *et al.*, 2008; Lamb *et al.*, 2011; Vitalini *et al.*, 2007).

In parallel to our work, the group of Alfredo Herrera-Estrella (Irapuato, Mexico) found in *T. atroviride* that blue light untilizes the MAPK Tmk3 pathway, homologous to the SakA

pathway, for light signaling (Esquivel-Naranjo *et al.*, 2016). The MAPK Tmk3 was phosphorylated immediately when the mycelia was exposed to light, which was dependent of the blue light receptor Blr1. However, how the light signal is transmitted to the Tmk3 pathway still remains elusive. Additionally, light stimulated the tolerance to osmostic stress independently of Blr1. Mutants lacking Tmk3 and the MAPKK Pbs2 were all highly sensitive to osmotic and oxidative stresses, cell wall damage, high temperature, cadmium, and UV light.

In *A. nidulans*, the SakA pathway responds to oxidative stress, osmolarity and fungicide treatment (Hagiwara *et al.*, 2009a; Kawasaki *et al.*, 2002). Results in this study definitely show *A. nidulans* responds to light through the SakA pathway. In immunostaining analyses, blue light also phosphorylated SakA in an FphA-dependent manner, but LreA and LreB were not essential. This implies that other blue light receptors perhaps play a role in this case. The recombinant bacterial phytochrome Cph2 has the ability to sense blue light (Wu and Lagarias, 2000). Therefore, FphA possibly also senses blue light. SakA shuttling under salt stress was independent of FphA, which demonstrates HKs but not FphA are involved in osmosensing. Under oxidative stress, SakA physically and functionally interacts with the bZIP transcription factor AtfA, when oxidative stress stress is imposed (Balazs *et al.*, 2010; Lara-Rojas *et al.*, 2011). It would be interesting to check whether and which light condition can stimulate the interaction, and whether this interaction depends on FphA. The parent strain and the *sakA*-recomplemented mutant (M6-9+*sakA*) could grow at 42 °C in the absence of uracil and uridine in the dark but mutant M6-9 cannot, suggesting that the *SakA* pathway probably is also involved in temperature sensing.

2.4 FphA transmits light signal with spatially cytoplasmic and nuclear manners

FphA interacts with the WCC that stimulates sexual development and mycotoxin biosynthesis. Deletion of LreA or lreB attenuates cleistothecia production and sterigmatocystin biosynthesis (Purschwitz *et al.*, 2009; Purschwitz *et al.*, 2008). Furthermore, FphA also interacts with VeA, which is a global regulator of sexual development and also regulates secondary metabolism (Bayram *et al.*, 2008b; Purschwitz *et al.*, 2009; Purschwitz *et al.*, 2008). However, these interactions all occur in the nucleus, though FphA localization is mainly cytoplasmic and VeA localizes in both cytoplasm and nucleus and accumulates in the nucleus in response to light (Bayram *et al.*, 2008b; Purschwitz *et al.*, 2008). Latest studies has revealed that FphA modulating *ccgA* expression involves different transcription factors and histone H3 modification. LreA interacts with the acetyltransferase GcnE and the histone deacetylase HadA respectively. VeA binds to the *ccgA* promoter in an FphA-dependent manner and LreA binds to the *ccgA* promoter in the dark in a VeA-dependent manner and is released in response to

light (Hedtke *et al.*, 2015).

Beyond the interaction between FphA and VeA, FphA inhibits *veA* expression somehow in light. To check if FphA directly binds to the *veA* promoter we performed many times chromatin immunoprecipitation (ChIP). However, we did not see the enrichment of FphA on the *veA* promoter (data not shown). How FphA regulates *veA* gene expression needs to be elucidated in the future. Moreover, the interaction between FphA and CryA (data not shown), makes the regulatory role of FphA more comlex and interesting.

Interaction beween FphA and YpdA is cytoplasmic, though YpdA localizes in both cytoplasm and nucleus. In *S. cerevisiae*, Ypd1 transmits the osmotic stress signal from Sln1p on the plasma membrane to Ssk1p in the cytosol and Skn7p in the nucleus (Lu *et al.*, 2003). Ssk1p activates the Hog1 pathway in the cytoplasm and Skn7p is a transcription factor in the nucleus controlling the expression of genes related to cell wall integrity and other processes (Levin, 2005; Morgan *et al.*, 1997; Posas *et al.*, 1996). However, translocation of YpdA upon illumination is not observed. Nuclear YpdA perhaps interacts with other HKs to respond to other internal or external signals. FphA localization is mainly cytoplasmic and the signal of GFP-tagged FphA expressed under the control of the *alcA* promoter in the nucleus is pretty weak in comparison to the signal in cytoplasm (Blumenstein *et al.*, 2005). FphA dimers also mainly distribute in the cytoplasm, which was verified with BiFC by tagging FphA to the N-terminus and the C-terminus of YFP respectively (Blumenstein *et al.*, 2005). Likely, dimerized FphA interacts with YpdA in the cytoplasm and FphA in the nucleus interacts with other components but not YpdA to transmit the light signal.

Based on this study we proposed the following models of light signaling in *A. nidulans* **(Fig. 37)**. In the cytoplasm, a FphA dimer activates the SakA pathway and the phosphorylated SakA translocates into nucleus, leading to gene expression; in the nucleus, FphA interacts with the WCC and VeA, to implement a subtle regulation of light response by modifying histone H9K acetylation.

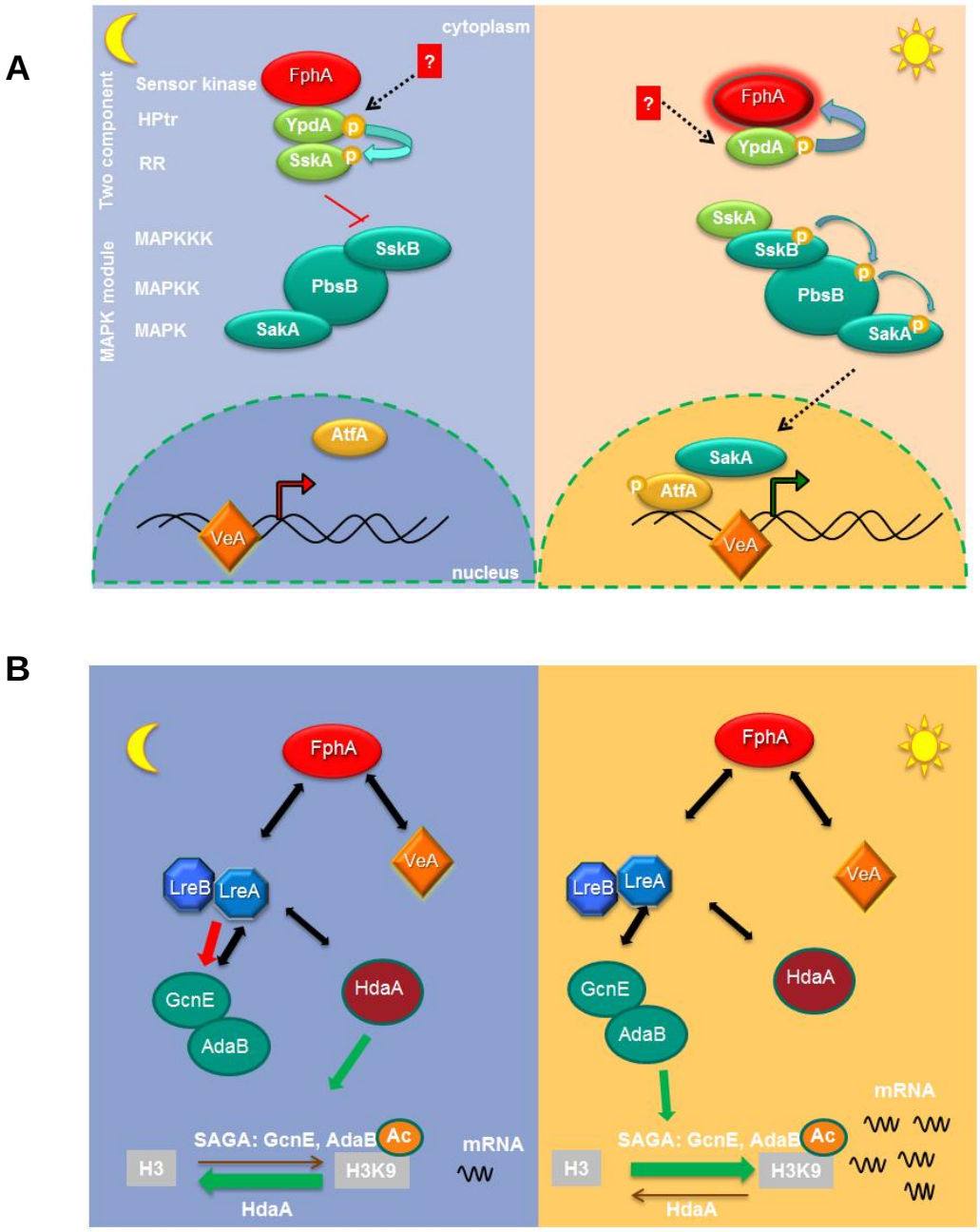

Fig. 37. Proposed model of light signaling in *A. nidulans.* (A) Light signaling starts from the cytoplasm. In the dark, phytochrome does not receive the phosphate from the histidine phosphotransferase YpdA that is probably phosphorylated by other histidine kinases. Phosphorylated YpdA donates the phosphate to the response regulator SskA. Phosphorylated SskA cannot bind to the MAPKKK SskB. In this case, SskB cannot undergo auto-phosphorylation leading to inactivation of the SakA pathway. Unphosphorylated SakA is retained in the cytoplasm and the transcription factor AtfA remains unphoshorylated. Light-inducible genes cannot be induced. On the contrary, upon light the response regulator of phytochrome accepts the phosphate from YpdA, which results in low levels of phosphorylated SskA. Unphosphorylated SskA binds to SskB that undergoes auto-phosphorylation activating the SakA pathway. Phosphorylated SakA shuttles into nucleus and phosphorylates AtfA. Phosphorylated AtfA

activates gene expression. **(B)** Light signaling modified by histone H3K9 acetylation. In the dark, LreA and VeA recruit both the acetyltransferase GcnE and the deacetylase HdaA to the *ccgA* promoter locus of light-inducible genes. The activity of GcnE is inhibited by LreA and thus *ccgA* is silenced. In light, LreA is released from the *ccgA* promoter. VeA and FphA promote GcnE activity and *ccgA* is induced.

2.5 TCS phosphorelays coordinate asexual and sexual development under different environmental cues through the SakA pathway

TcsA is not essential for vegetative growth but the *tscA*-deletion strain is unable to produce conidia on standard *A. nidulans* medium. However, this defect can be rescued by imposing salt stress (1M sorbitol) (Virginia *et al.*, 2000). The *tcsB*-deletion strain has no detectable phenotype (Furukawa *et al.*, 2005; Furukawa *et al.*, 2002). NikA also regulates asexual development, vegetative growth and conidiospore viability (Hagiwara *et al.*, 2007b; Hagiwara *et al.*, 2009b; Vargas-Perez *et al.*, 2007). The response regulators, SskA and SrrA are both involved in asexual development (Hagiwara *et al.*, 2007a). However, since most studies on TcsA, TcsB and NikA were performed with *veA1* background strains, whose sexual development is defective to some extent, the role of these HKs in sexual development is not well studied.

Light as an important extracellular signal regulates asexual and sexual development of *A. nidulans* (Blumenstein *et al.*, 2005; Mooney and Yager, 1990). In light, more conidia and less cleistothecia are produced than in the dark. FphA represses sexual development and the *fphA*-deletion strain produces more or less the same amount of cleistothecia in light than the wild type in the dark (Blumenstein *et al.*, 2005; Purschwitz *et al.*, 2006; Purschwitz *et al.*, 2008; Rodriguez-Romero *et al.*, 2010). Production of conidiospores in the *fphA*-deletion strain is slightly reduced. Therefore, it appears that some HKs are involved in asexual development but in light FphA controls sexual development. Different HKs collaborate to regulate development under ever-changing environmental signals through the SakA pathway, which is further proven with the phenotype of the *sakA*-deletion strain in a *veA* background. In the *sakA*-deletion strain, asexual development is shifted to sexual development, which means SakA has more comprehensive roles on controlling development than any single HK. In the *atfA*-deletion strain, sexual development is also de-repressed (Lara-Rojas *et al.*, 2011). The signals from different HKs are partially integrated at SskA and go into SakA pathway eventually. Indeed, the *sskA*-deletion strain in a *veA* background has similar phenotype as the *sakA*-deletion strain (data not shown). Therefore, TCS phosphorelays coordinate asexual and sexual development under different environmental cues through the SakA pathway.

3 MetR is involved in light signaling by controlling FphA expression

Sulfur is present in macromolecules (i.g. lipids, proteins, electron carriers and intermediary metabolites) that are essential for cellular functions of all organisms. The sulfur metabolism system has been well studied in fungal species such as *A. nidulans*, *N. crassa* and *S. cerevisiae* (Marzluf, 1997; Thomas and Surdin-Kerjan, 1997). In *N. crassa*, the expression of sulfur metabolism genes is coordinated by the positive regulator CYS3 that is a basic region-leucine zipper (bZIP) transcription factor and the negative regulator, SCON (sulfur controller). *N. crassa* CYS3 is one of the best studied bZIP transcription factors and the encoding gene *cys3* is highly induced when sulfur is limiting (Marzluf and Metzenberg, 1968; Paietta *et al.*, 1987). CYS3 is functional as a homodimer and recognizes a palindromic sequence ATGRYRYCAT in the promoter of sulfur metabolism genes (Kanaan *et al.*, 1992; Li and Marzluf, 1996). bZIP transcription factors controlling sulfur metabolism are also characterized in *S. cerevisiae*, *A. nidulans*, *A. fumigatus* and *Schizosaccharomyces pombe* (Amich *et al.*, 2013; Harrison *et al.*, 2005; Natorff *et al.*, 2003; Pilsyk *et al.*, 2015; Thomas and Surdin-Kerjan, 1997). The homolog of CYS3 in *A. nidulans* is MetR which controls sulfur assimilation (Natorff *et al.*, 2003). Becasue the bZIP domain of CYS3 can replace the function of bZIP domain of MetR, MetR likely can recognize the same palindromic sequence ATGRYRYCAT. However, in contrast to CYS3, MetR expression is not regulated by the sulfur status. Interestingly, another bZIP transcription factor MetZ, is regulated by the sulfur status and the expression of *metZ* is dependent on MetR (Pilsyk *et al.*, 2015). Constitutive expression of the *metZ* gene in the *metR*-deletion strain activates the expression of genes related to the sulfur metabolism and partially complements the phenotype of the *metR*-deletion strain (Pilsyk *et al.*, 2015).

In *S. cerevisiae*, an F-box protein can assemble with the SCF (Skplp/Cdc53p/F-box) complex which functions as E3 ubiquitin ligases. The F-box containing complex is responsible for ubiquitin-mediated proteolysis (Skowyra *et al.*, 1997; Zheng *et al.*, 2002). In the *S. cerevisiae* sulfur metabolism system, the F-box protein Met30 assembles with SCF to ubiquitinate the bZIP transcription factor Met4 (Kaiser *et al.*, 2000; Kuras *et al.*, 1996), resulting in the inactivation or degradation of Met4 (Kaiser *et al.*, 2000; Menant *et al.*, 2006). In *N. crassa*, SCON2 is an F-box protein and functions as a repressor of sulfur metabolism gene expression. SCON2 interacts with SCON3, which is the homologue of *S. cerevisiae* Skp1p and the interaction depends on the F-box. The homologues of Met30 and Skp1 in *A. nidulans* are SconB and SconC, respectively (Natorff *et al.*, 1998; Piotrowska *et al.*, 2000).

Sienko *et al.* has shown the mutations in *cysB*, *sconB* or *sconC* can induce the genes related to the stress response in *A. nidulans* (Sienko *et al.*, 2014). The *cysB* gene encodes the cysteine synthase that converts sulfide to cysteine (Topczewski *et al.*, 1997). In that scenario, microarray analysis was performed with three mutants (*cysB*, *sconB* and *sconC*) (Sienko *et al.*, 2014). The up-regulated genes related to TCSs, temperature response, heat shock response and osmosensing were present in all three mutants. HHKs encoding genes (*phkB*, *hk-8-1*, *hk-8-2* and *hk-8-3*) and the HPt encoding gene *ypdA*, were up-regulated in all three mutants and three other HHKs encoding genes (*tcsB*, *hk2*, and *hk-8-5*) only in the *sconC* mutant. Intriguingly, *sakA* and *aftA* were both up-regulated in all three mutants. MetR strictly controlled *fphA* expression by which it regulates the induction of *conJ* and *ccgA*, demonstrating the cross talk between sulfur metabolism and light sensing. Since earlier studies on sulfur metabolism were done in a *veA1* background strain, the regulatory role of MetR on sexual development was not analyzed. Our study clearly demonstrates MetR plays similar role as FphA on the repression of sexual development and the control of the light induction of *ccgA* and *conJ* genes. Beyond the interaction between FphA and VeA, MetR and FphA also repress *veA* gene expression when the mycelia are exposed to light, which suggests the connection between sulfur metabolism and secondary metabolism. It would be interesting to study the secondary metabolism in a *metR1* mutant.

4 FphA as a potential thermosensor

In response to heat shock, organisms encode more heat shock protiens (HSPs) to fulfill intracellular repair mechanisms (Guisbert *et al.*, 2008). Some of them are chaperones that aid in protein folding or target misfolded protein to protease for degradation (Vabulas *et al.*, 2010). The transcriptional response stimulated by heat shock is regulated by the heat shock transcription factors (HSFs), which are conserved from fungi to humans (Sorger *et al.*, 1987; Wiederrecht *et al.*, 1987). In *C. albicans*, Hsp90 regultes global gene expression by modulating nucleosome levels at promoters of stress-responsive genes and and protein homoeostasis via repressive effects on Hsf1 (Leach *et al.*, 2016).

In plants, crosstalk between light and temperature impacts on seed germination, shade avoidance and flowering. Temperature signaling is integrated into light signaling in plants but the light receptor as a themosensor has not been reported (Lorenzo *et al.*, 2016). Recently, temperature-dependent histidine kinase activity of bacterial phytochrome Agp1 from *Agrobacterium tumefaciens* has been revealed (Njimona and Lamparter, 2011; Njimona *et al.*, 2014). When the ambient temperature increases from 25 °C to 35 °C, the phosphorylation activity of far-red and red light irradiated holoprotein

decreases. The phosphorylation activity of holoprotein increases when the temperature increases from 5 °C to 25 °C (Njimona *et al.*, 2014). Similar temperature-dependent histidine activity of cyanobacterial phytochrome, Cph1, was also observed (Njimona *et al.*, 2014). The absorption spectra of the sensory core (PAS-GAF-PHY) of cyanobacterial phytochrome, is temperature-dependent and the spectra shifts are fully reversible in the range from 4 to 43 °C (Kim *et al.*, 2014). However, *in vivo* the effect of temperature sensing mediated by Agp1 and Cph1 remains obscure. The impact of Cph1 on gene expression is rather low (Hubschmann *et al.*, 2005).

In fungi, the SakA pathway plays a role in the adaption to temperature stress (Ji *et al.*, 2012). To adapt to temperature changes in the environment and host cells, *A. fumigatus* is able to grow at 50°C and even survives up to 75°C (Hartmann *et al.*, 2011). The vegetative growth of a *tcsB*-deletion stain is more sensitive to higher temperatures (48°C) in comparison to wild type and the germination rate of conidia is dramatically decreased at high temperature (Ji *et al.*, 2012). Cold stress can activate the SakA pathway in a TcsB-dependent manner (Ji *et al.*, 2012). In the koji mold *Aspergillus kawachii*, gene expression of *ypdA*, *hogA* and *atfA* in the HogA pathway is down-regulated when the temperature lowers from 40 to 30°C (Futagami *et al.*, 2015). In the pathogenic dimorphic fungus *Penicillium marneffei*, *atfA* is induced under heat stress at 42 °C (Nimmanee *et al.*, 2014).

Temperature-induction of *ccgA* and *conJ* was dependent of FphA and SakA, implying that FphA and the SakA pathway in *A. nidulans* are involved in temperature sensing. Since the absorption spectra of the sensory core (PAS-GAF-PHY) of cyanobacterial phytochrome depends on temperature (Kim *et al.*, 2014), the conformation of the sensor domain of FphA possibly is also affected by temperature. Therefore, a temperature shift causes the conformational change of the sensor domain, which perhaps is independent of the cysteine residue 195 (C195) **(Fig. 38)**. The conformational change causes the autophosphorylation of HKD, leading to the exposure of aspartate residue 1181 (D1181) to YpdA. Phosphoryl group transfer from YpdA to the RRD activates the SakA pathway.

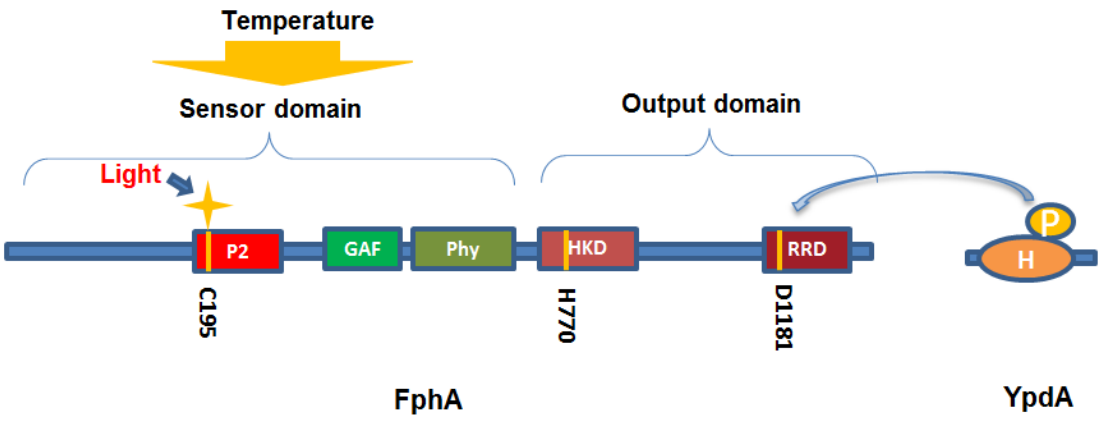

Fig. 38. Putative scheme of FphA as a photoreceptor and a potential thermosensor. As a photoreceptor, cysteine at postion 195 (C195) is essential. The light stimulus causes the conformational change of the bilin, resulting in the structural change of the sensor domain, which leads to the autophosphorylation of the HK domain. The autophophorylation of the HKD causes the structural change of the output domain and hence the RRD is exposed to YpdA and accepts the phosphoryl group. However, as a temperature sensor, C195 is not necessary. Temperature changes the conformation of the sensor domain and hence causes the autophosphorylation of HKD and the RRD is exposed to YpdA. The phosphoryl group is also transferred from YpdA to the RRD.

To prove that C195 is not essential, cycteine 195 can be changed to alanine (C195A) and in this case, FphA^{C185A} should still function as a themosensor. The necessity of histidine residue 770 can be analysed with the *fphA*^{H770A} and *fphA*^{H770Q} mutants. Since in the *fphA*^{H770Q} mutant, negatively charged glutamine may change the conformation of the output domain, *ccgA* and *conJ* are supposed to be induced constitutively. In the *fphA*^{D1811A} mutant, neither light stimulus nor temperature shift can activate the SakA pathway. Whether FphA participates in the HSP and HSF based heat shock response also needs to be elucidated in the future.

Materials and methods

1 Chemicals and equipment used in this study

The common chemicals used in this study were purchased from the company Roth (Karlsruhe), Roche (Mannheim), Sigma Aldrich (Seelze), Sigma (Taufkirchen)，Invitrogen (Karlsruhe), Applichem (Darmstadt) and Serva Feinbiochemica (Heidelberg). DNA polymerases for PCR, restriction endonucleases and makers for DNA and protein were produced by New England Biolabs (Frankfurt) and Fermentas (St-Leon-Rot). Other chemicals were indicated in the text. Equipment used in this study are listed in **Table 1**.

Table 1. Equipments used in this study

Equipment	Type	Manufacturer
Real-Time PCR	MyiQ^{TM} Single Color Real-Time	Bio-Rad, USA
Detection System	PCR Detection	
Microscopy	Axio Imager. Z1	Carl Zeiss Microlmaging GmbH, Germany
Autoclave	Systec 3850 ELV	Systec GmbH, Wettenberg
	Systec VE-75	Systec GmbH, Wettenberg
Digital camera	Canon PowerShot G15	Canon, Japan
Thermocycler	Labcycler & Gradient	SensoQuest GmbH
Heating block	Thermo mixer 5436	Eppendorf, Germany
Hybridization oven	UVP hb-1000 Hybridizer	UVP, USA
Power supply apparatus	Power Pac 3000	Bio-Rad, Munich
Shaker/ incubator	Heraeus-Brutschrank Baureihe 6000	Kendro, Langenselbold
	HT Infors	Infors AG, Switzerland
	Kleinschüttler KM-2	Edmund Bühler GmbH, Tübingen
UV-cross Linker	UV Stratalinker 2400	Stratagene, Heidelberg

pH meter	Hanna HI 208	Hanna, Romania
Magnetic stirrer	Heidolph MR3000	Heidolph, Germany
Homogenizer	Retsch MM200	Retsch, Germany
Speed Vac	Savant sc110	Savant, USA
Weighing instrument	Kern 440-47N	Sartorius, Göttingen
	Sartorius R200D	Kern, Germany

2 Microbiological methods

2.1 *Escherichia coli* cultivation and transformation

Competent cells were mixed with ligation samples and incubated on ice for 15~30 minutes. The mixture was incubated in 42 °C water bath for 2 minutes. 400 ml SOC medium was added and the mixture was incubated at 37 °C at 180 rpm for 1 hour. After the incubation 80 µl culture was added to a LB plate supplemented with ampicillin (100 µg/ml). The plates were incubated at 37 °C overnight. The colonies of *E. coli* were picked with toothpicks and cultured in test tubes. The positive clone was determined by colony PCR or by digesting the isolated plasmids with restriction enzyme. Medium used for *E. coli* cultivation are listed in **Table 2**.

Table 2. Medium for *E. coli*

Medium	Ingredients (1 liter)
Luria-Bertani (LB)	10 g Trypton; 10 g Yeast extract; 5 g NaCl; pH 7.5
SOC	20 g Trypton; 5 g Yeast extract; 0.58 g NaCl; 0.185 g KCl; 2.03 g $MgCl_2 \times 7H_2O$; 2.46 g $MgSO_4 \times 7H_2O$; 3.6 g glucose

2.2 *A. nidulans* transformation

Fresh conidia were inoculated in 500 ml supplemented liquid minimal medium and incubated at 37 °C at 180 rpm overnight. The mycelia were washed with solution 1 and harvested with sterilized miracloth by filtration. 1~2 g mycelia were added to a sterilized 50 ml falcon tube with 5 ml solution 2. 180 mg glucanex was dissolved in 1 ml H_2O and afterwards the solution was added to a falcon tube. The mixture was kept on ice for 5 minutes and further mixed with BSA solution (10 mg BSA in 0.5 ml H_2O). The mixture was moved to a 100 ml Erlenmeyer flask and incubated at 30 °C at 80 rpm for 1.5 hours. After the digestion, the mixture was added into a new 50 ml falcon tube and solution 3

was added on top the mixture very gently with a pipet. The falcon tubes were centrifuged 18 minutes at 5,000 rpm at 4°C. The interphase containing the potoplast was taken out with a 1 ml pipet to a new falcon tube. 10 ml solution 4 was added to the falcon tube and was centrifuged 15 minutes at 5,000 rpm at 4 °C. The supernatant was discarded and the pellet was resuspended with 1 ml solution 4. The mixture was moved to a 1 ml Eppendorf tube. After 5 minutes centrifuged at 2,800 rcf, the supernatant was discarded and the pellet was resuspended in 200 µl solution 5.

0.5~4 µg DNA was mixed with 200 µl protoplast and 50 µl solution 6 in a 10 ml falcon tube. The mixture was incubated on ice for 20 minutes. 1 ml solution 6 was added to the mixture and the falcon tube was kept at room temperature for 5 minutes. 5 ml solution 5 was added to dilute the mixture. 5 ml pre-warmed top-MMR medium was added and mixed by inverting. The mixture was poured on 3~5 supplemented MMR agar plates. The plates were incubated at 30 °C for 3~5 days.

Table 3. Solutions used for *A. nidulans* transformation.

Buffer or medium	Composition
Solution 1	0.6 M $MgSO_4$
Solution 2	1.2 M $MgSO_4$, 10 mM Na_3PO_4 buffer, pH 5.8
Solution 4	0.6 M sorbitol, 0.1 M Tris-HCl, pH 7.0
Solution 5	1.2 M sorbitol, 10 mM $CaCl_2$, 10 mM Tris-HCl, pH 7.5
Solution 6	60% PEG 4000, 10 mM $CaCl_2$, 10 mM Tris-HCl, pH 7.5
MMR	50 ml Salt stock solution; 1 ml Trace elements stock solution; 342 g saccharose; 15 g agar; pH 6.8; add 100 ml 10x glucose stock solution (200 g in 1 L H_2O) and 10 ml 100x Ammonium Tartrate stock solution (92 g in 1 L H_2O) after autoclaving
MMR-TOP	50 ml Salt stock solution; 1 ml Trace elements stock solution; 342 g saccharose; 6 g agar; pH 6.8

Table 4. Media and stock solutions for *A. nidulans* cultivation.

Medium or Stock	Ingredients (1 liter)
MM	50 ml 20x Salt stock solution; 1 ml 1000x Trace elements stock solution; 20 g glucose/20 g glycerol, 2 g glucose/20 g

	Threonin, 2 g glucose; pH 6.5
20x Salt stock solution	120 g $NaNO_3$; 10.4 g KCl; 10.4 g $MgSO_4$ x $7H_2O$; 30.4 g KH_2PO_4
1000x Trace elements stock solution	22 g $ZnSO_4$ x $7H_2O$; 11 g H_3BO_3; 5 g $MnCl_2$ x $4H_2O$; 5 g $FeSO_4$ x $7H_2O$; 1.6 g $CoCl_2$ x $5H_2O$; 1.6 g $CuSO_4$ x $5H_2O$; 1.1 g $(NH_4)_6Mo_7O_{24}$ x $4H_2O$; 50 g Na_4 EDTA; adjust pH to 6.5-6.8 using KOH
1000x Vitamin stock solution	0 .1 g D-Biotin; 0.1 g Pyrodoxin-HCl; 0.1 g Thiamin-HCl; 0.1 g Riboflavin; 0.1 g p-Aminobenzoic acid; 0.1 g Nicotinic acid

Table 5. Supplements of the medium.

Substance	Stock Concentration	Volume or weight per liter
Pyridoxin-HCl	0.1 %	1 ml
Arginin	500 mM	10 ml
Uracil	-	1 g
Uridin	-	1.2 g
p-Aminobenzoic acid (PABA)	0.1 %	1 ml
Riboflavin	0.25 %	1 ml

Table 6. Annotations of the genes shown in the genotypes.

Marker	Function	Chromosome	Reference
argB2	Arginine auxotrophy (ornithine carbamoyltransferase)	III	(Upshall et al., 1986)
bar	Glufosinate resistance	-	(Nayak et al., 2006)
biA1	Biotin auxotrophy	I	FGSC
pabaA1	Para aminobenzoic acid auxotrophy	I	FGSC
pyroA4	Pyridoxin auxotrophy	IV	FGSC

pyrG89	Uracil auxotrophy (orotidine-5'-phosphate decarboxylase)	I	(Balance et al., 1983)
riboB2	Riboflavin auxotrophy	VIII	(Kim et al., 2009)
trpC801	Tryptophan auxotrophy (phosphoribosylanthranilat isomerase)	VIII	(Yelton et al., 1984)
veA1	Truncated veA gene	VIII	FGSC
wA3	White spores (polyketide synthase)	II	(Mayorga & Timberlake, 1990)
yA2	Yellow spores (laccase)	I	(Aramayo et al., 1989)

Table 7. Strains used in this study.

Name	Genotype	Resource
SKV103	*pryG89; pyroA4; veA*$^{+}$	(Vienken and Fischer, 2006)
SJP1	*pyrG89; ΔargB::trpCDB; pyroA4; ΔfphA::argB; veA*$^{+}$	(Purschwitz *et al.*, 2008)
SJP70	*pyrG89; ΔlreB::argB; ΔargB::trpCDB; pyroA4; veA*$^{+}$	(Purschwitz *et al.*, 2008)
SJR2	*pryG89; pyroA4, nkuA::bar; veA*$^{+}$	(Herr and Fischer, 2014)
SJR10	*pyrG89; ΔargB::trpCΔB; pyroA4, nkuA::bar; ΔfphA::argB; veA*$^{+}$	(Hedtke *et al.*, 2015)
SSR66	*yA2; pyroA4, nkuA::bar; ΔlreA::ptrA; pabaA1; veA*$^{+}$	(Hedtke *et al.*, 2015)
SSR89	*yA2; ΔlreB::agrgB; pyroA4, nkuA::bar; ΔlreA::ptrA; pabaA1; veA*$^{+}$	(Hedtke *et al.*, 2015)
TδsskA-riboB	*pyrG89; ΔsskA::AfriboB, pyroA4, ΔnkuA::argB; riboB2, veA1**	(Vargas-Perez *et al.*, 2007)
TFLΔsakA-03	*pyrG89; ΔsakA::AfriboB; pyroA4, ΔnkuA::argB;*	(Lara-Rojas *et al.*,

	riboB2, veA1	2011)
TFLΔatfA-02	*yA2, pyrG89; ΔatfA::AfpyrG; pabaA1; veA1*	(Lara-Rojas *et al.*, 2011)
TFL6	*pyrG89; sakA(p)::sakA::GFP::AfpyrG; pyroA4, ΔnkuA::bar; veA1*	(Lara-Rojas *et al.*, 2011)
A1166	*pyrG89; wA3; argB2; nkuA::argB pyroA4; pbsB::AfpyrG, se15, nirA14, chaA1, fwA1*	(De Souza *et al.*, 2013)
A1293	*pyrG89; wA3; argB2; nkuA::argB pyroA4; sskB::AfpyrG, se15, nirA14, chaA1, fwA1*	(De Souza *et al.*, 2013)
GR5	*pyrG89; wA3; pyroA4; veA1*	(Waring *et al.*, 1989)
SSM9	GR5 transformed with *pJP2 (alcA::GFP::fphA)*	(Purschwitz *et al.*, 2008)
SJP109	SJP1 transformed with pJP8 (*alcA::GFP::HKRR*)	(Purschwitz *et al.*, 2009)
SJP66	GR5 transformed with pJP10 (*alcA::GFP::RR*)	(Purschwitz *et al.*, 2009)
RM114	*metR1; pyroA4; yA2*	(Natorff *et al.*, 2003)
SKV104	*yA2, pyrG89; pyroA4; pabaA1; veA*$^{+}$	this study
M1-22	Bind mutant from UV-mutagenesis	this study
M6-9	Bind mutant from UV-mutagenesis	this study
M7-25	Bind mutant from UV-mutagenesis	this study
M8-17	Bind mutant from UV-mutagenesis	this study
M10-13	Bind mutant from UV-mutagenesis	this study
M13-14	Bind mutant from UV-mutagenesis	this study
M15-1	Bind mutant from UV-mutagenesis	this study
M17-1	Mutant from UV-mutagenesis	this study
MD3-8	Dominant mutant from UV-mutagenesis	this study
MD6-6	Dominant mutant from UV-mutagenesis	this study
MD5-1	Dominant mutant from UV-mutagenesis	this study
MD15-16	Dominant mutant from UV-mutagenesis	this study
SZY17	SKV104 transformed with pZY19 (*conJ(p)::pyr4, pyroA4)*	this study
SJR3	*argB2; pyroA4, nkuA::bar; veA*$^{+}$	this study

SZY31	TFLDsakA-03 crossed to SJR3*; pyrG89; ΔsakA::AfriboB; pyroA4*, *ΔnkuA::argB; veA*$^+$	this study
SZY34	*pyrG89; sakA(p)::sakA::GFP::AfpyrG; pyroA4*, *nkuA::bar; VeA*$^+$	this study
SYZ35	*yA2; sakA(p)::sakA::GFP::AfpyrG; pyroA4*, *nkuA::bar; ΔlreA::ptrA; pabaA1; veA*$^+$	this study
SZY36	*pyrG89; ΔlreB::agrgB; sakA(p)::sakA::GFP::AfpyrG; pyroA4*, *nkuA::bar; veA*$^+$	this study
SZY37	*ΔargB::trpCΔB, sakA(p)::sakA::GFP::AfpyrG; pyroA4, nkuA::bar; ΔfphA::argB; veA*$^+$	this study
SZY38	*pyrG89; pyroA4; alcA::YFP-C::fphA::pyr4; alcA::YFP-N::ypdA::pyroA; alcA(p)::stuA(NLS)::DsRed; veA*$^+$	this study
SZY39	*pyrG89; pyroA4; alcA::YFP-C::fphA::pyr4; alcA::YFP-N::sskA::pyroA; alcA(p)::stuA(NLS)::DsRed; VeA*$^+$	this study
SZY41	TΔsskA-riboB crossed to SJR3*; pyrG89; ΔsskA::AfriboB, pyroA4*, *nkuA::bar; veA*$^+$	this study
SZY42	TFLΔatfA-02 crossed to SJR3; *yA2, pyrG89; pyroA4, nkuA::bar; ΔatfA::AfpyrG; pabaA1; veA*$^+$	this study
SZY44	*pyrG89; pyroA4; alcA::YFP-C::fphA::pyr4; alcA::YFP-N::TcsB::pyroA; alcA(p)::stuA(NLS)::DsRed; VeA*$^+$	this study
SZY45	M6-9 co-transformed with plasmid pCK17 (*pabaA1* gene) and pZY30 (*sakA* gene)	this study
SSM39	*alcA::fphA::3xHA; pyrG89, veA*$^+$	this study
SZY49	SKV103 transformed with plasmid pZY35	this study
SZY50	SSM39 transformed with plasmid pZY35	this study
SZY61	RM114 crossed to SJR3; *metR1, pyroA4, nku::bar, veA*$^+$	this study
SZY63	SJR2 transformed with plasmid pZY27	this study
SZY64	SZY17 crossed to SJR3; *argB2* background and harbors pZY19 (*conJ(p)::pyr4, pyroA4)*	this study

2.3 UV mutagenesis

Fresh conidiaspores were washed off from a newly-prepared plate with distilled water and the spore suspension in 10 ml falcon tube was incubated on ice for 20 minutes. The supernatant was moved into a new falcon tube and the mycelium pellet was discarded. The concentration of conidiaspores was diluted to 1.2×10^4 conidia/ml. 400 µl conidia suspension were added to Ø 14 cm Petri dish with 100 ml solid minimal medium supplemented with p-aminobenzoic acid (PABA). In order to make a survival rate curve, the plates were illuminated in a UV Stratalinker 1800 crosslinker (Stratagene, La Jolla, CA) with a dosage of 0 mJ, 10 mJ, 15 mJ, 20 mJ or 25 mJ. After UV treatment, the plates were incubated in white light at 37 °C for 3 days. The colonies on each plate were counted. The survival rate at the dosage of 0 mJ was set as 100% and the others were normalized to it. According to the survival rate curve, we used a dosage of 15 J to treat each plate to get a survival rate of 25%. 50 plates were treated for each round of screening. After UV treatment, the plates were incubated in white light at 37 °C for 3 days to screen *blind* mutants or in the dark to screen dominant mutants.

2.4 Quantification of conidiospores and cleistothicia

The fresh conidia were washed down with water from newly-cultivated plates. Top minimal medium (0.75 % agar) was heated until melted and then kept in 50 °C water bath to prevent the solidification. The conidia suspension was diluted in top minimal medium to get a final concentration of 10^4 conidia/ml. 2 ml top minimal medium was added on the surface of each minimal medium plate, which was incubated at 37 °C for 5 days in the dark or light afterwards. Agar pieces were cut out with Φ 8 mm puncher for quantification. The cleistothicia were counted on each agar piece under stereomicroscopy. The conidiospores on each agar piece were washed down with 2 ml of 2% Tween in a 2 ml Eppendorf tube by shaking at 37 °C for 1 hour. The spore suspensions were diluted and the number of conidiospores was counted with counting chamber.

3 Molecular biological methods

3.1 Polymerase Chain Reaction (PCR)

Polymerase chain reaction (PCR) was performed with Taq or Phusion polymerases from New England Biolabs (NEB, Frankfurt am Main) according to manufacturer protocols. Oligonucleotides synthesis was performed by MWG Biotech (Ebersberg), and the final concentration was 0.2 µM in 25 µl or 50 µl PCR reactions, in which ~10 ng plasmid DNA or ~100 ng genomic DNA were used as templates. dNTPs were purchased from Roth (Karlsruhe) and the final concentration is 200 µM. The PCR reactions were carried out in

SensoQuest Labcycler (Göttingen). The PCR programs are changeable due to the length of the amplified fragments. After pre-denaturation at 98°C or 95°C for 30 sec or 5 min respectively, 25~32 cycles are executed with 95 °C/30 sec (Taq) or 98°C/10 s (Phusion) denaturation, annealing at 55~65 °C for 30 sec and elongation at 72°C at a speed of 1 kb/min (Taq) or 72°C at 1 kb/30 s (Phusion). For colony PCR of *E. coli*, Taq polymerase was used and the pre-denaturation time was 10 minutes. As for fusion PCR, 10 cycles were performed in the absence of primes followed by another 32 cycles with primers. The primers used in this study are listed in **Table 8**.

Table 8. Primers used in this study.

Name	Sequence (5'-> 3')	
conJ(p)_fwd	ATAATCCTAGGCGTTCGCTAGATCTGGCTAAAAC	Parent strain construction
conJ(p)_rev	CTATGCTCGAGTTTGATGTATTTAAAGAATTGGTTGTGGTTTG	
pyr4_fwd	CTTTACTCGAGATGTCGACAAGTCAGGAAACGCAG	
pyr4_rev	CAGTTGGATCCGATCTTCATCATTCGTCGCTTTCGGG	
h2b-RT-F	CTGCCGAGAAGAAGCCTAGCAC	real-time PCR
h2b-RT-R	GAAGAGTAGGTCTCCTTCCTGGTC	
ccgA-RT-F	CGACGCTTCCCTCACTTCTC	
ccgA-RT-R	CATCATGGGACTTCTCGTCCTT	
conJ-RT-F	CTGAGAAGCAGCGCAACATC	
conJ-RT-R	CTCATCGCCAGGCTGGAA	
PJR54(veA)	CTCACAGCCGAAACCAATCC	
PJR55(veA)	AAAGTCGTGTCTGCGAACCC	
fphA_RTQ_fw	ATGGAGGCGCTGTTGGATACAA	
fphA_RTQ_rev	CAGATCTATGCTCATCGTCGGA	
pyr4-rt-f	GACGGCGAAAGCACGACAGAG	
pyr4-rt-r	TCCTCTCCTGGTGGCGGCAAC	
HogA_recom_F	AACATACAGAGCCATCTCGAG	Complementation

HogA_recom_R	CAAGGTGAGACCGGCTCCAG	
Nest-SakA-F	TTACAGCTATTTCGTCACGGAGC	GFP tagging
Nest-SakA-R	CGTGACTGGCAGACTTACCG	
YpdA_YFP_F	GGGGCGCGCCCATGGCGTCAACTACAAC CACCAAGAC	Split YFP strain construction
YpdA_YFP_R	CCTTAATTAATTATGCTTTGGCGTCTTTTTT GGATTCTTC	
SskA_YFP_F	GGGGCGCGCCCATGTCGGAACGACGCTG GTCC	
SskA_YFP_R	CCTTAATTAACTAGAGAGCCCCGTCCTGTA CCG	
TcsB_YFP_F	GGGGCGCGCCCATGCGCGTTCCTATTGC CGT	
TcsB_YFP_R	CCTTAATTAATCACATCTGCGGTTTCTCCG C	
atfA_seq_f	TCTTCCACTCGGGACCACGGAT	Sequencing
atfA_seq_r	TAGTTGTTACAGTACGCCCGAGCC	
sskB_seq_f1	TTCGAGCTAGGACATGTGGCCG	
sskB_seq_f2	AGCTGCACGTCCAGGAGGAT	
sskA_seq_f2	CACCTCCCGACTATGGGATCG	
sskA_seq_f1	GCGTTCCATTCCAGCATGACTGAT	
AtfA_in_F	CCCCAGACTTCATTAGCACCTCC	
AtfA_in_R	ATGCGGCCCAAAGTCGACTG	
VeA+1789_rev	GGAGCCTTATTTCAGGCCGC	
VeA+1034_rev	GTGTGTGGAGTGGAGGAGGCG	

3.2 DNA purification

After the digestion or PCR, the samples were loaded on the gel. Afterwards DNA fregments were recovered with Zymoclean Gel DNA Recovery Kit (Zymo Research, US). The fragments digested with restriction enzymes could also be recovered directly with

innuPREP PCRpure Kit (AJ Innuscreen GmbH, Berlin). All the DNA fragments were eluted in water. The concentration of the purified DNA was determined with Nano drop 3000 (PeQLab, Erlangen).

Table 9. Solutions used for DNA agarose gel electrophoresis.

Solution	Composition
50x TAE buffer	40 mM Tris-Acetate; 1 mM EDTA; pH 8.0
1x Loading buffer	15% Ficoll 400; 5 mM EDTA (pH 8.0); 1% SDS; 1.5 M Bromphenol blue

3.3 DNA digestion, ligation and sequencing

Plasmids (1~5 µg) or DNA (0.5~1µg) fragments were digested with restriction endonucleases (AscI, PacI, XhoI or AvrII) in corresponding reaction buffers (NEB). Generally, the restriction endonuclease digestion was performed in a total volume of 50 µl, with 1µl restriction enzyme and the samples were incubated from 1 hour at 37 °C provided by the manufacturer.

DNA ligation was performed using T4 ligase (NEB) and the provided reaction buffer at RT for 20 minutes in a volume of 20 µl. The molar ratio of vector to insert was 1: 6 for cohesive end ligation. With respect to blunt end fragments, pJET1.2/blunt Cloning Vector (Fermentas, St. Leon-Rot) was used. After the ligation, the sample was transformed to competent cells directly.

The DNA fragments used for sequencing were amplified with phusion DNA polymerase from plasmids or genomic DNA. DNA fragments (10~15 ng/µl) were premixed in water with sequencing primers before sent out for sequencing and DNA sequencing was done commercially by MWG Biotech (Ebersberg).

3.4 Plasmid extraction from *E. coli* cells

The plasmids used for transformation were isolated with a NucleoSpin Plasmid EasyPure kit (MACHEREY-NAGEL, Düren) according to the manufacturer's protocols. For quick miniprep of plasmid DNA, an alkali-lysis method was used (Sambrook *et al.*, 1989). *E. coli* was cultured overnight in liquid LB medium and centrifuged at 13000 rpm for 1 minute. The *E. coli* pellet was resuspended in 200 µl Tris-EDTA Buffer and 200 µl alkali-lysis buffer were added and mixed gently. 200 µl neutralization buffer were added into an Eppendorf tube which afterwards was inverted 5-7 times. The samples were incubated on ice for 5 minutes and then centrifuged for 5 minutes. The supernatants were moved into new 1.5 ml tubes with 0.7 volume of isopropanol. To precipitate the

plasmid DNA, the samples were centrifuged for 10 minutes at 4 °C. The pellets were washed with 500 µl of 70% ethanol and diluted in 20 µl TE buffer.

Table 10. Solutions used for plasmid DNA extraction (miniprep).

Solution	Ingredient
Tris-EDTA buffer	5 ml 1M Tris-HCl (pH 7.5); 2 ml 0.5M EDTA (pH 8.0); 10 mg RNase in 100 ml
Alkali-lysis buffer	0.2 M NaOH; 1% SDS
Neutralization buffer	1.5 M Potassium Acetate, pH 4.8
TE buffer	10 mM Tris-HCl; 1 mM EDTA; pH 8.0

Table 11. Plasmids used in this study.

Name	Genotype	Resource
pJP4	*alcA(p):: YFP-NT::fphA; pyroA4*	(Blumenstein *et al.*, 2005)
pCK17	*pabaA1* gene in pCR2.1 TOPO vector	(Grünbacher *et al.*, 2014)
pJP5	*alcA(p):: YFP-CT::FphA; pyr4*	(Blumenstein *et al.*, 2005)
pJW18	*alcA(p)::stuA(NLS)::DsRed* in pBluescript KS-	(Toews *et al.*, 2004)
pJP17	*fphA* gene in pCR2.1 TOPO vector	Janina Purschwitz, Karlsruhe
pZY21	*sakA* gene in vector pJet1.2	this study
pZY24	*alcA(p)::YFP-N::SskA; pyroA4*	this study
pZY25	*alcA(p)::YFP-N::YpdA; pyroA4*	this study
pZY19	*conJ(p)::pyr4 cassette* replaced *alcA(p)*::*fphA* cassette in plasmid pJP4	this study
pZY35	*alcA(p)::GFP::YpdA; pyr4*	this study

3.5 Genomic DNA extraction from *A. nidulans* cells

Conidia were inoculated with an inoculation loop on the surface of 3 ml supplemented minimal medium in a small Petri dish and incubated at 37 °C overnight. The mycelia were collected by filtration and approximately 50 mg wet mycelia were used for DNA purification. The mycelia were added to a 1.5 ml Eppendorf tube containing 700 µl Ustilago lysis buffer and an Ø 3 mm metal bead. The cells were broken with a cell

homogenizer at 30 hits/min for 15 minutes. The samples were incubated at 68 °C in a thermo mixer for 1 hour. 100 µl of 8 M potassium acetate were added. The samples were kept on ice for 30 minutes and inverted 5~6 times during the incubation. After that, the samples were centrifuged at 13,000 rpm and 700 µl of supernatant were moved to a new Eppendorf tube with 700 µl of 100% ethanol and mixed well. The samples were centrifuged again for 15 minutes at 13,000 rpm and afterwards the supernatants were discarded. To wash the pellets, 500 µl of 70% ethanol were added to the tube with the pellet. The tubes were centrifuged at 13,000 rpm for 5 minutes and the supernatants were discarded. The tubes were centrifuged again for 5 seconds and the remaining supernatants were taken out with a pipette. The pellets were dried for 2 minutes and 30~50 µl TE/RNase A (20 µg/ml) were added to dissolve the pellet by keeping the sample at 50 °C for 10 minutes or overnight. 1~2 µl genomic DNA were loaded on the gel to check the integrity.

To purify the genomic DNA for whole genome sequencing, all the progenies were inoculated on the surface of the plates separately and incubated at 37 °C overnight. The mycelia were washed with water and collected by filtration. Mycelia from 5~10 progenies were mixed and ground in a big mortar with liquid nitrogen to break the cells. The powder was collected in a 1.5 ml Eppendorf tube. Afterwards, the genomic DNA was extracted with DNeasy® Plant Mini Kit (QIAGEN GmbH, Germany). The concentration of the genomic DNA was determined with Nano drop 3000 (PeQLab, Erlangen) and was normalized to a final concentration of 80 ng/µl.

Table 12. Solutions used for genomic DNA extraction.

Solution	Composition
Extraction buffer	1% SDS, 50 mM EDTA, 50 mM pH 7.5 Tris-HCl, dilution 1:1 with 1x TE
8 M Potassium Acetat (pH 4.2)	Dissolve 29.4 g Potassium Acetat in 50 ml dd H_2O, then add 11.5 ml 100% Acetic Acid and adjust the pH to 4.2 with HCl. Fill up to 100 ml with H_2O

3.6 Next generation sequencing (NGS)

1 µg of genomic DNA for each sample was sheared to 180bp using a Covaris S2 device (peak incidence power 100 W, duty factor 10%, cycles per burst 200, 430 seconds) and ligated to 5' and 3' adapters following the TruSeq PCR-free (Illumina) standard guidlines.). Paired end reads (2 x 50 nucleotides) were obtained with a Hiseq1500 using SBS v3 kits (Illumina). Cluster detection and base calling were performed using RTAv1.14 and quality

of reads assessed with CASAVA v1.8.1 (Illumina). The sequencing resulted in at least 22 million pairs of 50 nt long reads for each sample, with a mean Phred quality score > 30. The sequencing reads were mapped against the genome of *A.nidulans* (ASM1142v1.25) with the gap aligner bwa version 0.7.10 (Li and Durbin, 2009). Identification of SNP and indels was performed with HaplotypeCaller from GATK version 3.2.2 using the options -recoverDanglingHeads -dontUseSoftClippedBases -stand_call_conf 20.0 -stand_emit_conf 20.0. (McKenna *et al.*, 2010). The identification of causative mutations was performed on pairs of mutant and corresponding wild type strains with VEP using the exon-exon annotations availed from Ensembl fungi (release 75) and the options --symbol --check_existing --check_alleles --check_svs --total_length --numbers. Putative mutations candidates specific to mutants strains were obtained by using a custom Perl script and checked by visualisation of BAM files in the IGV genome browser. Depth of coverage was computed using with DepthOfCoverage from GATK version 3.2.2 with a bin size of 2000 base pair and the options --minMappingQuality 15 --minBaseQuality 10, averaged score coverage were scaled from 0 to 1 and visualise as wig file in the IGV genome browser.

3.7 RNA isolation and quantitative real-time PCR

Fresh conidia were inoculated on the surface of liquid supplemented minimal medium in Ø 3.5 cm petri dishes and cultivated in the dark for 18 hours. The mycelium was harvested in dim-green light directly or after 30 minutes illumination and frozen immediately in liquid nitrogen. A Fungal RNA Extraction kit from Omega was used to isolate RNA and cell disruption was performed with a cell homogenizer at 30 hits/min for 5 minutes. RNA was treated with TURBO DNA-free kit and diluted to 50 ng/µl with DEPC water. Quantitative real-time PCR was performed with SensiFAST SYBR & Fluorescein One-Step Kit from Bioline (Lueckenwalde). Each reaction is 25 µl with 0.2 µM primers and 100 ng RNA. The program starts with 10 minutes of reverse transcription reaction at 45 °C, followed 2.5 minutes at 95 °C for the inactivation reaction of reverse transcriptase and 40 cycles of polymerase chain reaction (10 s at 95 °C and then 30 s at 58 °C). To assess the dissociation-characteristics of two-stranded DNA, melting curve analyses were carried out (80 cycles, 95 °C to 58 °C with 10 s per step). H2B was used for normalization. Each expression level is the average of three biological replicates. Primers used for real-time PCR are listed in **Table 8**.

3.8 Tagging of proteins with GFP, split YFP and HA

In order to localize SakA in wild type and the *fphA*-deletion strain under different illumination conditions, we used primers Nest-SakA-F and Nest-SakA-R to amplify a 5-kb

sakA::*GFP* transformation cassette from genomic DNA of strain TFL6. This cassette was transformed into wild type (SJR2), *ΔfphA* (SJR10), *ΔlreA* (SSR66) and *ΔlreB* (SJR70). The ORF of *ypdA*, *sskA* and *tcsB* were amplified with the following primers, YpdA_YFP_F, YpdA_YFP_R, SskA_YFP_F, SskA_YFP_R, TcsB_YFP_F and TcsB_YFP_R. These fragments replaced the *fphA* fragment in plasmids pJP4, yielding plasmids pZY25, pZY24 and pYZ30. Three plasmids were separately co-transformed with pJP5 and pJW18 into SKV103 strain.

3.9 Microscopy

For the study of SakA localization in wild type and the *fphA*-deletion strain in different light conditions, fresh conidia were inoculated on coverslips with supplemented minimal medium and incubated overnight in the dark at 28 °C. In order to avoid the effect of temperature shifts, the samples were placed at room temperature for 2 hours before microscopy analysis. For light stimuli, the samples were illuminated in white, red or blue light for 5 minutes. For salt stress, the minimal medium on coverslips was replaced by minimal medium containing 0.5 M NaCl and incubated 10 minutes in the dark. After illumination or salt stimulation, the samples were fixed with minimal medium containing 4% formaldehyde for 15 minutes and then washed once with PBS. For the analysis of bimolecular fluorescence complementation (BiFC), conidia were incubated on coverslips with supplemented minimal medium containing 2% threonine and 0.2% glucose overnight in the dark at 28 °C.

4 Biochemistry methods

4.1 Protein extraction

Fresh conidia were inoculated on the surface of the plates with 25 ml minimal medium containing appropriate supplements and incubated for 20 hours in the dark at 37 °C. White, red and blue light were switched on to illuminate the mycelia. The mycelia were harvested immediately and frozen in liquid nitrogen for protein extraction. Mycelia were ground in a mortar with liquid nitrogen and afterwards the mycelia powder was collected into the Eppendorf tubes. 0.8 ml protein extraction buffer (20 mM Tris–HCl, pH 8, 0.05% Triton-X-100, 150 mM NaCl) containing a protease inhibitor cocktail and 1 mM PMSF was added into each Eppendorf tube and incubated on ice for 20 minutes. The samples were centrifuged twice at 13,000 rpm at 4 °C. After each centrifugation, the supernatants were moved to the new Eppendorf tubes and the pellets were discarded. The concentration of the total protein was measured by Brandford protein assay which

performed on Thermo Nanodrop 2000C. All the samples were normalized to the same concentration with protein extraction buffer.

4.2 Bradford assay

Protein concentration was determined by Bradford protein (Bradford, 1976). This measurement is based upon Coomassie Brilliant Blue G-250 dye-binding assay. The standard curve was established with bovine serum albumin (BSA) according to **Table 13**. 200 µl of Roti-Quant Reagent (Roth, Karlsruhe) were added to each sample (1 µl protein sample in 800 µl ddH_2O), after gently mixing and incubation of 5 minutes, the absorbance was measured with Nano drop 2000C.

Table 13. Preparation of BSA standards for standard curve.

	10 µg/ml	8 µg/ml	6 µg/ml	4 µg/ml	2 µg/ml	1µg/ml	blank
BSA 100 µg/ml	100 µl	80 µl	60 µl	40 µl	20 µl	10 µl	0 µl
H_2O	700 µl	720 µl	740 µl	760 µl	780 µl	790 µl	800 µl
Roti-Quant Reagent	200 µl	200 µl	200 µl	200 µl	200 µl	200 µl	200 µl

4.3 SDS polyacrylamide gel electrophoresis

Solutions used for preparing the SDS polyacrylamide gel were listed in **Table 14**. The resolving gel was casted between the glass plates and overlaid with 2 ml isopropanol. After polymerization, the isopropanol was removed and the gel chamber was filled up with stacking gel. Protein samples mixed with 4 x SDS loading buffer were denatured by heating at 95 °C for 7 minutes and loaded onto the gel. 35 µg of total protein were loaded to a 10% polyacrylamide SDS gel and blotted to nitrocellulose membrane. Electrophoresis was performed at RT, first at 70 V until the sample entered resolving gel and then 150 V until the tracking dye reached the bottom of the gel.

Table 14. Solutions used for SDS-PAGE.

Solution	Composition
5% Stacking gel	0.83 ml 30% Acrylamid-Mix; 0.63 ml 1 M Tris pH 6.8; 0.05 ml 10% SDS; 0.1 ml 10% APS; 0.006 ml TEMED; 4.6 ml ddH_2O
10% Resolving gel	3.3 ml 30% Acrylamid-Mix; 2.5 ml 1.5 M Tris pH 8.8; 0.1 ml 10% SDS ; 0.1 ml 10% APS; 0.006 ml TEMED; 4 ml

1x SDS gel running buffer	ddH_2O 3 g Tris-base; 18.8 g Glycine; 10 ml 10% SDS-solution in 1 liter of ddH_2O

4.4 Western blot

All the samples were adjusted to the same concentration with protein extraction buffer. After denaturation, samples were loaded onto a 10% sodium dodecyl sulfate polyacrylamide gel and blotted to a nitrocellulose membrane. The membranes were incubated in blocking solution for 1 h at RT, subsequently incubated with the first antibody diluted in blocking solution overnight at 4 °C. Afterwards, the membranes were washed 3 x 10 minutes with TBST and incubated for 1 h at RT with the secondary antibody diluted in TBS-T and followed by 3 x 10 minutes washing with TBST before detection. After the detection, the membrances were stripped in stripping buffer for 30 minutes at 50 °C.

For immunodetection, anti-phospho-p38 MAP kinase (The180/Tyr182) antibodies (#4092; Cell Signaling Technology; Bevertly, MA; dilution 1:1000) against phosphorylated HogA, anti-Hog1p C-terminus antibody (y-215; Santa Cruz Biotechnology; California, USA; dilution 1:500) against SakA/HogA and anti-rabbit IgG (whole molecular)-peroxidase antibody (A0545; Sigma–Aldrich; München, Germany; dilution 1:80,000) were used. Solutions used here are listed in **Table 15**.

Table 15. Solutions used for Western blot.

Solution	Composition
10x Transfer buffer	30.3 g Tris; 144 g Glycine in 1 liter of ddH_2O
1x Transfer buffer	100 ml 10x Transfer buffer, 200 ml Methanol, 700 ml ddH_2O
10x TBS	24.2 g Tris, 80 g NaCl in 1 liter of ddH_2O, pH 7.6
1x TBST	1x TBS, 0.1% Tween 20 (100%)
Blocking solution	TBS-T with 5% BSA
Luminol solution	1 ml solution A (50 mg Luminol in 200 ml 0.1 M Tris-HCl pH 8.6); 0.1 ml solution B (11 mg p-Hydroxycoumarin acid in 10 ml DMSO); 0.3 µl 35 % H_2O_2
Stripping buffer	1x TBS; 2 % SDS; 0.1 M beta-Mercaptoethanol

4.5 Co-immunoprecipitation (CoIP)

Fresh conidia were incubated in liquid minimal medium at 37 °C containing 2% threonine and 0.2% glucose for 24 hours at 180 rpm, and then the mycelia were harvested by filtration and frozen in liquid nitrogen. Protein extraction was done as described above and 7 mg raw protein were used for co-immunoprecipitation. 80 µl of HA epitope tag antibody (ThemoFischer scientific) were added to each sample and incubated at 4 °C for 3 hours, rotating gently. After the incubation the beads were washed five times with extraction buffer. To release the protein, the SDS buffer (4× SDS sample buffer: 240 mM Tris-HCl pH 6.8; 400 mM DTT; 8% SDS; 0.04% bromphenol blue; 30% Glycerol) was added to the pelleted beads and boiled at 100 °C for 5 minutes. Western blot anaylsis was performed as described above. For the detection of GFP, Anti-GFP, N-terminal antibody ((#G1544; Sigma–Aldrich; München, Germany; dilution 1:1,000) and as secondary antibody anti-rabbit IgG (whole molecular)-peroxidase antibody (A0545; Sigma–Aldrich; München, Germany; dilution 1:80,000) were used. The HA tagg was detected with the Monoclonal Anti-HA antibody (H9658; Sigma–Aldrich; München, Germany; dilution 1:10,000) and anti-mouse IgG (whole molecule)–peroxidase antibody (A9044; Sigma–Aldrich; München, Germany; dilution 1:80,000) as secondary antibody.

4.6 Immunofluorescence

Sterilized coverslips were placed in the Petri dish. 450 µl supplemented minimal medium were added onto each coverslip. Fresh conidia were inoculated on the coverslips to get a final concentration of 10^3 spores/ml and cultivated for 18 hours in the dark at RT. The samples were exposed to light or kept in the dark for 5 minutes before fixation. To fix the samples, the medium was removed and the fixation solution was added immediately on the coverslips. After 30 minutes incubation at RT, the coverslips were washed three times (10 minutes/time) with 1 x PBS buffer. After washing, the coverslips were switched to a new Petri dishes. The coverslips were incubated with 200 µl digestion solution for 1h at RT. The coverslips were washed three times (10 minutes/time) with 1 x PBS buffer. –20°C precooled methanol was added to the Petri dishes to submerge the coverslips. The Petri dishes were incubated at –20°C for 10 minutes. Subsequently, the coverslips were washed two times (5 minutes/time) with 1 x PBS buffer. 200 µl blocking solution (1x TBST + 5% skim milk) were added to each coverslips. After 15 minutes incubation in blocking solution, the coverslips were switched to the new Petri dishes. Afterwards, the coverslips were incubated with antiphospho-p38 MAP kinase (The180/Tyr182) antibodies (#9211; Cell Signaling Technology; Bevertly, MA; dilution 1:400) in TBST buffer with 5% BSA overnight at 4 °C and washed three times (10 minutes/time) with 1 x

TBST after that. Cy3-conjugated anti-rabbit IgG secondary antibody (Jackson Immuno Research, USA) was used at a 1:200 dilution in 5% BSA in TBST. After 1 hour incubation, the coverslips were washed three times (10 minutes/time) with TBST and mounted on microscope slides with a drop of mounting medium with DAPI from VECTASHIELD for observation. For the long-term storage, the coverslips were sealed with nail polish and stored at 4 °C until observation.

Table 16. Solutions for immunofluorescence

Solution	Composition
Fixation solution	50 ml, 200mM PIPES pH6.7 with 10N NaOH; 10 ml, 500mM EGTA pH8.5 with NaOH; 1 ml, 1M $MgSO_4$; 10 ml, DMSO; 21.6 ml, Formaldehyde (37%)
10 x PBS (1L)	80 g, NaCl; 2 g, KCl; 14.4 g, Na_2HPO_4; 2.4 g, KH_2PO_4; pH7.4
1 x PBS (1L)	100 ml, 10 x PBS; H_2O
50mM sodium citrate (50 ml)	80 g, NaCl; 2 g, KCl; 14.4 g, Na_2HPO_4; 2.4 g, KH_2PO_4; pH7.4
50mM sodium citrate (50 ml)	12.9 g, sodium citrate; pH5.8
Digestion solution (5 ml)	100 mg, Driselase (solved in 600 µl 50mM sodium citrate pH5.8); 20 µl, Zymolase (5U/ µl); 800 mg, GlucanX (solved in 1 ml 50 mM sodium citrate pH 5.8); subject to 2.5 ml with 50mM NaCitrat; 2.5 ml, egg white
10x TBS (1L)	24.2 g, Tris/HCl, pH 7.6; 80 g, NaCl.
1x TBST (1L)	100 ml, 10xTBS; 1ml, Tween20; H_2O
Blocking sulution (100 ml)	10 ml, 1xTBST; 5 g, BSA

References

Aasland, R., Gibson, T. J., and Stewart, A. F. (1995). The PHD finger: implications for chromatin-mediated transcriptional regulation. *Trends Biochem Sci* **20**, 56-59.

Abdolrasouli, A., Rhodes, J., Beale, M. A., Hagen, F., Rogers, T. R., Chowdhary, A., Meis, J. F., Armstrong-James, D., and Fisher, M. C. (2015). Genomic context of azole resistance mutations in *Aspergillus fumigatus* determined using whole-genome sequencing. *MBio* **6**, e00536-00515.

Abe, H., Yamamoto, K. T., Nagatani, A., and Furuya, M. (1985). Characterization of Green Tissue-Specific Phytochrome Isolated Immunochemically from Pea Seedlings. *Plant Cell Physiol* **26**, 1387-1399.

Adams, T. H., Wieser, J. K., and Yu, J. H. (1998). Asexual sporulation in *Aspergillus nidulans*. *Microbiol Mol Biol Rev* **62**, 35-54.

Ahmed, Y. L., Gerke, J., Park, H. S., Bayram, O., Neumann, P., Ni, M., Dickmanns, A., Kim, S. C., Yu, J. H., Braus, G. H., and Ficner, R. (2013). The velvet family of fungal regulators contains a DNA-binding domain structurally similar to NF-kappaB. *PLoS Biol* **11**, e1001750.

Alonso-Monge, R., Navarro-Garcia, F., Molero, G., Diez-Orejas, R., Gustin, M., Pla, J., Sanchez, M., and Nombela, C. (1999). Role of the mitogen-activated protein kinase Hog1p in morphogenesis and virulence of *Candida albicans*. *J Bacteriol* **181**, 3058-3068.

Alvarez, A. F., Barba-Ostria, C., Silva-Jimenez, H., and Georgellis, D. (2016). Organization and mode of action of two component system signaling circuits from the various kingdoms of life. *Environ Microb*iol，doi: 10.1111/1462-2920.

Amich, J., Schafferer, L., Haas, H., and Krappmann, S. (2013). Regulation of sulphur assimilation is essential for virulence and affects iron homeostasis of the human-pathogenic mould *Aspergillus fumigatus*. *PLoS Pathog* **9**, e1003573.

Ariyoshi, M., and Schwabe, J. W. (2003). A conserved structural motif reveals the essential transcriptional repression function of Spen proteins and their role in developmental signaling. *Genes Dev* **17**, 1909-1920.

Arpaia, G., Carattoli, A., and Macino, G. (1995). Light and development regulate the expression of the albino-3 gene in *Neurospora crassa*. *Dev Biol* **170**, 626-635.

Azuma, N., Kanamaru, K., Matsushika, A., Yamashino, T., Mizuno, T., Kato, M., and Kobayashi, T. (2007). In vitro analysis of His-Asp phosphorelays in *Aspergillus nidulans*: the first direct biochemical evidence for the existence of His-Asp phosphotransfer systems in filamentous fungi. *Biosci Biotechnol Biochem* **71**, 2493-2502.

Bae, G., and Choi, G. (2008). Decoding of light signals by plant phytochromes and their interacting proteins. *Annu Rev Plant Biol* **59**, 281-311.

Bahn, Y. S. (2008). Master and commander in fungal pathogens: the two-component system and the HOG signaling pathway. *Eukaryot Cell* **7**, 2017-2036.

Bahn, Y. S., Xue, C., Idnurm, A., Rutherford, J. C., Heitman, J., and Cardenas, M. E. (2007). Sensing the environment: lessons from fungi. *Nat Rev Microbiol* **5**, 57-69.

Baima, S., Macino, G., and Morelli, G. (1991). Photoregulation of the *albino-3* gene in *Neurospora crassa*. *J Photochem Photobiol B* **11**, 107-115.

Baker, C. L., Kettenbach, A. N., Loros, J. J., Gerber, S. A., and Dunlap, J. C. (2009). Quantitative proteomics reveals a dynamic interactome and phase-specific phosphorylation in the *Neurospora* circadian clock. *Mol Cell* **34**, 354-363.

Balazs, A., Pocsi, I., Hamari, Z., Leiter, E., Emri, T., Miskei, M., Olah, J., Toth, V., Hegedus, N., Prade, R. A., Molnar, M., and Pocsi, I. (2010). AtfA bZIP-type transcription factor regulates oxidative and osmotic stress responses in *Aspergillus nidulans*. *Mol Genet Genomics* **283**, 289-303.

Ballario, P., and Macino, G. (1997). White collar proteins: PASsing the light signal in *Neurospora crassa*. *Trends Microbiol* **5**, 458-462.

Ballario, P., Talora, C., Galli, D., Linden, H., and Macino, G. (1998). Roles in dimerization and blue light photoresponse of the PAS and LOV domains of *Neurospora crassa* white collar proteins. *Mol Microbiol* **29**, 719-729.

Ballario, P., Vittorioso, P., Magrelli, A., Talora, C., Cabibbo, A., and Macino, G. (1996). White collar-1, a central regulator of blue light responses in *Neurospora*, is a zinc finger protein. *Embo j* **15**, 1650-1657.

Banno, S., Noguchi, R., Yamashita, K., Fukumori, F., Kimura, M., Yamaguchi, I., and Fujimura, M. (2007). Roles of putative His-to-Asp signaling modules HPT-1 and RRG-2, on viability and sensitivity to osmotic and oxidative stresses in *Neurospora crassa*. *Curr Genet* **51**, 197-208.

Bayram, O., Biesemann, C., Krappmann, S., Galland, P., and Braus, G. H. (2008a). More than a repair enzyme: *Aspergillus nidulans* photolyase-like CryA is a regulator of sexual development. *Mol Biol Cell* **19**, 3254-3262.

Bayram, O., and Braus, G. H. (2012). Coordination of secondary metabolism and development in fungi: the velvet family of regulatory proteins. *FEMS Microbiol Rev* **36**, 1-24.

Bayram, O., Braus, G. H., Fischer, R., and Rodriguez-Romero, J. (2010). Spotlight on *Aspergillus nidulans* photosensory systems. *Fungal Genet Biol* **47**, 900-908.

Bayram, O., Krappmann, S., Ni, M., Bok, J. W., Helmstaedt, K., Valerius, O., Braus-Stromeyer, S., Kwon, N. J., Keller, N. P., Yu, J. H., and Braus, G. H. (2008b). VelB/VeA/LaeA complex coordinates light signal with fungal development and secondary metabolism. *Science* **320**, 1504-1506.

Bhoo, S. H., Davis, S. J., Walker, J., Karniol, B., and Vierstra, R. D. (2001). Bacteriophytochromes are photochromic histidine kinases using a biliverdin chromophore. *Nature* **414**, 776-779.

Bieszke, J. A., Braun, E. L., Bean, L. E., Kang, S., Natvig, D. O., and Borkovich, K. A. (1999a). The nop-1 gene of *Neurospora crassa* encodes a seven transmembrane helix retinal-binding protein homologous to archaeal rhodopsins. *Proc Natl Acad Sci* **96**, 8034-8039.

Bieszke, J. A., Li, L., and Borkovich, K. A. (2007). The fungal opsin gene nop-1 is negatively-regulated by a component of the blue light sensing pathway and influences conidiation-specific gene expression in *Neurospora crassa*. *Curr Genet* **52**, 149-157.

Bieszke, J. A., Spudich, E. N., Scott, K. L., Borkovich, K. A., and Spudich, J. L. (1999b). A eukaryotic protein, NOP-1, binds retinal to form an archaeal rhodopsin-like photochemically reactive pigment. *Biochemistry* **38**, 14138-14145.

Blackwell, M. (2011). The fungi: 1, 2, 3 ... 5.1 million species? *Am J Bot* **98**, 426-438.

Blum, A., Benfield, A. H., Stiller, J., Kazan, K., Batley, J., and Gardiner, D. M. (2016). High-throughput FACS-based mutant screen identifies a gain-of-function allele of the *Fusarium graminearum* adenylyl cyclase causing deoxynivalenol over-production. *Fungal Genet Biol* **90**, 1-11.

Blumenstein, A., Vienken, K., Tasler, R., Purschwitz, J., Veith, D., Frankenberg-Dinkel, N., and Fischer, R. (2005). The *Aspergillus nidulans* phytochrome FphA represses sexual development in red light. *Curr Biol* **15**, 1833-1838.

Bok, J. W., and Keller, N. P. (2004). LaeA, a regulator of secondary metabolism in *Aspergillus* spp. *Eukaryot Cell* **3**, 527-535.

Borkovich, K. A., Alex, L. A., Yarden, O., Freitag, M., Turner, G. E., Read, N. D., Seiler, S., Bell-Pedersen, D., Paietta, J., Plesofsky, N., Plamann, M., Goodrich-Tanrikulu, M., Schulte, U., Mannhaupt, G., Nargang, F. E., Radford, A., Selitrennikoff, C., Galagan, J. E., Dunlap, J. C., Loros, J. J., Catcheside, D., Inoue, H., Aramayo, R., Polymenis, M., Selker, E. U., Sachs, M. S., Marzluf, G. A., Paulsen, I., Davis, R., Ebbole, D. J., Zelter, A., Kalkman, E. R., O'Rourke, R., Bowring, F., Yeadon, J., Ishii, C., Suzuki, K., Sakai, W., and Pratt, R. (2004). Lessons from the genome sequence of *Neurospora crassa*: tracing the path from genomic blueprint to multicellular organism. *Microbiol Mol Biol Rev* **68**, 1-108.

Borthwick, H. A., and Hendricks, S. B. (1960). Photoperiodism in Plants. *Science* **132**, 1223-1228.

Boylan, M. T., and Quail, P. H. (1996). Are the phytochromes protein kinases? *Protoplasma* **195**, 12-17.

Bradford, M. M. (1976). A rapid and sensitive method for the quantitation of microgram quantities of protein utilizing the principle of protein-dye binding. *Anal Biochem* **72**, 248-254.

Brandt, S., von Stetten, D., Gunther, M., Hildebrandt, P., and Frankenberg-Dinkel, N. (2008). The fungal phytochrome FphA from *Aspergillus nidulans*. *J Biol Chem* **283**, 34605-34614.

Brenna, A., Grimaldi, B., Filetici, P., and Ballario, P. (2012). Physical association of the WC-1 photoreceptor and the histone acetyltransferase NGF-1 is required for blue light signal transduction in *Neurospora crassa*. *Mol Biol Cell* **23**, 3863-3872.

Brown, G. D., Denning, D. W., Gow, N. A., Levitz, S. M., Netea, M. G., and White, T. C. (2012). Hidden killers: human fungal infections. *Sci Transl Med* **4**, 165rv113.

Brown, L. S. (2004). Fungal rhodopsins and opsin-related proteins: eukaryotic homologues of bacteriorhodopsin with unknown functions. *Photochem Photobiol Sci* **3**, 555-565.

Buchberger, T., and Lamparter, T. (2015). Streptophyte phytochromes exhibit an N-terminus of cyanobacterial origin and a C-terminus of proteobacterial origin. *Protoplasma* **8**, 144.

Buhler, R. M., Muller, B. L., Moritz, D. E., Vendruscolo, F., de Oliveira, D., and Ninow, J. L. (2015). Influence of light Intensity on growth and pigment production by *Monascus ruber* in Submerged Fermentation. *Appl Biochem Biotechnol* **176**, 1277-1289.

Butler, W. L., Norris, K., Siegelman, H., and Hendricks, S. (1959). Detection, assay, and preliminary purification of the pigment controlling photoresponsive development of plants. *Proc Natl Acad Sci* **45**, 1703-1708.

Camps, S. M., Dutilh, B. E., Arendrup, M. C., Rijs, A. J., Snelders, E., Huynen, M. A., Verweij, P. E., and Melchers, W. J. (2012). Discovery of a HapE mutation that causes azole resistance in *Aspergillus fumigatus* through whole genome sequencing and sexual crossing. *PLoS One* **7**, e50034.

Capra, E. J., and Laub, M. T. (2012). Evolution of two-component signal transduction systems. *Annu Rev Microbiol* **66**, 325-347.

Carattoli, A., Kato, E., Rodriguez-Franco, M., Stuart, W. D., and Macino, G. (1995). A chimeric light-regulated amino acid transport system allows the isolation of blue light regulator (*blr*) mutants of *Neurospora crassa*. *Proc Natl Acad Sci* **92**, 6612-6616.

Casas-Flores, S., Rios-Momberg, M., Bibbins, M., Ponce-Noyola, P., and Herrera-Estrella, A. (2004). BLR-1 and BLR-2, key regulatory elements of photoconidiation and mycelial growth in *Trichoderma atroviride*. *Microbiology* **150**, 3561-3569.

Cashmore, A. R., Jarillo, J. A., Wu, Y. J., and Liu, D. (1999). Cryptochromes: blue light receptors for plants and animals. *Science* **284**, 760-765.

Catlett, N. L., Yoder, O. C., and Turgeon, B. G. (2003). Whole-genome analysis of two-component signal transduction genes in fungal pathogens. *Eukaryotic Cell* **2**, 1151-1161.

Cha, J., Chang, S. S., Huang, G., Cheng, P., and Liu, Y. (2008). Control of WHITE COLLAR localization by phosphorylation is a critical step in the circadian negative feedback process. *EMBO J* **27**, 3246-3255.

Cha, J., Huang, G., Guo, J., and Liu, Y. (2007). Posttranslational control of the *Neurospora* circadian clock. *Cold Spring Harb Symp Quant Biol* **72**, 185-191.

Cha, J., Zhou, M., and Liu, Y. (2013). CATP is a critical component of the *Neurospora* circadian clock by regulating the nucleosome occupancy rhythm at the frequency locus. *EMBO Rep* **14**, 923-930.

Chakraborty, S., Gupta, R., Jain, K. K., and Kuhad, R. C. (2016). Cost-effective production of cellulose hydrolysing enzymes from *Trichoderma* sp. RCK65 under SSF and its evaluation in saccharification of cellulosic substrates. *Bioprocess Biosyst Eng*.

Chen, C. H., DeMay, B. S., Gladfelter, A. S., Dunlap, J. C., and Loros, J. J. (2010). Physical interaction between VIVID and white collar complex regulates photoadaptation in *Neurospora*. *Proc Natl Acad Sci* **107**, 16715-16720.

Chen, C. H., Ringelberg, C. S., Gross, R. H., Dunlap, J. C., and Loros, J. J. (2009). Genome-wide analysis of light-inducible responses reveals hierarchical light signalling in *Neurospora*. *EMBO J* **28**, 1029-1042.

Cheng, P., He, Q., Yang, Y., Wang, L., and Liu, Y. (2003). Functional conservation of light, oxygen, or voltage domains in light sensing. *Proc Natl Acad Sci* **100**, 5938-5943.

Cheng, P., Yang, Y., Gardner, K. H., and Liu, Y. (2002). PAS domain-mediated WC-1/WC-2 interaction is essential for maintaining the steady-state level of WC-1 and the function of both proteins in circadian clock and light responses of *Neurospora*. *Mol Cell Biol* **22**, 517-524.

Chory, J. (1993). Out of darkness: mutants reveal pathways controlling light-regulated development in plants. *Trends Genet* **9**, 167-172.

Collett, M. A., Garceau, N., Dunlap, J. C., and Loros, J. J. (2002). Light and clock expression of the *Neurospora* clock gene frequency is differentially driven by but dependent on WHITE COLLAR-2. *Genetics* **160**, 149-158.

Daiyasu, H., Ishikawa, T., Kuma, K., Iwai, S., Todo, T., and Toh, H. (2004). Identification of cryptochrome DASH from vertebrates. *Genes Cells* **9**, 479-495.

Dasgupta, A., Fuller, K. K., Dunlap, J. C., and Loros, J. J. (2016). Seeing the world differently: variability in the photosensory mechanisms of two model fungi. *Environ Microbiol* **18**, 5-20.

Davis, S. J., Vener, A. V., and Vierstra, R. D. (1999). Bacteriophytochromes: phytochrome-like photoreceptors from nonphotosynthetic eubacteria. *Science* **286**, 2517-2520.

de Menezes, H. D., Massola, N. S., Jr., Flint, S. D., Silva, G. J., Jr., Bachmann, L., Rangel, D. E., and Braga, G. U. (2015). Growth under visible light increases conidia and mucilage production and tolerance to UV-B radiation in the plant pathogenic fungus *Colletotrichum acutatum*. *Photochem Photobiol* **91**, 397-402.

de Paula, R. M., Lamb, T. M., Bennett, L., and Bell-Pedersen, D. (2008). A connection between MAPK pathways and circadian clocks. *Cell Cycle* **7**, 2630-2634.

De Souza, C. P., Hashmi, S. B., Osmani, A. H., Andrews, P., Ringelberg, C. S., Dunlap, J. C., and Osmani, S. A. (2013). Functional analysis of the *Aspergillus nidulans* kinome. *PLoS One* **8**, e58008.

Degli-Innocenti, F., and Russo, V. E. (1984). Isolation of new white collar mutants of *Neurospora crassa* and studies on their behavior in the blue light-induced formation of protoperithecia. *J Bacteriol* **159**, 757-761.

Dufosse, L., Fouillaud, M., Caro, Y., Mapari, S. A., and Sutthiwong, N. (2014). Filamentous fungi are large-scale producers of pigments and colorants for the food industry. *Curr Opin Biotechnol* **26**, 56-61.

Esquivel-Naranjo, E. U., Garcia-Esquivel, M., Medina-Castellanos, E., Correa-Perez, V. A., Parra-Arriaga, J. L., Landeros-Jaime, F., Cervantes-Chavez, J. A., and Herrera-Estrella, A. (2016). A *Trichoderma atroviride* stress-activated MAPK pathway integrates stress and light signals. *Mol Microbiol* **100**, 860-876.

Fischer, R. (2008). Developmental biology. Sex and poison in the dark. *Science* **320**, 1430-1431.

Fisher, M. C., Henk, D. A., Briggs, C. J., Brownstein, J. S., Madoff, L. C., McCraw, S. L., and Gurr, S. J. (2012). Emerging fungal threats to animal, plant and ecosystem health. *Nature* **484**, 186-194.

Franchi, L., Fulci, V., and Macino, G. (2005). Protein kinase C modulates light responses in *Neurospora* by regulating the blue light photoreceptor WC-1. *Mol Microbiol* **56**, 334-345.

Froehlich, A. C., Chen, C. H., Belden, W. J., Madeti, C., Roenneberg, T., Merrow, M., Loros, J. J., and Dunlap, J. C. (2010). Genetic and molecular characterization of a cryptochrome from the filamentous fungus *Neurospora crassa*. *Eukaryot Cell* **9**, 738-750.

Froehlich, A. C., Liu, Y., Loros, J. J., and Dunlap, J. C. (2002). White Collar-1, a circadian blue light photoreceptor, binding to the frequency promoter. *Science* **297**, 815-819.

Froehlich, A. C., Noh, B., Vierstra, R. D., Loros, J., and Dunlap, J. C. (2005). Genetic and molecular analysis of phytochromes from the filamentous fungus *Neurospora crassa*. *Eukaryot Cell* **4**, 2140-2152.

Furukawa, K., Hoshi, Y., Maeda, T., Nakajima, T., and Abe, K. (2005). *Aspergillus nidulans* HOG pathway is activated only by two-component signalling pathway in response to osmotic stress. *Mol Microbiol* **56**, 1246-1261.

Furukawa, K., Katsuno, Y., Urao, T., Yabe, T., Yamada-Okabe, T., Yamada-Okabe, H., Yamagata, Y., Abe, K., and Nakajima, T. (2002). Isolation and functional analysis of a gene, *tcsB*, encoding a transmembrane hybrid-type histidine kinase from *Aspergillus nidulans*. *Appl Environ Microbiol* **68**, 5304-5310.

Futagami, T., Mori, K., Wada, S., Ida, H., Kajiwara, Y., Takashita, H., Tashiro, K., Yamada, O., Omori, T., Kuhara, S., and Goto, M. (2015). Transcriptomic analysis of temperature responses of *Aspergillus kawachii* during barley koji production. *Appl Environ Microbiol* **81**, 1353-1363.

Garcia-Esquivel, M., Esquivel-Naranjo, E. U., Hernandez-Onate, M. A., Ibarra-Laclette, E., and Herrera-Estrella, A. (2016). The *Trichoderma atroviride* cryptochrome/photolyase genes regulate the expression of *blr1*-independent genes both in red and blue light. *Fungal Biol* **120**, 500-512.

Gessler, N. N., Aver'yanov, A. A., and Belozerskaya, T. A. (2007). Reactive oxygen species in regulation of fungal development. *Biochemistry (Mosc)* **72**, 1091-1109.

Grünbacher, A., Throm, T., Seidel, C., Gutt, B., Röhrig, J., Strunk, T., Vincze, P., Walheim, S., Schimmel, T., and Wenzel, W. (2014). Six hydrophobins are involved in hydrophobin rodlet formation in *Aspergillus nidulans* and contribute to hydrophobicity of the spore surface. *PloS one* **9**, e94546.

Grimaldi, B., Coiro, P., Filetici, P., Berge, E., Dobosy, J. R., Freitag, M., Selker, E. U., and Ballario, P. (2006). The *Neurospora crassa* White Collar-1 dependent blue light response requires acetylation of histone H3 lysine 14 by NGF-1. *Mol Biol Cell* **17**, 4576-4583.

Guisbert, E., Yura, T., Rhodius, V. A., and Gross, C. A. (2008). Convergence of molecular, modeling, and systems approaches for an understanding of the *Escherichia coli* heat shock response. *Microbiol Mol Biol R* **72**, 545-554.

Gustin, M. C., Albertyn, J., Alexander, M., and Davenport, K. (1998). MAP kinase pathways in the yeast *Saccharomyces cerevisiae*. *Microbiol Mol Biol Rev* **62**, 1264-1300.

Hagiwara, D., Asano, Y., Marui, J., Furukawa, K., Kanamaru, K., Kato, M., Abe, K., Kobayashi, T., Yamashino, T., and Mizuno, T. (2007a). The SskA and SrrA response regulators are implicated in oxidative stress responses of hyphae and asexual spores in the phosphorelay signaling network of *Aspergillus nidulans*. *Biosci Biotechnol Biochem* **71**, 1003-1014.

Hagiwara, D., Asano, Y., Marui, J., Yoshimi, A., Mizuno, T., and Abe, K. (2009a). Transcriptional profiling for *Aspergillus nidulans* HogA MAPK signaling pathway in response to fludioxonil and osmotic stress. *Fungal Genet Biol* **46**, 868-878.

Hagiwara, D., Matsubayashi, Y., Marui, J., Furukawa, K., Yamashino, T., Kanamaru, K., Kato, M., Abe, K., Kobayashi, T., and Mizuno, T. (2007b). Characterization of the NikA histidine kinase implicated in the phosphorelay signal transduction of *Aspergillus nidulans*, with special reference to fungicide responses. *Biosci Biotechnol Biochem* **71**, 844-847.

Hagiwara, D., Mizuno, T., and Abe, K. (2009b). Characterization of NikA histidine kinase and two response regulators with special reference to osmotic adaptation and asexual development in *Aspergillus nidulans*. *Biosci Biotechnol Biochem* **73**, 1566-1571.

Hagiwara, D., Sakamoto, K., Abe, K., and Gomi, K. (2016). Signaling pathways for stress responses and adaptation in *Aspergillus* species: stress biology in the post-genomic era. *Biosci Biotechnol Biochem*, 1-14.

Harding, R. W., and Melles, S. (1983). Genetic analysis of phototropism of *Neurospora crassa* perithecial beaks using white collar and albino mutants. *Plant Physiol* **72**, 996-1000.

Harrison, C., Katayama, S., Dhut, S., Chen, D., Jones, N., Bahler, J., and Toda, T. (2005). SCF(Pof1)-ubiquitin and its target Zip1 transcription factor mediate cadmium response in fission yeast. *EMBO J* **24**, 599-610.

Hartmann, T., Sasse, C., Schedler, A., Hasenberg, M., Gunzer, M., and Krappmann, S. (2011). Shaping the fungal adaptome--stress responses of *Aspergillus fumigatus*. *Int J Med Microbiol* **301**, 408-416.

Hartwell, L. H. (1967). Macromolecule synthesis in temperature-sensitive mutants of yeast. *J Bacteriol* **93**, 1662-1670.

Hartwell, L. H., Culotti, J., and Reid, B. (1970). Genetic control of the cell-division cycle in yeast, I. Detection of mutants. *Proc Natl Acad Sci* **66**, 352-359.

Hayashi, S., Yoshioka, M., Matsui, T., Kojima, K., Kato, M., Kanamaru, K., and Kobayashi, T. (2014). Control of reactive oxygen species (ROS) production through histidine kinases in *Aspergillus nidulans* under different growth conditions. *FEBS Open Bio* **4**, 90-95.

He, Q., Cha, J., He, Q., Lee, H. C., Yang, Y., and Liu, Y. (2006). CKI and CKII mediate the FREQUENCY-dependent phosphorylation of the WHITE COLLAR complex to close the *Neurospora circadian* negative feedback loop. *Genes Dev* **20**, 2552-2565.

He, Q., Cheng, P., Yang, Y., Wang, L., Gardner, K. H., and Liu, Y. (2002). White collar-1, a DNA binding transcription factor and a light sensor. *Science* **297**, 840-843.

He, X., Li, S., and Kaminskyj, S. G. (2014). Using *Aspergillus nidulans* to identify antifungal drug resistance mutations. *Eukaryot Cell* **13**, 288-294.

Hedayati, M. T., Pasqualotto, A. C., Warn, P. A., Bowyer, P., and Denning, D. W. (2007). *Aspergillus flavus*: human pathogen, allergen and mycotoxin producer. *Microbiology* **153**, 1677-1692.

Hedtke, M., Rauscher, S., Rohrig, J., Rodriguez-Romero, J., Yu, Z., and Fischer, R. (2015). Light-dependent gene activation in *Aspergillus nidulans* is strictly dependent on phytochrome and involves the interplay of phytochrome and white collar-regulated histone H3 acetylation. *Mol Microbiol* **97**, 733-745.

Heintzen, C., Loros, J. J., and Dunlap, J. C. (2001). The PAS protein VIVID defines a clock-associated feedback loop that represses light input, modulates gating, and regulates clock resetting. *Cell* **104**, 453-464.

Herr, A., and Fischer, R. (2014). Improvement of *Aspergillus nidulans* penicillin production by targeting AcvA to peroxisomes. *Metab Eng* **25**, 131-139.

Hohmann, S. (2002). Osmotic stress signaling and osmoadaptation in yeasts. *Microbiol Mol Biol Rev* **66**, 300-372.

Huang, G., Chen, S., Li, S., Cha, J., Long, C., Li, L., He, Q., and Liu, Y. (2007). Protein kinase A and casein kinases mediate sequential phosphorylation events in the circadian negative feedback loop. *Genes Dev* **21**, 3283-3295.

Huang, M., Bai, Y., Sjostrom, S. L., Hallstrom, B. M., Liu, Z., Petranovic, D., Uhlen, M., Joensson, H. N., Andersson-Svahn, H., and Nielsen, J. (2015). Microfluidic screening and whole-genome sequencing identifies mutations associated with improved protein secretion by yeast. *Proc Natl Acad Sci* **112**, E4689-4696.

Hubschmann, T., Yamamoto, H., Gieler, T., Murata, N., and Borner, T. (2005). Red and far-red light alter the transcript profile in the cyanobacterium *Synechocystis* sp. PCC 6803: impact of cyanobacterial phytochromes. *FEBS Lett* **579**, 1613-1618.

Hunt, S. M., Thompson, S., Elvin, M., and Heintzen, C. (2010). VIVID interacts with the WHITE COLLAR complex and FREQUENCY-interacting RNA helicase to alter light and clock responses in *Neurospora*. *Proc Natl Acad Sci* **107**, 16709-16714.

Idnurm, A., and Heitman, J. (2005). Light controls growth and development via a conserved pathway in the fungal kingdom. *PLoS Biol* **3**, e95.

Idnurm, A., Rodriguez-Romero, J., Corrochano, L. M., Sanz, C., Iturriaga, E. A., Eslava, A. P., and Heitman, J. (2006). The *Phycomyces madA* gene encodes a blue-light photoreceptor for phototropism and other light responses. *Proc Natl Acad Sci* **103**, 4546-4551.

Idnurm, A., Verma, S., and Corrochano, L. M. (2010). A glimpse into the basis of vision in the kingdom *Mycota*. *Fungal Genet Biol* **47**, 881-892.

Innocenti, F. D., Pohl, U., and Russo, V. E. (1983). Photoinduction of protoperithecia in *Neurospora crassa* by blue light. *Photochem Photobiol* **37**, 49-51.

Ji, Y., Yang, F., Ma, D., Zhang, J., Wan, Z., Liu, W., and Li, R. (2012). HOG-MAPK signaling regulates the adaptive responses of *Aspergillus fumigatus* to thermal stress and other related stress. *Mycopathologia* **174**, 273-282.

Johnson, R. T., and Downes, C. S. (2002). Heroes for a heroic age. *Cell Cycle* **1**, 6-7.

Jones, C. A., Greer-Phillips, S. E., and Borkovich, K. A. (2007). The response regulator RRG-1 functions upstream of a mitogen-activated protein kinase pathway impacting asexual development, female fertility, osmotic stress, and fungicide resistance in *Neurospora crassa*. *Mol Biol Cell* **18**, 2123-2136.

Kafer, E. (1965). Origins of translocations in Aspergillus nidulans. *Genetics* **52**, 217-232.

Kaiser, P., Flick, K., Wittenberg, C., and Reed, S. I. (2000). Regulation of transcription by ubiquitination without proteolysis: Cdc34/SCF(Met30)-mediated inactivation of the transcription factor Met4. *Cell* **102**, 303-314.

Kami, C., Lorrain, S., Hornitschek, P., and Fankhauser, C. (2010). Light-regulated plant growth and development. *Curr Top Dev Biol* **91**, 29-66.

Kanaan, M. N., Fu, Y. H., and Marzluf, G. A. (1992). The DNA-binding domain of the Cys-3 regulatory protein of *Neurospora crassa* is bipartite. *Biochemistry* **31**, 3197-3203.

Kaneko, T., Sato, S., Kotani, H., Tanaka, A., Asamizu, E., Nakamura, Y., Miyajima, N., Hirosawa, M., Sugiura, M., Sasamoto, S., Kimura, T., Hosouchi, T., Matsuno, A., Muraki, A., Nakazaki, N., Naruo, K., Okumura, S., Shimpo, S., Takeuchi, C., Wada, T., Watanabe, A., Yamada, M., Yasuda, M., and Tabata, S. (1996). Sequence analysis of the genome of the unicellular cyanobacterium *Synechocystis* sp. strain PCC6803. II. Sequence determination of the entire genome and assignment of potential protein-coding regions. *DNA Res* **3**, 109-136.

Karim, F. D., Chang, H. C., Therrien, M., Wassarman, D. A., Laverty, T., and Rubin, G. M. (1996). A screen for genes that function downstream of Ras1 during *Drosophila* eye development. *Genetics* **143**, 315-329.

Karniol, B., Wagner, J. R., Walker, J. M., and Vierstra, R. D. (2005). Phylogenetic analysis of the phytochrome superfamily reveals distinct microbial subfamilies of photoreceptors. *Biochem J* **392**, 103-116.

Kato, N., Brooks, W., and Calvo, A. M. (2003). The expression of sterigmatocystin and penicillin genes in *Aspergillus nidulans* is controlled by veA, a gene required for sexual development. *Eukaryot Cell* **2**, 1178-1186.

Kawasaki, L., Sanchez, O., Shiozaki, K., and Aguirre, J. (2002). SakA MAP kinase is involved in stress signal transduction, sexual development and spore viability in *Aspergillus nidulans*. *Mol Microbiol* **45**, 1153-1163.

Kehoe, D. M., and Grossman, A. R. (1996). Similarity of a chromatic adaptation sensor to phytochrome and ethylene receptors. *Science* **273**, 1409-1412.

Kim, H., Han, K., Kim, K., Han, D., Jahng, K., and Chae, K. (2002). The *veA* gene activates sexual development in *Aspergillus nidulans*. *Fungal Genet Biol* **37**, 72-80.

Kim, J. Y. (2016). Human fungal pathogens: Why should we learn? *J Microbiol* **54**, 145-148.

Kim, P. W., Rockwell, N. C., Martin, S. S., Lagarias, J. C., and Larsen, D. S. (2014). Dynamic inhomogeneity in the photodynamics of cyanobacterial phytochrome Cph1. *Biochemistry* **53**, 2818-2826.

Kooss, S., and Lamparter, T. (2016). Cyanobacterial origin of plant phytochromes. *Protoplasma*, 1-5.

Krantz, M., Ahmadpour, D., Ottosson, L. G., Warringer, J., Waltermann, C., Nordlander, B., Klipp, E., Blomberg, A., Hohmann, S., and Kitano, H. (2009). Robustness and fragility in the yeast high osmolarity glycerol (HOG) signal-transduction pathway. *Mol Syst Biol* **5**, 281.

Krantz, M., Becit, E., and Hohmann, S. (2006). Comparative genomics of the HOG-signalling system in fungi. *Curr Genet* **49**, 137-151.

Kuras, L., Cherest, H., Surdin-Kerjan, Y., and Thomas, D. (1996). A heteromeric complex containing the centromere binding factor 1 and two basic leucine zipper factors, Met4 and Met28, mediates the transcription activation of yeast sulfur metabolism. *EMBO J* **15**, 2519-2529.

Lamb, J. S., Zoltowski, B. D., Pabit, S. A., Li, L., Crane, B. R., and Pollack, L. (2009). Illuminating solution responses of a LOV domain protein with photocoupled small-angle X-ray scattering. *J Mol Biol* **393**, 909-919.

Lamb, T. M., Finch, K. E., and Bell-Pedersen, D. (2012). The *Neurospora crassa* OS MAPK pathway-activated transcription factor ASL-1 contributes to circadian rhythms in pathway responsive clock-controlled genes. *Fungal Genet Biol* **49**, 180-188.

Lamb, T. M., Goldsmith, C. S., Bennett, L., Finch, K. E., and Bell-Pedersen, D. (2011). Direct transcriptional control of a p38 MAPK pathway by the circadian clock in *Neurospora crassa*. *PLoS One* **6**, e27149.

Lamparter, T., Carrascal, M., Michael, N., Martinez, E., Rottwinkel, G., and Abian, J. (2004). The biliverdin chromophore binds covalently to a conserved cysteine residue in the N-terminus of *Agrobacterium* phytochrome Agp1. *Biochemistry* **43**, 3659-3669.

Lamparter, T., and Marwan, W. (2001). Spectroscopic detection of a phytochrome-like photoreceptor in the myxomycete *Physarum polycephalum* and the kinetic mechanism for the photocontrol of sporulation by Pfr. *Photochem Photobiol* **73**, 697-702.

Lamparter, T., Mittmann, F., Gartner, W., Borner, T., Hartmann, E., and Hughes, J. (1997). Characterization of recombinant phytochrome from the cyanobacterium *Synechocystis*. *Proc Natl Acad Sci* **94**, 11792-11797.

Lara-Rojas, F., Sanchez, O., Kawasaki, L., and Aguirre, J. (2011). *Aspergillus nidulans* transcription factor AtfA interacts with the MAPK SakA to regulate general stress responses, development and spore functions. *Mol Microbiol* **80**, 436-454.

Larrondo, L. F., Olivares-Yanez, C., Baker, C. L., Loros, J. J., and Dunlap, J. C. (2015). Circadian rhythms. Decoupling circadian clock protein turnover from circadian period determination. *Science* **347**, 1257277.

Lauter, F. R., Marchfelder, U., Russo, V. E. A., Yamashiro, C. T., Yatzkan, E., and Yarden, O. (1998). Photoregulation of *cot-1*, a kinase-encoding gene involved in hyphal growth in *Neurospora crassa*. *Fungal Genet Biol* **23**, 300-310.

Leach, M. D., Farrer, R. A., Tan, K., Miao, Z., Walker, L. A., and Cuomo, C. A. (2016). Hsf1 and Hsp90 orchestrate temperature-dependent global transcriptional remodelling and chromatin architecture in *Candida albicans*. *Nat commun* **7**, 11704.

Lee, J., Godon, C., Lagniel, G., Spector, D., Garin, J., Labarre, J., and Toledano, M. B. (1999). Yap1 and Skn7 control two specialized oxidative stress response regulons in yeast. *J Biol Chem* **274**, 16040-16046.

Lee, K., Dunlap, J. C., and Loros, J. J. (2003). Roles for WHITE COLLAR-1 in circadian and general photoperception in *Neurospora crassa*. *Genetics* **163**, 103-114.

Levin, D. E. (2005). Cell wall integrity signaling in *Saccharomyces cerevisiae*. *Microbiol Mol Biol R* **69**, 262-291.

Li, F. W., Melkonian, M., Rothfels, C. J., Villarreal, J. C., Stevenson, D. W., Graham, S. W., Wong, G. K., Pryer, K. M., and Mathews, S. (2015). Phytochrome diversity in green plants and the origin of canonical plant phytochromes. *Nat Commun* **6**, 7852.

Li, H., and Durbin, R. (2009). Fast and accurate short read alignment with Burrows-Wheeler transform. *Bioinformatics* **25**, 1754-1760.

Li, Q., and Marzluf, G. A. (1996). Determination of the *Neurospora crassa* CYS 3 sulfur regulatory protein consensus DNA-binding site: amino-acid substitutions in the CYS3 bZIP domain that alter DNA-binding specificity. *Curr Genet* **30**, 298-304.

Li, S., Ault, A., Malone, C. L., Raitt, D., Dean, S., Johnston, L. H., Deschenes, R. J., and Fassler, J. S. (1998). The yeast histidine protein kinase, Sln1p, mediates phosphotransfer to two response regulators, Ssk1p and Skn7p. *EMBO J* **17**, 6952–6962.

Lichius, A., Bidard, F., Buchholz, F., Le Crom, S., Martin, J., Schackwitz, W., Austerlitz, T., Grigoriev, I. V., Baker, S. E., Margeot, A., Seiboth, B., and Kubicek, C. P. (2015). Genome sequencing of the *Trichoderma reesei* QM9136 mutant identifies a truncation of the transcriptional regulator XYR1 as the cause for its cellulase-negative phenotype. *BMC Genomics* **16**, 326.

Linden, H., and Macino, G. (1997). White collar 2, a partner in blue-light signal transduction, controlling expression of light-regulated genes in *Neurospora crassa*. *EMBO J* **16**, 98-109.

Liu, B., Yang, Z., Gomez, A., Liu, B., Lin, C., and Oka, Y. (2016). Signaling mechanisms of plant cryptochromes in *Arabidopsis thaliana*. *J Plant Res* **129**, 137-148.

Lorenzo, C. D., Sanchez-Lamas, M., Antonietti, M. S., and Cerdan, P. D. (2016). Emerging Hubs in Plant Light and Temperature Signaling. *Photochem Photobiol* **92**, 3-13.

Lu, J. M., Deschenes, R. J., and Fassler, J. S. (2003). *Saccharomyces cerevisiae* histidine phosphotransferase Ypd1p shuttles between the nucleus and cytoplasm for SLN1-dependent phosphorylation of Ssk1p and Skn7p. *Eukaryot Cell* **2**, 1304-1314.

Maeda, T., Takekawa, M., and Saito, H. (1995). Activation of yeast PBS2 MAPKK by MAPKKKs or by binding of an SH3-containing osmosensor. *Science* **269**, 554-558.

Maeda, T., Wurgler-Murphy, S. M., and Saito, H. (1994). A two-component system that regulates an osmosensing MAP kinase cascade in yeast. *Nature* **369**, 242-245.

Malzahn, E., Ciprianidis, S., Kaldi, K., Schafmeier, T., and Brunner, M. (2010). Photoadaptation in *Neurospora* by competitive interaction of activating and inhibitory LOV domains. *Cell* **142**, 762-772.

Marzluf, G. A. (1997). Molecular genetics of sulfur assimilation in filamentous fungi and yeast. *Annu Rev Microbiol* **51**, 73-96.

Marzluf, G. A., and Metzenberg, R. L. (1968). Positive control by the cys-3 locus in regulation of sulfur metabolism in *Neurospora*. *J Mol Biol* **33**, 423-437.

Mascher, T., Helmann, J. D., and Unden, G. (2006). Stimulus perception in bacterial signal-transducing histidine kinases. *Microbiol Mol Biol Rev* **70**, 910-938.

McCluskey, K., Wiest, A. E., Grigoriev, I. V., Lipzen, A., Martin, J., Schackwitz, W., and Baker, S. E. (2011). Rediscovery by Whole Genome Sequencing: Classical Mutations and Genome Polymorphisms in *Neurospora crassa*. *G3 (Bethesda)* **1**, 303-316.

McKenna, A., Hanna, M., Banks, E., Sivachenko, A., Cibulskis, K., Kernytsky, A., Garimella, K., Altshuler, D., Gabriel, S., Daly, M., and DePristo, M. A. (2010). The Genome Analysis Toolkit: a MapReduce framework for analyzing next-generation DNA sequencing data. *Genome Res* **20**, 1297-1303.

Menant, A., Baudouin-Cornu, P., Peyraud, C., Tyers, M., and Thomas, D. (2006). Determinants of the ubiquitin-mediated degradation of the Met4 transcription factor. *J Biol Chem* **281**, 11744-11754.

Mooney, J. L., and Yager, L. N. (1990). Light is required for conidiation in *Aspergillus nidulans*. *Genes Dev* **4**, 1473-1482.

Morgan, B. A., Banks, G. R., †, W. M. T., Raitt, D., Kuge, S., and Johnston, L. H. (1997). The Skn7 response regulator controls gene expression in the oxidative stress response of the budding yeast *Saccharomyces cerevisiae*. *EMBO J* **16**, 1035–1044.

Morris, N. (1976). A temperature-sensitive mutant of *Aspergillus nidulans* reversibly blocked in nuclear division. *Exp Cell Res* **98**, 204-209.

Morris, N. R. (1975). Mitotic mutants of *Aspergillus nidulans*. *Genet Res* **26**, 237-254.

Mosier, A. C., Miller, C. S., Frischkorn, K. R., Ohm, R. A., Li, Z., LaButti, K., Lapidus, A., Lipzen, A., Chen, C., Johnson, J., Lindquist, E. A., Pan, C., Hettich, R. L., Grigoriev, I. V., Singer, S. W., and Banfield, J. F. (2016). Fungi contribute critical but spatially varying roles in nitrogen and carbon cycling in acid mine drainage. *Front Microbiol* **7**, 238.

Natorff, R., Piotrowska, M., and Paszewski, A. (1998). The *Aspergillus nidulans* sulphur regulatory gene *sconB* encodes a protein with WD40 repeats and an F-box. *Mol Gen Genet* **257**, 255-263.

Natorff, R., Sienko, M., Brzywczy, J., and Paszewski, A. (2003). The *Aspergillus nidulans metR* gene encodes a bZIP protein which activates transcription of sulphur metabolism genes. *Mol Microbiol* **49**, 1081-1094.

Nelson, M. A., Morelli, G., Carattoli, A., Romano, N., and Macino, G. (1989). Molecular cloning of a *Neurospora crassa* carotenoid biosynthetic gene (*albino-3*) regulated by blue light and the products of the white collar genes. *Mol Cell Biol* **9**, 1271-1276.

Ni, M., and Yu, J. H. (2007). A novel regulator couples sporogenesis and trehalose biogenesis in *Aspergillus nidulans*. *PLoS One* **2**, e970.

Nielsen, K., and Heitman, J. (2007). Sex and virulence of human pathogenic fungi. *Adv Genet* **57**, 143-173.

Nimmanee, P., Woo, P. C., Vanittanakom, P., Youngchim, S., and Vanittanakom, N. (2014). Functional analysis of atfA gene to stress response in pathogenic thermal dimorphic fungus *Penicillium marneffei*. *PLoS One* **9**, e111200.

Niu, J., Arentshorst, M., Nair, P. D., Dai, Z., Baker, S. E., Frisvad, J. C., Nielsen, K. F., Punt, P. J., and Ram, A. F. (2016). Identification of a classical mutant in the industrial host *Aspergillus niger* by systems genetics: LaeA is required for citric acid production and regulates the formation of some secondary metabolites. *G3 (Bethesda)* **6**, 193-204.

Nixon, B. T., Ronson, C. W., and Ausubel, F. M. (1986). Two-component regulatory systems responsive to environmental stimuli share strongly conserved domains with the nitrogen assimilation regulatory genes *ntrB* and *ntrC*. *Proc Natl Acad Sci* **83**, 7850-7854.

Njimona, I., and Lamparter, T. (2011). Temperature effects on *Agrobacterium* phytochrome Agp1. *PLoS One* **6**, e25977.

Njimona, I., Yang, R., and Lamparter, T. (2014). Temperature effects on bacterial phytochrome. *PLoS One* **9**, e109794.

Noguchi, R., Banno, S., Ichikawa, R., Fukumori, F., Ichiishi, A., Kimura, M., Yamaguchi, I., and Fujimura, M. (2007). Identification of OS-2 MAP kinase-dependent genes induced in response to osmotic stress, antifungal agent fludioxonil, and heat shock in *Neurospora crassa*. *Fungal Genet Biol* **44**, 208-218.

O'Brien, H. E., Parrent, J. L., Jackson, J. A., Moncalvo, J. M., and Vilgalys, R. (2005). Fungal community analysis by large-scale sequencing of environmental samples. *Appl Environ Microbiol* **71**, 5544-5550.

Olmedo, M., Ruger-Herreros, C., Luque, E. M., and Corrochano, L. M. (2010). A complex photoreceptor system mediates the regulation by light of the conidiation genes *con-10* and *con-6* in *Neurospora crassa*. *Fungal Genet Biol* **47**, 352-363.

Ono, D., Honma, S., and Honma, K.-i. (2013). Cryptochromes are critical for the development of coherent circadian rhythms in the mouse suprachiasmatic nucleus. *Nat commun* **4**, 1666.

OSMANI, S. A. (1996). Cell cycle regulation in *Aspergillus* by two protein kinases. *Biochemical journal* **317**, 633-641.

Paietta, J. V., Akins, R. A., Lambowitz, A. M., and Marzluf, G. A. (1987). Molecular cloning and characterization of the *cys-3* regulatory gene of *Neurospora crassa*. *Mol Cell Biol* **7**, 2506-2511.

Palmer, J. M., Theisen, J. M., Duran, R. M., Grayburn, W. S., Calvo, A. M., and Keller, N. P. (2013). Secondary metabolism and development is mediated by LlmF control of VeA subcellular localization in *Aspergillus nidulans*. *PLoS Genet* **9**, e1003193.

Park, H. S., Nam, T. Y., Han, K. H., Kim, S. C., and Yu, J. H. (2014). VelC positively controls sexual development in *Aspergillus nidulans*. *PLoS One* **9**, e89883.

Pedmale, U. V., Huang, S.-s. C., Zander, M., Cole, B. J., Hetzel, J., Ljung, K., Reis, P. A., Sridevi, P., Nito, K., and Nery, J. R. (2016). Cryptochromes interact directly with PIFs to control plant growth in limiting blue light. *Cell* **164**, 233-245.

Pilsyk, S., Natorff, R., Sienko, M., Skoneczny, M., Paszewski, A., and Brzywczy, J. (2015). The *Aspergillus nidulans metZ* gene encodes a transcription factor involved in regulation of sulfur metabolism in this fungus and other *Eurotiales*. *Curr Genet* **61**, 115-125.

Piotrowska, M., Natorff, R., and Paszewski, A. (2000). *sconC*, a gene involved in the regulation of sulphur metabolism in *Aspergillus nidulans*, belongs to the *SKP1* gene family. *Mol Gen Genet* **264**, 276-282.

Posas, F., and Saito, H. (1997). Osmotic activation of the HOG MAPK pathway via Ste11p MAPKKK: scaffold role of Pbs2p MAPKK. *Science* **276**, 1702-1705.

Posas, F., and Saito, H. (1998). Activation of the yeast SSK2 MAP kinase kinase kinase by the SSK1 two-component response regulator. *EMBO J* **17**, 1385-1394.

Posas, F., Wurgler-Murphy, S. M., Maeda, T., Witten, E. A., Thai, T. C., and Saito, H. (1996). Yeast HOG1 MAP kinase cascade is regulated by a multistep phosphorelay mechanism in the SLN1-YPD1-SSK1 "two-component" osmosensor. *Cell* **86**, 865-875.

Purschwitz, J., Muller, S., and Fischer, R. (2009). Mapping the interaction sites of *Aspergillus nidulans* phytochrome FphA with the global regulator VeA and the White Collar protein LreB. *Mol Genet Genomics* **281**, 35-42.

Purschwitz, J., Muller, S., Kastner, C., and Fischer, R. (2006). Seeing the rainbow: light sensing in fungi. *Curr Opin Microbiol* **9**, 566-571.

Purschwitz, J., Muller, S., Kastner, C., Schoser, M., Haas, H., Espeso, E. A., Atoui, A., Calvo, A. M., and Fischer, R. (2008). Functional and physical interaction of blue- and red-light sensors in *Aspergillus nidulans*. *Curr Biol* **18**, 255-259.

Rangel, D. E., Fernandes, E. K., Braga, G. U., and Roberts, D. W. (2011). Visible light during mycelial growth and conidiation of *Metarhizium robertsii* produces conidia with increased stress tolerance. *FEMS Microbiol Lett* **315**, 81-86.

Rauscher, S., Pacher, S., Hedtke, M., Kniemeyer, O., and Fischer, R. (2016). A phosphorylation code of the *Aspergillus nidulans* global regulator VelvetA (VeA) determines specific functions. *Mol Microbiol* **99**, 909-924.

Rodriguez-Romero, J., and Corrochano, L. M. (2006). Regulation by blue light and heat shock of gene transcription in the fungus *Phycomyces*: proteins required for photoinduction and mechanism for adaptation to light. *Mol Microbiol* **61**, 1049-1059.

Rodriguez-Romero, J., Hedtke, M., Kastner, C., Muller, S., and Fischer, R. (2010). Fungi, hidden in soil or up in the air: light makes a difference. *Annu Rev Microbiol* **64**, 585-610.

Rohrig, J., Kastner, C., and Fischer, R. (2013). Light inhibits spore germination through phytochrome in *Aspergillus nidulans*. *Curr Genet* **59**, 55-62.

Ronson, C. W., Nixon, B. T., and Ausubel, F. M. (1987). Conserved domains in bacterial regulatory proteins that respond to environmental stimuli. *Cell* **49**, 579-581.

Rottwinkel, G., Oberpichler, I., and Lamparter, T. (2010). Bathy phytochromes in rhizobial soil bacteria. *J Bacteriol* **192**, 5124-5133.

Ruesch, C. E., Ramakrishnan, M., Park, J., Li, N., Chong, H. S., Zaman, R., Joska, T. M., and Belden, W. J. (2014). The histone H3 lysine 9 methyltransferase DIM-5 modifies chromatin at frequency and represses light-activated gene expression. *G3 (Bethesda)* **5**, 93-101.

Ruger-Herreros, C., Rodriguez-Romero, J., Fernandez-Barranco, R., Olmedo, M., Fischer, R., Corrochano, L. M., and Canovas, D. (2011). Regulation of conidiation by light in *Aspergillus nidulans*. *Genetics* **188**, 809-822.

Sambrook, J., Fritsch, E., and Maniatis, T. (1989). Molecular cloning: a laboratory manual, 2nd edn. Cold Spring Laboratory Press. *Cold Spring Harbor, USA* **18**, 86.

Sancar, A. (1994). Structure and function of DNA photolyase. *Biochemistry* **33**, 2-9.

Sancar, C., Ha, N., Yilmaz, R., Tesorero, R., Fisher, T., Brunner, M., and Sancar, G. (2015). Combinatorial control of light induced chromatin remodeling and gene activation in *Neurospora*. *PLoS Genet* **11**, e1005105.

Sancar, G. B. (1990). DNA photolyases: physical properties, action mechanism, and roles in dark repair. *Mutat Res* **236**, 147-160.

Sanchez-Arreguin, A., Perez-Martinez, A. S., and Herrera-Estrella, A. (2012). Proteomic analysis of *Trichoderma atroviride* reveals independent roles for transcription factors BLR-1 and BLR-2 in light and darkness. *Eukaryot Cell* **11**, 30-41.

Santos, J. L., and Shiozaki, K. (2001). Fungal histidine kinases. *Sci STKE* **2001**, re1.

Sanz, C., Rodriguez-Romero, J., Idnurm, A., Christie, J. M., Heitman, J., Corrochano, L. M., and Eslava, A. P. (2009). *Phycomyces* MADB interacts with MADA to form the primary photoreceptor complex for fungal phototropism. *Proc Natl Acad Sci* **106**, 7095-7100.

Sarikaya-Bayram, O., Bayram, O., Feussner, K., Kim, J. H., Kim, H. S., Kaever, A., Feussner, I., Chae, K. S., Han, D. M., Han, K. H., and Braus, G. H. (2014). Membrane-bound methyltransferase complex VapA-VipC-VapB guides epigenetic control of fungal development. *Dev Cell* **29**, 406-420.

Sarikaya-Bayram, O., Palmer, J. M., Keller, N., Braus, G. H., and Bayram, O. (2015). One Juliet and four Romeos: VeA and its methyltransferases. *Front Microbiol* **6**, 1.

Sarikaya Bayram, O., Bayram, O., Valerius, O., Park, H. S., Irniger, S., Gerke, J., Ni, M., Han, K. H., Yu, J. H., and Braus, G. H. (2010). LaeA control of velvet family regulatory proteins for light-dependent development and fungal cell-type specificity. *PLoS Genet* **6**, e1001226.

Schafmeier, T., Diernfellner, A., Schäfer, A., Dintsis, O., Neiss, A., and Brunner, M. (2008). Circadian activity and abundance rhythms of the *Neurospora* clock transcription factor WCC associated with rapid nucleo–cytoplasmic shuttling. *Genes & Development* **22**, 3397-3402.

Schafmeier, T., Haase, A., Kaldi, K., Scholz, J., Fuchs, M., and Brunner, M. (2005). Transcriptional feedback of *Neurospora* circadian clock gene by phosphorylation-dependent inactivation of its transcription factor. *Cell* **122**, 235-246.

Schmidhauser, T. J., Lauter, F. R., Russo, V. E., and Yanofsky, C. (1990). Cloning, sequence, and photoregulation of al-1, a carotenoid biosynthetic gene of Neurospora crassa. *Mol Cell Biol* **10**, 5064-5070.

Schwerdtfeger, C., and Linden, H. (2001). Blue light adaptation and desensitization of light signal transduction in *Neurospora crassa*. *Mol Microbiol* **39**, 1080-1087.

Schwerdtfeger, C., and Linden, H. (2003). VIVID is a flavoprotein and serves as a fungal blue light photoreceptor for photoadaptation. *EMBO J* **22**, 4846-4855.

Selby, C. P., and Sancar, A. (2006). A cryptochrome/photolyase class of enzymes with single-stranded DNA-specific photolyase activity. *Proc Natl Acad Sci* **103**, 17696-17700.

Shi, X., Kachirskaia, I., Walter, K. L., Kuo, J. H., Lake, A., Davrazou, F., Chan, S. M., Martin, D. G., Fingerman, I. M., Briggs, S. D., Howe, L., Utz, P. J., Kutateladze, T. G., Lugovskoy, A. A., Bedford, M. T., and Gozani, O. (2007). Proteome-wide analysis in *Saccharomyces cerevisiae* identifies several PHD fingers as novel direct and selective binding modules of histone H3 methylated at either lysine 4 or lysine 36. *J Biol Chem* **282**, 2450-2455.

Sienko, M., Natorff, R., Skoneczny, M., Kruszewska, J., Paszewski, A., and Brzywczy, J. (2014). Regulatory mutations affecting sulfur metabolism induce environmental stress response in *Aspergillus nidulans*. *Fungal Genet Biol* **65**, 37-47.

Skerker, J. M., Prasol, M. S., Perchuk, B. S., Biondi, E. G., and Laub, M. T. (2005). Two-component signal transduction pathways regulating growth and cell cycle progression in a bacterium: a system-level analysis. *PLoS Biol* **3**, e334.

Skowyra, D., Craig, K. L., Tyers, M., Elledge, S. J., and Harper, J. W. (1997). F-box proteins are receptors that recruit phosphorylated substrates to the SCF ubiquitin-ligase complex. *Cell* **91**, 209-219.

Smith, K. M., Sancar, G., Dekhang, R., Sullivan, C. M., Li, S., Tag, A. G., Sancar, C., Bredeweg, E. L., Priest, H. D., McCormick, R. F., Thomas, T. L., Carrington, J. C., Stajich, J. E., Bell-Pedersen, D., Brunner, M., and Freitag, M. (2010). Transcription factors in light and circadian clock signaling networks revealed by genomewide mapping of direct targets for *Neurospora* white collar complex. *Eukaryot Cell* **9**, 1549-1556.

Sorger, P. K., Lewis, M. J., and Pelham, H. R. (1987). Heat shock factor is regulated differently in yeast and HeLa cells. *Nature* **329**, 81-84.

Sprote, P., and Brakhage, A. A. (2007). The light-dependent regulator velvet A of *Aspergillus nidulans* acts as a repressor of the penicillin biosynthesis. *Arch Microbiol* **188**, 69-79.

Stinnett, S. M., Espeso, E. A., Cobeno, L., Araujo-Bazan, L., and Calvo, A. M. (2007). *Aspergillus nidulans* VeA subcellular localization is dependent on the importin alpha carrier and on light. *Mol Microbiol* **63**, 242-255.

Stock, A. M., Robinson, V. L., and Goudreau, P. N. (2000). Two-component signal transduction. *Annu Rev Biochem* **69**, 183-215.

Suzuki, A., Kanamaru, K., Azuma, N., Kato, M., and Kobayashi, T. (2008). GFP-tagged expression analysis revealed that some histidine kinases of

Aspergillus nidulans show temporally and spatially different expression during the life cycle. *Biosci Biotechnol Biochem* **72**, 428-434.

Suzuki, S., Sarikaya Bayram, O., Bayram, O., and Braus, G. H. (2013). *conF* and *conJ* contribute to conidia germination and stress response in the filamentous fungus *Aspergillus nidulans*. *Fungal Genet Biol* **56**, 42-53.

Tan, K., Roberts, A. J., Chonofsky, M., Egan, M. J., and Reck-Peterson, S. L. (2014). A microscopy-based screen employing multiplex genome sequencing identifies cargo-specific requirements for dynein velocity. *Mol Biol Cell* **25**, 669-678.

Tataroglu, O., Lauinger, L., Sancar, G., Jakob, K., Brunner, M., and Diernfellner, A. C. (2012). Glycogen synthase kinase is a regulator of the circadian clock of *Neurospora crassa*. *J Biol Chem* **287**, 36936-36943.

Thomas, D., and Surdin-Kerjan, Y. (1997). Metabolism of sulfur amino acids in *Saccharomyces cerevisiae*. *Microbiol Mol Biol Rev* **61**, 503-532.

Todo, T., Ryo, H., Yamamoto, K., Toh, H., Inui, T., Ayaki, H., Nomura, T., and Ikenaga, M. (1996). Similarity among the *Drosophila* (6-4)photolyase, a human photolyase homolog, and the DNA photolyase-blue-light photoreceptor family. *Science* **272**, 109-112.

Toews, M. W., Warmbold, J., Konzack, S., Rischitor, P., Veith, D., Vienken, K., Vinuesa, C., Wei, H., and Fischer, R. (2004). Establishment of mRFP1 as a fluorescent marker in *Aspergillus nidulans* and construction of expression vectors for high-throughput protein tagging using recombination in vitro (GATEWAY). *Current genetics* **45**, 383-389.

Topczewski, J., Sienko, M., and Paszewski, A. (1997). Cloning and characterization of the *Aspergillus nidulans cysB* gene encoding cysteine synthase. *Curr Genet* **31**, 348-356.

Tuncher, A., Reinke, H., Martic, G., Caruso, M. L., and Brakhage, A. A. (2004). A basic-region helix-loop-helix protein-encoding gene (*devR*) involved in the development of *Aspergillus nidulans*. *Mol Microbiol* **52**, 227-241.

Vabulas, R. M., Raychaudhuri, S., Hayer-Hartl, M., and Hartl, F. U. (2010). Protein folding in the cytoplasm and the heat shock response. *Cold Spring Harb Perspect Biol* **2**, a004390.

Vaidya, A. T., Chen, C. H., Dunlap, J. C., Loros, J. J., and Crane, B. R. (2011). Structure of a light-activated LOV protein dimer that regulates transcription. *Sci Signal* **4**, ra50.

van der Schalie, E., and Green, C. B. (2005). Cryptochromes. *Curr Biol* **15**, R785.

Vargas-Perez, I., Sanchez, O., Kawasaki, L., Georgellis, D., and Aguirre, J. (2007). Response regulators SrrA and SskA are central components of a phosphorelay system involved in stress signal transduction and asexual sporulation in *Aspergillus nidulans*. *Eukaryot Cell* **6**, 1570-1583.

Vienken, K., and Fischer, R. (2006). The $Zn(II)_2Cys_6$ putative transcription factor NosA controls fruiting body formation in *Aspergillus nidulans*. *Mol Microbiol* **61**, 544-554.

Vihtelic, T. S., and Hyde, D. R. (2002). Zebrafish mutagenesis yields eye morphological mutants with retinal and lens defects. *Vision research* **42**, 535-540.

Virginia, M., Appleyard, C. L., McPheat, W. L., and Stark, M. J. (2000). A novel 'two-component' protein containing histidine kinase and response regulator domains required for sporulation in *Aspergillus nidulans*. *Curr Genet* **37**, 364-372.

Vitalini, M. W., de Paula, R. M., Goldsmith, C. S., Jones, C. A., Borkovich, K. A., and Bell-Pedersen, D. (2007). Circadian rhythmicity mediated by temporal regulation of the activity of p38 MAPK. *Proc Natl Acad Sci* **104**, 18223-18228.

Vitalini, M. W., Morgan, L. W., March, I. J., and Bell-Pedersen, D. (2004). A genetic selection for circadian output pathway mutations in *Neurospora crassa*. *Genetics* **167**, 119-129.

Wagner, D., Koloszvari, M., and Quail, P. H. (1996). Two small spatially distinct regions of phytochrome B are required for efficient signaling rates. *Plant Cell* **8**, 859-871.

Wagner, J. R., Brunzelle, J. S., Forest, K. T., and Vierstra, R. D. (2005). A light-sensing knot revealed by the structure of the chromophore-binding domain of phytochrome. *Nature* **438**, 325-331.

Wagner, J. R., Zhang, J., Brunzelle, J. S., Vierstra, R. D., and Forest, K. T. (2007). High resolution structure of *Deinococcus* bacteriophytochrome yields new insights into phytochrome architecture and evolution. *J Biol Chem* **282**, 12298-12309.

Wang, B., Kettenbach, A. N., Gerber, S. A., Loros, J. J., and Dunlap, J. C. (2014). *Neurospora* WC-1 recruits SWI/SNF to remodel frequency and initiate a circadian cycle. *PLoS Genet* **10**, e1004599.

Wang, Z., Li, N., Li, J., Dunlap, J. C., Trail, F., and Townsend, J. P. (2016). The fast-evolving *phy-2* gene modulates sexual development in response to light in the model fungus *Neurospora crassa*. *MBio* **7**, e02148-15.

Waring, R. B., May, G. S., and Morris, N. R. (1989). Characterization of an inducible expression system in *Aspergillus nidulans* using *alcA* and tubulin-coding genes. *Gene* **79**, 119-130.

Wiederrecht, G., Shuey, D. J., Kibbe, W. A., and Parker, C. S. (1987). The *Saccharomyces* and *Drosophila* heat shock transcription factors are identical in size and DNA binding properties. *Cell* **48**, 507-515.

Wu, C., Yang, F., Smith, K. M., Peterson, M., Dekhang, R., Zhang, Y., Zucker, J., Bredeweg, E. L., Mallappa, C., Zhou, X., Lyubetskaya, A., Townsend, J. P., Galagan, J. E., Freitag, M., Dunlap, J. C., Bell-Pedersen, D., and Sachs, M. S. (2014). Genome-wide characterization of light-regulated genes in *Neurospora crassa*. *G3 (Bethesda)* **4**, 1731-1745.

Wu, S. H., and Lagarias, J. C. (2000). Defining the bilin lyase domain: lessons from the extended phytochrome superfamily. *Biochemistry* **39**, 13487-13495.

Wuichet, K., Cantwell, B. J., and Zhulin, I. B. (2010). Evolution and phyletic distribution of two-component signal transduction systems. *Curr Opin Microbiol* **13**, 219-225.

Yin, C., Wang, B., He, P., Lin, Y., and Pan, L. (2014). Genomic analysis of the aconidial and high-performance protein producer, industrially relevant *Aspergillus niger* SH2 strain. *Gene* **541**, 107-114.

Zalokar, M. (1954). Studies on biosynthesis of carotenoids in *Neurospora crassa*. *Arch Biochem Biophys* **50**, 71-80.

Zhang, X., He, H., Yin, Y., Zhou, W., Cai, M., Zhou, X., and Zhang, Y. (2016). A light-dark shift strategy derived from light-responded metabolic behaviors for polyketides production in marine fungus *Halorosellinia* sp. *J Biotechnol* **221**, 34-42.

Zheng, N., Schulman, B. A., Song, L., Miller, J. J., Jeffrey, P. D., Wang, P., Chu, C., Koepp, D. M., Elledge, S. J., Pagano, M., Conaway, R. C., Conaway, J. W., Harper, J. W., and Pavletich, N. P. (2002). Structure of the Cul1-Rbx1-Skp1-F boxSkp2 SCF ubiquitin ligase complex. *Nature* **416**, 703-709.

Zoltowski, B. D., and Crane, B. R. (2008). Light activation of the LOV protein vivid generates a rapidly exchanging dimer. *Biochemistry* **47**, 7012-7019.

Zoltowski, B. D., Schwerdtfeger, C., Widom, J., Loros, J. J., Bilwes, A. M., Dunlap, J. C., and Crane, B. R. (2007). Conformational switching in the fungal light sensor Vivid. *Science* **316**, 1054-1057.

Zoltowski, B. D., Vaccaro, B., and Crane, B. R. (2009). Mechanism-based tuning of a LOV domain photoreceptor. *Nat Chem Biol* **5**, 827-834.

Appendix

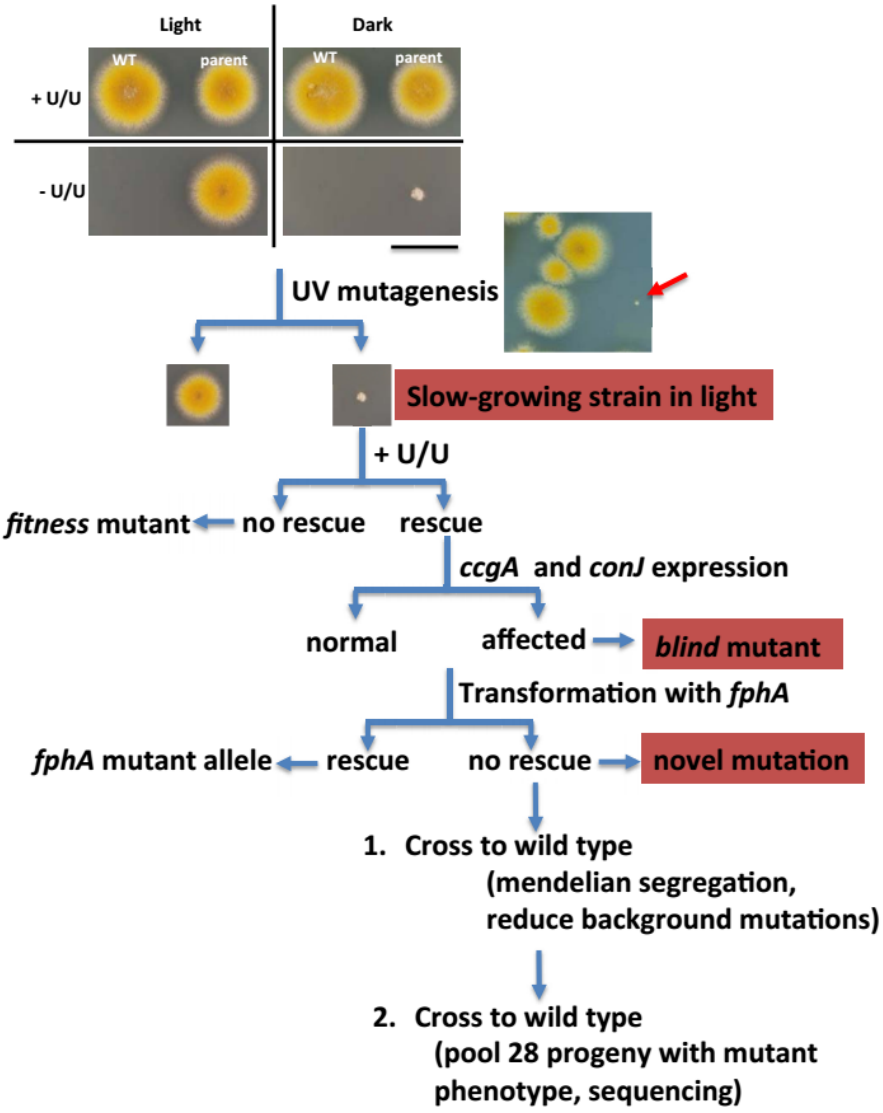

Suppl. Fig. S1. Scheme of whole-genome sequencing based screening for novel components involved in light signaling. Parent strain grows like wild type in light on minimal medium without uracil and uridine, but grows very slowly in the dark. After UV treatment, the putative *blind* mutants showed a slow-growing phenotype on minimal medium without uracil and uridine in light. These slow-growing mutants were transferred to minimal medium with uracil and uridine to eliminate fitness mutants. The mutants, whose phenotype could not be rescued, were further confirmed by checking light inducible genes *ccgA* and *conJ* expression in the dark and light with real-time RT-PCR. The *blind* mutants were the ones in which *ccgA* and *conJ* could not be induced by light. These *blind* mutants were complemented with *fphA* to eliminate *fphA* mutagenesis. In order to reduce background mutations, all *blind* mutants were crossed to wild type. After two subsequent crosses, progeny were sorted by phenotype. 28 progenies with a slow-growing phenotype and 28 progenies with normal growth were used for multiplex whole-genome sequencing.

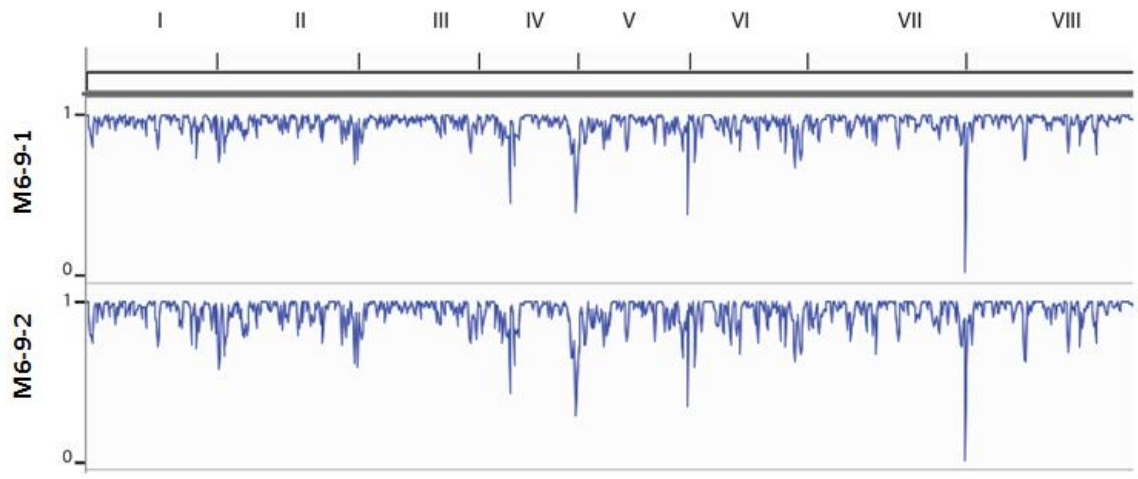

Suppl. Fig. S2: Coverage analysis shows that the genomes of M6-9-1 (only background mutations) and M6-9-2 (putative phenotype-causing mutation and background mutations) are identical. No big deletions or insertions were observed.

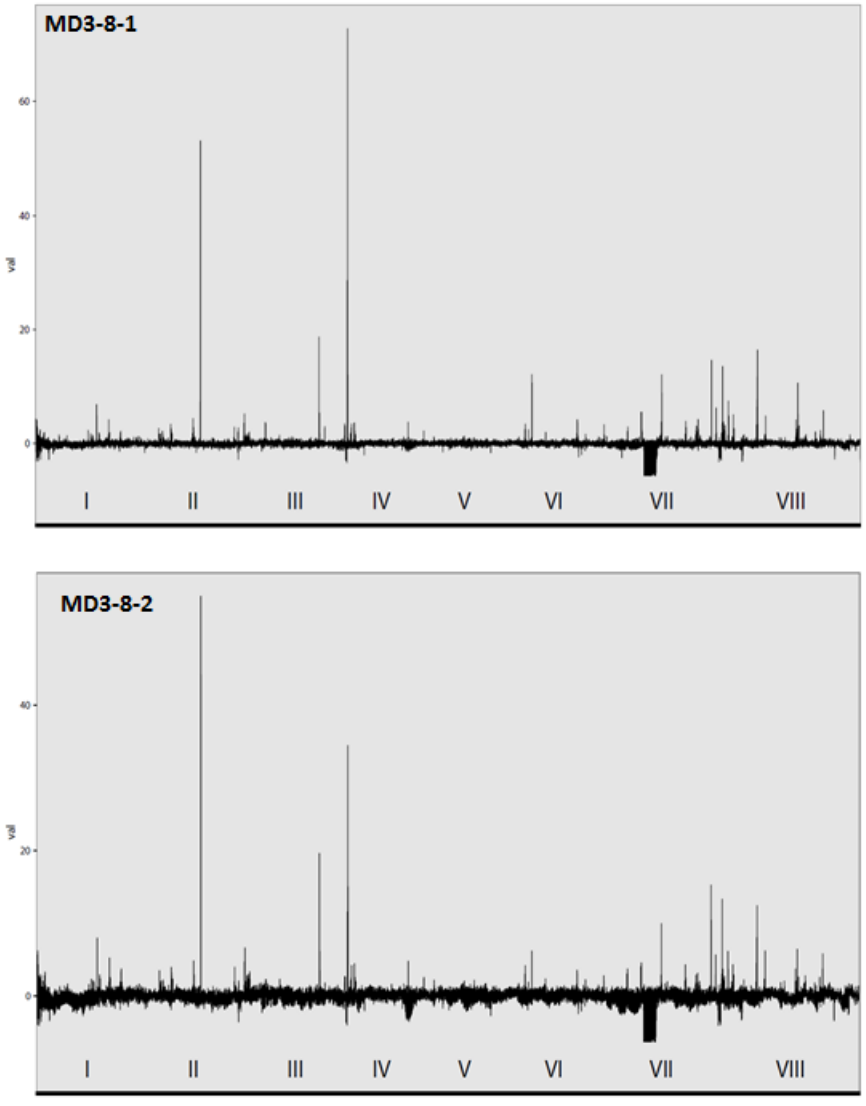

Suppl. Fig. S3. Coverage analysis shows that the genomes of MD3-8-1 (putative phenotype-causing mutation and background mutations) and MD3-8-2 (only background mutations) are identical. No big deletions or insertions were observed.

Acknowledgement

Special thanks to my supervisor, Prof. Dr. Reinhard Fischer. I am grateful for the chances he offered me to study and do the research in his laboratory and the supports he gave me in the course of studying, planning and performing the project, publishing the paper and writing the dissertation. I also thank him for the financial support that he gave me in the fourth year of my doctoral study.

I appreciate it very much that Olivier Armant and Victor Gourain helped me to analyze the genome sequences of the mutants.

I do not forget to thank China Scholarship Council (CSC) for the financial support in the first three years of my doctoral study. I feel like thanking the embassy staff in China embassy in Germany for the help in the beginning of my oversea study.

I also want to thank Dr. Julian Benjamin Röhrig, Dr. Stefan Rauscher, Dr. Maren Hedtke and Dr. Ying Zhang for the help and suggestions in the beginning of my doctoral study.

I am extremely grateful to Prof. Dr. Jesús Aguirre for the gift of the strains and plasmids that saved me a lot of time.

I thank Dr. Jerzy Brzywczy for sharing the new finding in their transcriptomic analysis with us.

I do not forget to thank my colleagues, Birgit Schreckenberger, Elke Wohlmann, Chris Streng and Jennifer Hübner for helping me in my project. I also want to thank other colleagues in the laboratory for some assistance.

I thank the Requena and the Kämper group for the help and suggestions in some experiments.

Last but not the least, I am grateful to my girlfriend Xiangru Li and my parents for the understanding and support.